From the
Institute of Veterinary Pathology
Faculty of Veterinary Medicine
Freie Universität Berlin

Therapeutic approaches to minimise acute renal failure in an animal model of myoglobinuria

Inaugural dissertation
to attain the degree of
Doctor of Veterinary Medicine
at the
Freie Universität Berlin

Submitted by
Ludwig K. Groebler
Veterinarian from Berlin

Berlin 2012

Journal-No.: 3587

Aus dem Institut für Tierpathologie
des Fachbereichs Veterinärmedizin
der Freien Universität Berlin

Therapeutische Ansätze zur Verminderung von akutem Nierenversagen in einem Tiermodell der Myoglobinurie

Inaugural-Dissertation
zur Erlangung des Grades eines
Doktors der Veterinärmedizin
an der
Freien Universität Berlin

vorgelegt von
Ludwig K. Gröbler
Tierarzt
aus Berlin

Berlin 2012

Journal-Nr.: 3587

Gedruckt mit Genehmigung des Fachbereichs Veterinärmedizin

der Freien Universität Berlin

Dekan: Univ.-Prof. Dr. Leo Brunnberg

Erster Gutachter: Univ.-Prof. Dr. Achim Gruber

Zweiter Gutachter: Prof. Dr. Paul Witting

Dritter Gutachter: Univ.-Prof. Dr. Barbara Kohn

Deskriptoren (nach CAB-Thesaurus):
rhabdomyolysis, myoglobinuria, renal failure, oxidative stress, antioxidants, deferoxamine, ascorbic acid

Tag der Promotion: 12. Februar 2013

CONTENT

CONTENT

ARF	Acute Renal Failure
AKI	Acute Kidney Injury
α-TOH	α-Tocopherol (biologically active Vitamin E)
ATP	Adenosine Triphosphate
BP	Bisphenol (3,3',5,5'-tetra-*tert*-butylbiphenyl-4,4'-diol)
CE	Cholesteryl Esters
cGMP	Cyclic Guanylyl Monophosphate
DFOB	Desferrioxamine B
DFOB-AdA$_{OH}$	DFOB-*N*-(3-hydroxyadamant-1-yl)carboxamide
eNOS	Endothelial Nitric Oxide Synthase
EPR	Electron Paramagnetic Resonance
Fe^{2+}	Ferrous Iron (II)
Fe^{3+}	Ferric Iron (III)
Fe^{4+}	Ferryl Iron (IV)
GPx	Glutathione Peroxidase
GSH	Glutathione
HO-1	Heme Oxygenase-1
H_2O_2	Hydrogen Peroxide
Hp	Haptoglobin
ICAM	Intracellular Adhesion Molecule
KIM-1	Kidney Injury Molecule-1
Mb	Myoglobin
MCP-1	Monocyte Chemotactic Protein 1
MDCK II	Madin-Darby Canine Kidney II cell
MTT	Tetrazolium Salt
NF-κB	Nuclear Factor κB
$\bullet$NO	Nitric Oxide
NTBI	Non-Transferrin-Bound-Iron
$^1O_2$	Singlet Oxygen
$O_2^{\bullet-}$	Superoxide Anion Radical
$\bullet$OH	Hydroxyl Radical
PBS	Phosphate Buffered Saline
RM	Rhabdomyolysis

ROS   Reactive Oxygen Species

sGC   Soluble Guanylyl Cyclase

SOD-1   Copper-Zinc Superoxide Dismutase

SOD-2   Manganese Superoxide Dismutase

% TBSA   Percentage Total Body Surface Area

TNF-α Tumor Necrosis Factor α

VCAM   Vascular Cell Adhesion Molecule

Vit C   Vitamin C

VSMC   Vascular Smooth Muscle Cells

1   Introduction

In 1941, during the London bombardment, the British physician Eric Bywaters (1910-2003) studied victims of the bombing. They had suffered from crushed limbs and – even if initially appeared in a good condition - developed kidney failure after release of the crushing pressure. This sequence became known as the "crush syndrome". Bywaters observed dark brown casts in the urine and casts in the renal tubules containing brown pigment. Ironically, Bywaters himself was rejected from military service because of a kidney problem. A few years later, in 1944, he showed that leakage of muscle contents, as a consequence of ischemia and reperfusion of the affected body parts, into the circulation caused renal failure as demonstrated by experiments he performed by injecting myoglobin (or myohaemoglobin as it was called at that time) into rabbits. This condition, termed rhabdomyolysis (RM), can have various causes such as trauma, exertion, muscle hypoxia, genetic defects, infections, changes in body temperature, metabolic and electrolyte disorders, drugs and toxins or may be idiopathic. Depending on the cause, there is a moderate to high risk for patients to develop acute renal failure (ARF) with fatal outcome. Almost 70 years after Bywaters observations, little is known about the precise molecular events leading to this pathology and further investigation on the mechanism of renal damage and therapeutic approaches to combat this are warranted. Over a long period, renal vasoconstriction, direct heme protein-induced cytotoxicity and intraluminal cast formation have been proposed as the main pathophysiological factors involved in RM-induced renal failure and this has lead to a number of proposed treatments, which were more or less unsuccessful. Recent studies have highlighted the importance of oxidative injury to the kidney in the development of RM-induced renal failure. This work aims to elucidate the role of myoglobin-mediated oxidative stress and how renal tissue may be protected against it. We used both an *in vitro* cell model and an *in vivo* rat model to simulate the conditions as they appear under myoglobinuric conditions. We tested selected iron chelators and antioxidants in regards of inhibiting oxidative stress and correlated this with protection from renal dysfunction. The data obtained in these studies may help to gain a deeper understanding of the molecular processes that are initiated by myoglobin and may contribute to develop new strategies to combat ARF after RM.

2   Literature Review

2.1   Clinical Background: Rhabdomyolysis

Pathophysiologically, rhabdomyolysis (RM) can be defined as "an injury to the sarcolemma of skeletal muscle, resulting in leakage of its components into the blood or urine" (Knochel 1993). Though the syndrome has been recognized for a few thousand years (Moses), renal failure and RM was ultimately linked for the first time by the classic description of the crush syndrome after London bombardment during the World War II (Bywaters and Beall 1941). Later, the authors could show the presence of abnormal levels of myoglobin (Mb) in the urine of these patients (Bywaters, Delory et al. 1941).

Excessive RM, and hence Mb-release, may be caused by a variety of factors, the most common of them in adults range from illicit drugs, alcohol abuse, medical drugs, muscle diseases, trauma, neuroleptic malignant syndrome, seizures and immobility. In paediatric patients lysis of myocytes is most commonly caused by viral myositis, trauma, connective tissue disorders, exercise, and drug overdose (Khan 2009). Ischemia or metabolic disorders can also cause RM leading to hypokalemia, hypernatremia, or hypophosphatemia.

Burns are one of the main causes leading to RM. Burns may be caused due to thermal, chemical or electrical injuries. Thermal and chemical injuries lead to coagulative necrosis of the skin and the underlying subcutaneous tissue including muscle cells. The major determinants of burn severity are extent (as determined by percentage of involved body surface area) and depth (partial – or full thickness) of the injury (Bellomo, Kellum et al. 2008). It has been shown that severe burn injury and systemic inflammatory response syndrome can initiate serious systemic illness often accompanied by various clinical complications. Multi-organ injury following severe burn has been reported in up to 50% of mortality cases (Sabry, Wafa et al. 2009).

2.2   Acute Renal Failure

One of the significant clinical pathologies that develop in burns patients is acute renal failure (ARF). This subset is reported to have a mortality rate of 85% on average (Mustonen and Vuola 2008) indicating that while ARF occurs in a small fraction of

burns patients, it is often associated with unacceptably high rates of mortality. The occurrence of ARF in burn patients can be promoted by several variables such as occurrence of septicemia, fluid loss, muscle damage, hypotension, cardiopulmonary failure and use of nephrotoxic agents (Holm, Hörbrand et al. 1999). In addition, renal insult subsequent to severe burns can be measured by the level of intensive acute phase response as an indicator of extensive inflammation in the kidney (Sabry, Wafa et al. 2009). Yet, there are different criteria suggested in the literature to conclude from burn severity to ARF what makes them difficult to compare. Despite this complication, the link between burn severity and the likelihood and severity of ARF is not disputed (Mustonen and Vuola 2008).

2.3   Myoglobin

Due to the lysis of peripheral muscle cells, large amounts of salts, enzymes (aldolase, creatine kinase, lactate dehydrogenase), and Mb are released into the systemic circulation which leads to electrolyte disturbances, hypovolemia, metabolic acidocis, coagulation defects and importantly, ARF due to the accumulation of extracellular Mb (Criddle 2003). Mb is a 17 kDa small intracellular heme protein that is found in the skeletal, smooth and cardiac muscle (Perkoff, Hill et al. 1962; Lewin and Moscarello 1966). It has a porphyrin moiety with an iron centre, which is surrounded by four alpha-helical loops. The primary function of Mb within muscle tissues is the transport and the storage of di-oxygen and the release if required, *e.g.*, under hypoxic conditions, to the mitochondria for oxidative phosphorylation. The maintenance of cellular energetics through the sustained production of ATP is essential for the cellular response to insult, which is linked to cell viability (Gordon 1986).

2.4   Pathophysiology

Current data indicates that RM leads to ARF in burns victims via the effect of extracellular Mb on the kidneys (Khan 2009). However, the exact pathogenesis of Mb induced/mediated renal failure is still a matter of contention. The theme of this particular thesis will be focused on enhanced oxidative stress as a causal factor in early onset ARF, and whether amelioration of oxidative stress with a suitable iron chelator, synthetic or natural antioxidants will be of benefit in an animal model of ARF. Rhabdomyolysis results in both the initiation of an endotoxin cascade (Zager 1996) and

volume depletion, which can lead to ischemia/reperfusion injury in the kidneys. At the same time, the extracellular Mb causes physical and chemical damage.

Some level of RM is normal and occurs on a daily basis in response to mechanical stress (Vanholder, Sever et al. 2000). In a normal functioning system, extracellular Mb is easily cleared away by a plasma protein, haptoglobin (Hp) (Sakata, Yoshioka et al. 1986; Vanholder, Sever et al. 2000). Often the amount of extracellular Mb reaching the proximal tubule cells through passive filtration exceeds their ability to convert iron to ferritin, the circulating Mb damages the kidney by renal tubular obstruction and necrosis, which are accompanied by intense renal vasoconstriction leading to intracellular ferrihemate accumulation (Sharp, Rozycki et al. 2004). Finally, extracellular Mb reaches the urine. This phenomenon is closely related to complications in burns victims as hypermyoglobinemia occurs in up to 88.5% of the patients (Walsh, Miller et al. 1982).

Rhabdomyolysis affects about 1 in 10,000 persons in the United States and accounts for an estimated 8 to 15% of all cases of ARF (www.rhabdomyolysis.org). About 5% of RM cases result in death (about 1500 for the United States). Some data suggest that the number of patients with RM after trauma may be underestimated and that the current treatments may not improve the outcome in a large proportion of patients with renal failure after RM.

The current therapy in RM is conservative and aims to stabilize the patient and to prevent ARF. Aggressive repletion with fluids is indicated to maintain kidney function and microvascular circulation and can be forced by addition of mannitol. In despite, the alkalinization of urine with bicarbonate to stabilize the heme group from dissociation has no or little clinical evidence (Huerta-Alardin, Varon et al. 2005). Upon failure of conservative treatment and onset of ARF, patients require emergency hemodialysis, although this does not remove Mb from the renal system. In conclusion, there is a necessity to explore new therapeutic avenues for the prevention of RM-induced ARF.

It is also known that Mb scavenges endothelial nitric oxide (•NO) (Kavdia, Tsoukias et al. 2002). This property of Mb plays a role in vasoconstriction by restraining •NO-bioavailability (Andriambeloson and Witting 2002). As a consequence, this could be a reason for cast development in the kidney (Zager, 1996). Although, it is not clear if

these casts are the result of the renal failure, occurring during tubular stasis, or causally related (Zager 1996).

Precipitation of Mb within the tubular cells could act as a physical barrier to glomerular filtration at higher Mb concentrations. However, renal dysfunction may also occur at relatively low levels of Mb, suggesting that an alternative mechanism of damage may be operative. For example, prior research has shown that cultured kidney epithelial cells are sensitive to low concentrations of extracellular Mb (in the range 0-100 μM) (Parry, Ellis et al. 2008). These cells showed signs of decreased monolayer permeability, decreased transferrin endocytosis, and increased expression of antioxidant genes along with increased activity of antioxidant proteins (Parry 2006; Parry, Ellis et al. 2008). A possible reason for such Mb-induced epithelial cell dysfunction could be enhanced oxidative stress.

Mb can exhibit a pro-oxidant activity, but this activity is modulated by an associated reductase enzyme that maintains the heme iron primarily in the Fe(II) redox state for the binding of molecular oxygen (Ueda, Baliga et al. 1996). Because of its relatively small protein size, extracellular Mb is filtered through the glomeruli and reabsorbed in the proximal tubules by endocytosis. Under acidic conditions (pH<5.6) the iron-containing ferric-hemate group is released from the globin portion of the protein. This degradation normally happens in the lysosome within the cell cytoplasm, where free iron released by this process is rapidly bound to ferritin where it is rendered redox inactive (Sharp, Rozycki et al. 2004). In the extracellular environment, the release of heme or free iron results in increased oxidative stress through the action of these pro-oxidants. For example, it has been suggested that the iron within Mb becomes released from its heme moiety. Redox available iron has the ability to donate and accept electron as well as the capability to generate free oxygen radicals. This leads to oxidative stress and injury of the renal cell through its role in Fenton chemistry, as a catalyst of the Haber-Weiss reaction (Vanholder, Sever et al. 2000). The Haber-Weiss reaction generates the hydroxyl radical from superoxide radical anion and hydrogen peroxide catalyzed by iron (refer to schematic below) (Fenton 1894; Haber and Weiss 1932), which can then damage cellular targets including lipids, protein and DNA, and contribute to enhanced oxidative stress (Winterbourn 1995).

$$Fe^{3+(aq)} + O_2{}^{\bullet-} \rightarrow Fe^{2+}{}_{(aq)} + O_{2\ (g)}$$

$$Fe^{2+}{}_{(aq)} + H_2O_2 \rightarrow {}^{\bullet}OH + OH^-{}_{(aq)}$$

***Net reaction*: $O_2{}^{\bullet-} + H_2O_2$ (Fe catalyst) $\rightarrow {}^{\bullet}OH + OH^- + O_{2\ (g)}$**
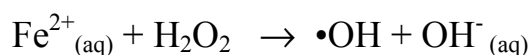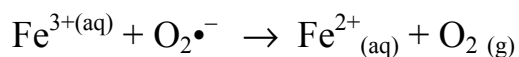
2.5   Oxidative Stress

Oxidative stress is defined as a disturbance in the equilibrium between pro- and antioxidant factors in the normal redox state within the biological system. This imbalance can be caused during the over-production of free radicals or the body's inability to readily detoxify the reactive intermediates or repair the resulting damage (Pentón-Rol, Cervantes-Llanos et al. 2009). Free radicals such as reactive oxygen species (ROS) are stable, but highly reactive species with one unpaired valence electron. Once formed, ROS react rapidly with neighboring species, including lipids, proteins and a wide range of other biomolecules, causing changes and/or damages in the target molecule and disturbing their function. Subsequently, they pass on the unpaired electron to create a secondary free radical. The secondary free radical then reacts in turn with its adjacent species to continue the cycle of damage (Halliwell 2007).

ROS can be produced by various mechanisms including generation during oxidative phosphorylation in the mitochondria as a by-product of normal cellular aerobic metabolism (Davies 1995; Ide, Tsutsui et al. 1999). Free radicals are usually oxygen- or nitrogen-centered and always contain a single unpaired electron.

Characterized as a di-radical, molecular oxygen (O_2) possess a property that permits liquid oxygen to be attracted to the poles of a magnet. This property also dictates that full chemical reduction of oxygen to water is the terminal event in the electron transport chain overall requiring 4 electrons. The sequential donation of electrons to oxygen during this process can generate ROS as intermediates, and "electron leakage" can also contribute to the formation of ROS (Davies 1995; Genova, Pich et al. 2003; Miwa and Brand 2003). Various ROS are produced in the mitochondria including:

➢   Donation of a single electron to molecular oxygen results in the formation of the superoxide radical ($O_2{}^{\bullet-}$).

➢ Donation of a second electron yields peroxide, which then undergoes protonation to yield hydrogen peroxide (H_2O_2).

➢ Donation of a third electron, such as occurs in the Fenton reaction ($Fe^{2+} + H_2O_2 \rightarrow Fe^{3+} + \bullet OH + OH^-$), results in production of the highly reactive hydroxyl radical ($\bullet OH$).

➢ Donation of a fourth electron yields water.

➢ Singlet oxygen ($^1O_2$), a very short-lived and reactive form of molecular oxygen in which the outer electrons are raised to a higher energy state, can be formed by a variety of mechanisms, including the Haber-Weiss reaction (see above) (Toufektsian, Boucher et al. 2001).

2.6   Iron Chelation

Due to its ability to inhibit the redox activity of transition metals through chelation, desferrioxamine B (referred to henceforth as DFOB-AdA$_{OH}$; structure shown in Figure 1) has been used to examine the mechanisms of oxidative stress caused by iron in many disease states (Gabutti and Piga 1996). As a result of the increased heme catabolism, the iron released saturates the binding capacity of transferrin, resulting in a pool of non-transferrin-bound-iron (NTBI) or iron overload similar to patients with Thalassemia (α and β), hemochromatosis or hemodialysis (Valko, Rhodes et al. 2006). Humans do not have an active iron excretion mechanism and the excess iron causes organ dysfunction from the unregulated production of ROS and cardiac siderosis; this iron overload requires treatment with iron chelators (Nick 2007). The first-line treatment for iron overload is Desferal$^\circledR$, which is the mesylate salt of the trihydroxamate-based siderophore, desferrioxamine B (DFOB).
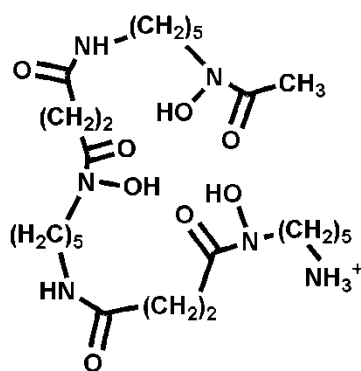
Figure 1   Chemical structure of the therapeutic iron chelator DFOB.

Reprinted with permission from Liu, Obando et al. Conjugates of desferrioxamine B (DFOB) with derivatives of adamantane or with orally available chelators as potential agents for treating iron overload. Journal of medicinal chemistry. 53(3), 1370-1382. Copyright © 2010, American Chemical Society.

Siderophores are low-molecular-weight compounds produced by both non-pathogenic and pathogenic bacteria in response to Fe deprivation. DFOB is the siderophore native to the soil bacterium *Streptomyces pilosus*; the use of DFOB in the clinic for almost 50 years underscores the value of mapping bioactive compounds from nature (Stintzi, Barnes et al. 2000). Previous studies have shown that desferrioxamine decreased RM-induced renal injury in the rat and prevented cell toxicity induced by direct exposure to Mb (Boutaud and Roberts 2011). Desferal® is not orally active and requires treatment through subcutaneous or intravenous infusions. The water solubility ~ 0.4 M of DFOB impacts significantly on the ability of this hydrophilic agent to cross cell membranes to access intracellular iron pools and this has a marked impact on the efficacy of this chelator. The hydrophilicity of DFOB manifests as rapid clearance of the drug with a short plasma half-life ($t_{1/2}$ ~ 5.5-12 min) (Porter, Rafique et al. 2005). The aqueous solubility of DFOB is attributable in part to the positive charge at the amine tail at physiological pH values.

The low membrane partition coefficient of DFOB (P = 0.02) describes a drug, which is unable to readily traverse the cell membrane to access intracellular iron pool. With this background in mind, Liu *et al.* aimed to modify DFOB without compromising the Fe(III)-binding ability but gaining superior pharmacokinetics (Liu, Obando et al. 2009). First, they designed covalent adducts between DFOB and adamantane-based

compounds that have analogues in the clinic which are orally available and generally well tolerated by patients. Adamantane-1-carboxylic acid belongs to a family of functionalized polycyclic cage-based compounds with several compounds in use to treat influenza A (amantadine, rimantadine), and Parkinson's disease (amantadine), Alzheimer's disease (memantine) and pulmonary tuberculosis (SQ109) (Spasov, Khamidova et al. 2000). Each of amantadine, rimantadine and memantine are orally active and are generally well tolerated by patients (Ison and Hayden 2001). Second, they designed conjugates of DFOB, which would have greater partition coefficients relative to DFOB (see Figure 2).
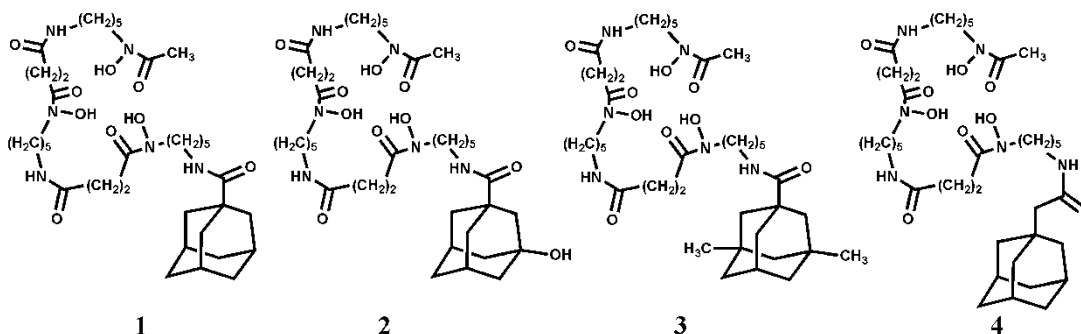
Figure 2   Desferrioxamine B conjugates

DFOB-AdA (1), DFOB-AdA$_{OH}$ (2), DFOB-AdA$_{dMe}$ (3), DFOB-AdAc (4)
Reprinted with permission from Liu, Obando et al. Conjugates of desferrioxamine B (DFOB) with derivatives of adamantane or with orally available chelators as potential agents for treating iron overload. Journal of medicinal chemistry. 53(3), 1370-1382. Copyright © 2010, American Chemical Society.

The ability of selected compounds to inhibit cellular proliferation of Madin−Darby canine kidney type II (MDCK II) cells was assessed using the [3-(4,5-dimethylthiazol-2-yl)-2,5-diphenyltetrazolium bromide] (MTT) assay (Mosmann 1983) (Table 1). Compounds that are well tolerated by cells will not affect regular cellular proliferation or growth and will have high IC$_{50}$ (or LD$_{50}$) values relative to more cytotoxic compounds.

Table 1   IC50 Values (μM) of 1−5 in Madin−Darby Canine Kidney Type II (MDCK II)

Compound	IC50 (μM)
DFOB	9.49 ± 1.24
DFOB-AdA	118.86 ± 1.16
DFOB-AdA$_{OH}$	> 100
DFOB-AdA$_{dMe}$	163.37 ± 1.52
DFOB-AdAc	225.56 ± 1.28

Adapted from Liu, J.; Obando, D.; Schipanski, L. G.; Groebler, L. K.; Witting, P. K.; Kalinowski, D. S.; Richardson, D. R.; Codd, R. J. Med. Chem. 2010, 53, 1370-1382

The cell viability data using the human SK-N-MC neuroepithelioma cell type reflects similar trends as observed in the MDCK II cell line. Importantly, in both cell types, all of the conjugates showed less cytotoxicity than DFOB itself but similar Fe chelating efficacy. In this work, we tested the ability of DFOB-*N*-(3-hydroxyadamant-1-yl)carboxamide to protect cultured kidney epithelial cells in an established cell model of RM that mimics urinary Mb levels detected in severe electrical burn-induced muscle myolysis (Parry, Ellis et al. 2008).

2.7   Antioxidants

Antioxidants are agents capable of interfering with processes involved in oxidative stress (Sies 1997). The specific effects of antioxidants, which include the regulation of gene expression, have been revealing but not yet fully understood. There has been some progress in the use of antioxidants to treat oxidative damage but there is certainly considerable work remaining. Antioxidants are widely used as constituents in dietary supplements in the hope of maintaining health and preventing oxidation related diseases (Ames, Shigenaga et al. 1993).

2.7.1 Naturally occurring Antioxidants

Natural antioxidants play a vital role by participating in the body's endogenous defense. Oxidation reactions are crucial for life and represent a major mechanism for the production of cellular energy required for normal function. However, in some pathologies the depletion of natural antioxidants is a hallmark. For example, during acute cerebral ischemia plasma content of low-molecular weight antioxidants are consumed (Hendryk, Czuba et al. 2010).

Antioxidant potency can be measured by the redox potential, which is a thermodynamic parameter that determines efficacy in a defined system. The lower the value of the redox potential, the greater the antioxidant activity for the agent; although kinetic effects must also be considered when assigning antioxidant efficacy. For example, glutathione has a redox potential of 920 mV and comparably lower antioxidant activity than Vitamin C (ascorbate, 280 mV), α-tocopherol (480 mV) and flavonoids (510 mV) (Jovanovic, Steenken et al. 1996). However, the relatively high abundance of glutathione in cells and tissues can compensate for its relatively low redox potential as rates of reaction are defined by both thermodynamic and quantity parameters.

2.7.2 Ascorbic Acid

Vitamin C (Vit C) or L-Ascorbate is a hexose sugar derivative that is a highly effective antioxidant in living organisms (see Figure 3). It has been known for a long time to be essential for protection of humans against scurvy. It is also known for its role in collagen production, leukocyte function, tissue metabolism and adrenocortico-hormone (Dylewski and Froman 1992). The main part of the molecule with regards to its biological activity is the ene-diol group at carbon atoms 2 and 3. This group gives the molecule its acidic nature and chemical reducing properties as it can ionise (pK_a = 4.17 and 11.17) and readily donate an electron to form a stable ascorbyl radical that decays to a non-radical product (dehydroascorbate). The latter can be taken up by cells and recycled to regenerate ascorbate making this a highly effective radical-scavenger (Smirnoff, Running et al. 2004).
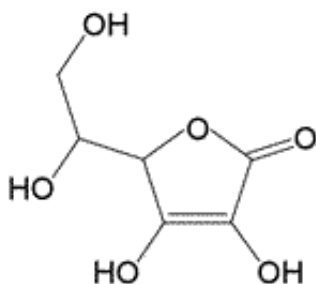
Figure 3   Structure of vitamin C

Chemical structure of water-soluble vitamin C showing the ene-diol group at carbon atoms 2 and 3.

Due to its low redox potential, Vit C is capable of reducing an array of reactive species such as oxygen-related radicals (superoxide, hydroxyl radical, peroxyl radicals), sulphur radicals and nitrogen-oxygen radicals (Padayatty, Katz et al. 2003). In addition, it can regenerate/recycle other phenolic antioxidants such as α-tocopheroxyl, urate and β-carotene. An example of this radical scavenging mechanism of Vit C is shown below (Figure 4):
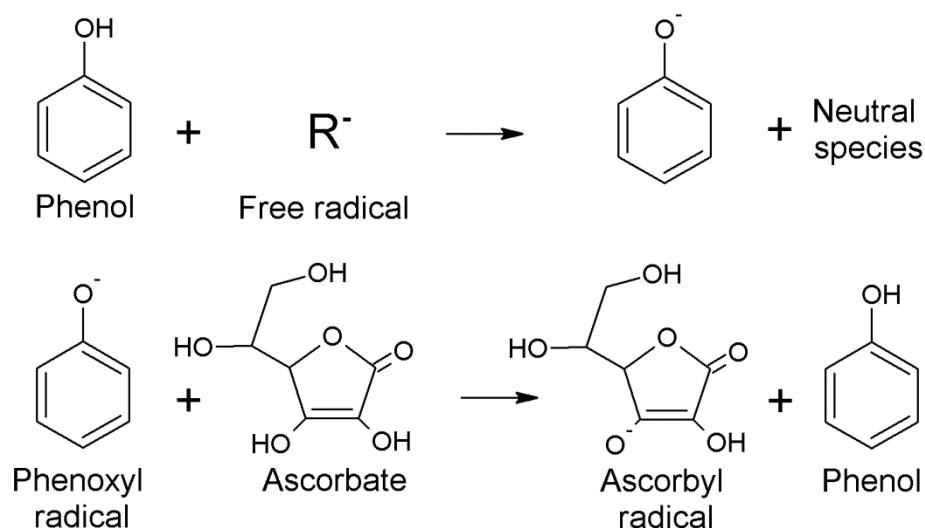
Figure 4 Regeneration of phenolic radicals by ascorbate/vitamin C
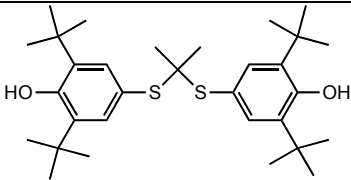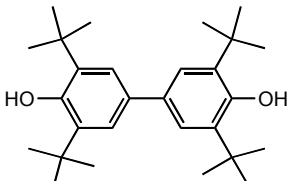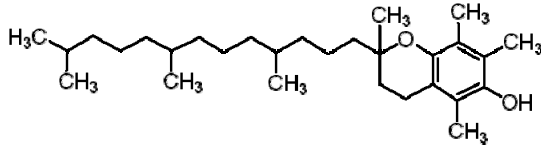
The figure shows a phenol molecule retaining with free radical producing neutral species and a phenoxyl radical. The phenoxyl radical reacts with the ascorbate to produce ascorbyl radical and regenerate the original phenolic compound. The ascorbyl radical is biologically inert and decomposes to yield dehydroascorbate (Smirnoff, Running et al. 2004). Figure created with ACD/ChemSketch freeware.

2.7.3 Bisphenol

Phenolic compounds are prototype chain-breaking antioxidants during the autoxidation of lipids (Sies 1997). The synthetic antioxidant 3,3',5,5'-tetra-t-butyl-biphenyl-4,4'-diol (Bisphenol) was designed through a structure activity study (Witting, Westerlund et al. 1996). The redox potential measured for Bisphenol (BP) is significantly less positive than that for other common synthetic or natural phenols. This is indicative of the increased antioxidant activity *in vitro* (see Table 2). For reference, the redox potential for the two common phenols probucol and vitamin E (as α-tocopherol) are shown together with their respective octanol-water partition coefficients.

In general, by lowering the redox potential in the design of the synthetic polyphenol without significantly altering lipophilicity, they have enhanced the antioxidant activity of BP in biological systems. The bisphenol BP is superior to methyl-BP because the redox potential increases markedly when -OH groups are replaced by a shielding methyl group and the presence of the phenol group imparts the antioxidant activity to this compound.

Table 2   Redox potentials and partition coefficients for natural and synthetic phenols

Agent	Structure	Redox potential (mV)[a]	Partition value[b]
Probucol		545	12.1
Bisphenol		307	10.3
α-TOH		600	12.2

[a] Redox potentials were determined with cyclic voltammetry and analytically pure samples as described previously (Wu, Kathir et al. 2006). [b] Corresponding octanol-water partition coefficients as determined by Kim *et al.* Free radical research. 2011, 45(9): 1000-1012.

2.8   Rationale for Antioxidant Selection

Bisphenol (BP) has been adopted in this study for two reasons. As described in the previous section, the activity of this synthetic compound is superior to many other natural antioxidants. It is more important, however, to note that BP was designed as a potent antioxidant with a potential to exert biological benefits primarily via reducing oxidative stress. The idea to use antioxidants as inhibitors of RM-induced ARF has some merit (Stefanovic, Savic et al. 2000; Chander, Singh et al. 2003; Rodrigo, Bosco et al. 2004), although not all studies reported improved renal function with antioxidant supplementation (Aydogdu, Atmaca et al. 2006; Vlahovic, Cvetkovic et al. 2007).

These conflicting outcomes may have arisen from different biological activities of the test compounds with some antioxidants capable of exhibiting other activities including anti-inflammatory and cell signaling capacity when employed at relative high concentrations *e.g.*, the case for vitamin E which can provide anti-inflammatory activity such as gene regulatory actions independent of anti-inflammatory activity (Azzi 2007).

The use of BP either alone or in combination with Vit C may assist in resolving the question on whether antioxidants are useful in the setting of RM-induced ARF as lower doses of the antioxidant can be employed due to the relatively high degree of antioxidant activity. To be an efficient antioxidant, bisphenol needs to react with initial free radicals, such as lipid peroxyl radicals, at suitable rates and interact with Vit C for its own regeneration and to enhance antioxidant activity (Sies 1997).

2.9   Statement of Hypothesis and Aims

In this work we propose to ascertain whether chelators or antioxidants are able to ameliorate ARF through inhibiting oxidative stress.

The objectives/aims of the study are to:

1) Assess the efficacy of a novel chelator to inhibit Mb-mediated oxidative damage in a cell model using cultured kidney epithelial cells.
2) Assess the efficacy of combined antioxidant therapy in an animal model of RM.

3   Publication 1

Conjugates of desferrioxamine B (DFOB) with derivatives of adamantane or with orally available chelators as potential agents for treating iron overload

Konjugate von Desferrioxamin B (DFOB) mit Derivaten von Adamantan oder oral verfügbaren Chelatoren als potentielle Wirkstoffe zur Behandlung von Eisenüberschuss

3.1   Abstract (German Translation)

Konjugate von Desferrioxamin B (DFOB) mit Adamantan-1-carbozyklischer Säure, 3-hydroxyadamantan-1-carbozyklischer Säure, 3,5-dimethyladamantan-1-carbozyklischer Säure, Adamantan-1-Essigsäure, 4-methylphenoxy-Essigsäure, 3-hydroxy-2-methyl-4-oxo-1-pyridin-Essigsäure (N-Essigsäure-Derivat von Deferiprone), oder 4-[3,5-bis(2-hydroxyphenyl)-1,2,4-triazol-1-yl]-Benzoesäure (Deferasirox) wurden synthetisiert und

die Integrität der Fe(III)-Bindung dieser Wirkstoffe wurde mittels Elektrosprayionisation-Massenspektromie und RP-HPLC-Messungen untersucht. Die von der DFOB-3,5-dimethyladamantan-1-carbozyklischen Säureverbindung mobilisierte Menge an intrazellulärem 59Fe war 3-mal höher als bei DFOB allein, und der IC50-Wert dieser Verbindung war 6- oder 15-mal höher als bei DFOB in zwei verschiedenen Zelltypen. Die Beziehung zwischen logP und 59Fe-Mobilisierung ergab bei den DFOB-Konjugaten, dass die maximale Mobilisierung von 59Fe bei einem logP-Wert von 2.3 geschieht. Dieser Parameter scheint, mehr als die Fe(III)-Affinität, das Ausmass der intrazellulären 59Fe-Moblisierung zu beeinflussen. Die Effizienz der hohen Eisenmobilisierung bei niedriger Toxizität von ausgewählten, auf Adamantan basierenden DFOB-Konjugaten untermauert das Potential dieser Wirkstoffe Erkrankungen durch Eisenüberschuss bei Patienten mit transfusionsabhängigen Störungen wie β-Thalassemie zu behandeln.

3.2   Original Publication

Journal of
**Medicinal
Chemistry**
Article

Conjugates of Desferrioxamine B (DFOB) with Derivatives of Adamantane or with Orally Available Chelators as Potential Agents for Treating Iron Overload

Joe Liu,[†] Daniel Obando,[†] Liam G. Schipanski,[†] Ludwig K. Groebler,[‡] Paul K. Witting,[‡]
Danuta S. Kalinowski,[‡] Des R. Richardson,[‡] and Rachel Codd*,[†]

[†] *School of Medical Sciences* (*Pharmacology*) *and Bosch Institute, University of Sydney, New South Wales 2006, Australia and* [‡] *School of Medical Sciences* (*Pathology*) *and Bosch Institute, University of Sydney, New South Wales 2006, Australia*

Desferrioxamine B (DFOB) conjugates with adamantane-1-carboxylic acid, 3-hydroxyadamantane-1-carboxylic acid, 3,5-dimethyladamantane-1-carboxylic acid, adamantane-1-acetic acid, 4-methylphenoxyacetic acid, 3-hydroxy-2-methyl-4-oxo-1-pyridineacetic acid (*N*-acetic acid derivative of deferiprone), or 4-[3,5-bis(2-hydroxyphenyl)-1,2,4-triazol-1-yl]benzoic acid (deferasirox) were prepared and the integrity of Fe(III) binding of the compounds was established from electrospray ionization mass spectrometry and RP-HPLC measurements. The extent of intracellular ^{59}Fe mobilized by the DFOB-3,5-dimethyladamantane-1-carboxylic acid adduct was 3-fold greater than DFOB alone, and the IC_{50} value of this adduct was 6- or 15-fold greater than DFOB in two different cell types. The relationship between log$P$ and ^{59}Fe mobilization for the DFOB conjugates showed that maximal mobilization of intracellular ^{59}Fe occurred at a log$P$ value $\sim$2.3. This parameter, rather than the affinity for Fe(III), appears to influence the extent of intracellular ^{59}Fe mobilization. The low toxicity-high Fe mobilization efficacy of selected adamantane-based DFOB conjugates underscores the potential of these compounds to treat iron overload disease in patients with transfusional-dependent disorders such as β-thalassemia.

Introduction

Inheritable disorders of hemoglobin arising from monogenic defects are the most common diseases in the world, with about 7% of people estimated as carriers.[1,2] Each year, 300000−500000 children are born with severe hemoglobin disorders, which include sickle cell anemia and the thalassemias.[1] Without treatment for their anemia, these infants die in the first few years of life.[1] Patients with severe forms of β-thalassemia require lifelong blood transfusions at 2−4 weekly intervals.[3] These regular blood transfusions increase macrophage-induced heme catabolism, which releases iron into the serum. This saturates the iron transport protein, transferrin, resulting in an increased pool of nontransferrin-bound-iron (NTBI[a]).[4] Humans do not have an active iron excretion mechanism, and levels of NTBI in excess of the normal, tightly regulated Fe(III) concentrations (about 10^{-24} M) can generate reactive oxygen species (ROS) that can cause dysfunction of the heart, liver, anterior pituitary, and pancreas.[5] Therefore, β-thalassemia patients must undergo, in addition to their blood transfusions, treatment with chelating

agents that coordinate the excess iron and form complexes that are excreted via the urinary and/or fecal route.[6,7] Before the advent of chelation therapy in 1962, β-thalassemia patients maintained on prophylactic blood transfusions would die in early adulthood from complications arising from iron overload.[3]

The first-line treatment for iron overload is the mesylate salt of the trihydroxamic acid-based siderophore, desferrioxamine B (DFOB; **1**), produced by the bacterium *Streptomyces pilosus* (Figure 1).[8] Siderophores are low-molecular-weight organic compounds produced by nonpathogenic and pathogenic bacteria in response to Fe deprivation.[9−12] With poor gastrointestinal absorption and a short plasma half-life ($t_{1/2} \sim$ 12 min),[13] DFOB·mesylate is not orally active, which requires that patients are treated via subcutaneous or intravenous infusion for about 60 h per week.[3] This arduous treatment regimen has a negative impact upon the quality of life of patients. Poor compliance with chelation therapy can lead to siderotic cardiac disease, which accounts for 71% of the mortality from thalassemia.[5,14] Significant drawbacks in the efficacy of the monocationic, hydrophilic **1** (water solubility $\sim$ 0.4 M) as a chelation agent, include both its rapid clearance (reflected in the treatment regimen) and its inability to readily cross cell membranes to access intracellular iron pools.[15] The distinguishing attribute of **1**, which confers value upon its clinical use, is the very high affinity toward Fe(III), forming a stable 1:1 Fe(III):**1** hexadentate complex via the three hydroxamic acid functional groups (logβ_{110} = 30.5).[16−18] The drawbacks of **1** have prompted research efforts to find orally available iron chelating agents.[5,6,19] Two of these candidates, deferiprone (1,2-dimethyl-3-hydroxypyrid-4-one, L1 (**2**)) and

[a] Abbreviations: AdAc, adamantane-1-acetic acid; AdA, adamantane-1-carboxylic acid; L_{DX}, 4-[3,5-bis(2-hydroxyphenyl)-1,2,4-triazol-1-yl]benzoic acid (deferasirox); DFOB, desferrioxamine B; AdA_{dMe}, 3,5-dimethyladamantane-1-carboxylic acid; ESI-MS, electrospray ionization mass spectrometry; ^{59}Fe-Tf, ^{59}Fe-labeled transferrin; AdA_{OH}, 3-hydroxyadamantane-1-carboxylic acid; Dp44mT, di-2-pyridyl ketone 4,4-dimethyl-3-thiosemicarbazone; MPOAc, 4-methylphenoxyacetic acid; L_{1D}, 3-hydroxy-2-methyl-4-oxo-1-pyridineacetic acid; NTBI, nontransferrin-bound-iron; ROS, reactive oxygen species; RP-HPLC, reversed-phase high pressure liquid chromatography.
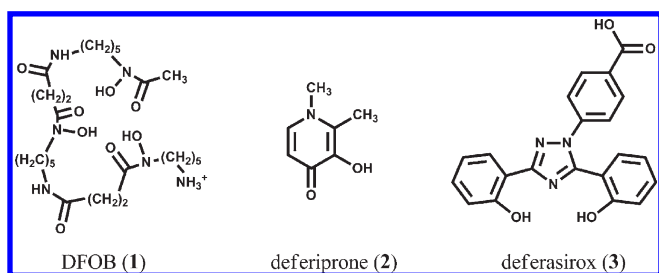
Figure 1. Schematic of the clinically used iron chelators used in this study: desferrioxamine B, DFOB (**1**); deferiprone (**2**); deferasirox (**3**).

deferasirox (4-[3,5-bis(2-hydroxyphenyl)-1,2,4-triazol-1-yl]-benzoic acid, ICL670 (**3**)) (Figure 1), both of which are orally active, have varied profiles in the clinic.[19−21]

Deferiprone (**2**) is an orally active, three-times-daily, α-ketohydroxypyridine-based bidentate iron chelator, which can remove iron from noncardiac parenchyma, macrophages, transferrin, ferritin, and hemosiderin.[19] Deferiprone is not as effective as **1** at removing Fe(III) and has toxicity issues, including agranulocytosis.[5,22,23] Its use is largely limited to the European Union as a second-line treatment for patients intolerant to **1**. Currently, **2** is not approved for use in the USA. Deferasirox (**3**) is a tridentate, one dose-per-day, orally administered iron chelator in use since 2005 in the USA, Switzerland, and Europe.[19,20] Deferasirox crosses hepatocyte and cardiac myocyte cell membranes and has shown good tolerance and safety with side effects that include mild gastro-intestinal symptoms and mild aminotransferase elevation.[24,25] The first-in-class thiazolecarboxylic acid-based iron chelator, desferrithiocin, showed good iron clearance in monkeys but was severely nephrotoxic.[26,27] The less toxic derivative, defer-itrin, showed favorable pharmacokinetics in rats, dogs, and monkeys[28] and is currently in phase II clinical trials.[19] Renal toxicity has also been observed in some patients treated with **3**.[29,30] The development of acceptable iron chelating drugs for iron overload, therefore, requires consideration of efficacy of Fe-binding, renal toxicity, and other potential side effects. Other drugs in development as iron chelators include the deferiprone derivative L1NA11,[19] hydroxypyridinone-based compounds,[31] isonicotinoyl hydrazones,[32−35] and thiosemicarbazones;[32,36−40] the latter two classes of compounds being developed principally as anticancer agents.

An alternative approach toward the design of new iron chelating compounds for the treatment of iron overload involves **1**-based semisynthesis, where ancillary compounds are appended to **1** via the free primary amine group, which itself is not involved in the Fe(III)-**1** coordination sphere.[17] In this approach, the integrity of the **1**-derived Fe(III)-binding hydroxamic acid groups of the conjugate are retained, yet the properties of the compound may be tuned as a function of the ancillary fragments. Conjugates of **1** have been previously prepared with a variety of groups appended at the amine termi-nus, including fluorophores,[41−44] ferrocene,[45] hydroxypyridi-none-, or catecholate-based ligands[46−48] and others.[49−52] Most recently, the octanol−water partition coefficients of a series of alkylated **1** compounds were determined to be 200−3900 times that of free **1** at 25 °C.[51] This may have implications for improving the ability of free **1** to traverse cell membranes to access intracellular iron stores. Starch poly-mers of **1** have also been explored as a mechanism to improve the plasma half-life and toxicity.[52] In a more general context, conjugates of hydroxamic acid-based and catechol-based

siderophores have a rich research profile as potential anti-bacterial and anticancer agents.[44,53,54]

Here, we describe the synthesis, characterization, and structure−activity relationships of seven DFOB conjugates (**4−10**, Figure 2). These studies include examination of the integrity of Fe(III)-binding using electrospray ionization mass spectrometry (ESI-MS) and reversed-phase high pressure liquid chromatography (RP-HPLC). We report the determi-nation of the log*P* values of **4−10** in the absence and presence of Fe(III) and the iron chelation efficacy of **4−10** with regard to their ability to mobilize intracellular ^{59}Fe from SK-N-MC neuroepithelioma cells and to prevent ^{59}Fe uptake from ^{59}Fe-transferrin (^{59}Fe-Tf). Furthermore, we have examined the antiproliferative activity of **4−10** in SK-N-MC cells and in a renal epithelial cell type. Together, the results indicate that selected conjugates of **1** should be further evaluated as poten-tial new agents for the treatment of iron overload disease.

Results and Discussion

Rationale for Chelator Design. Semisynthesis was used to prepare conjugates between **1** and lipophilic compounds with structures similar to those of selected orally available compounds in clinical use. Our rationale was that the favor-able properties of the ancillary fragments (oral availability, lipophilicity, low toxicity) may be conferred upon the con-jugates of **1**. We selected adamantane-1-carboxylic acid-based ancillary fragments for conjugation to **1**, with several compounds of this class in use clinically to treat influenza A (amantadine, rimantadine),[55] Parkinson's disease (amanta-dine),[56] Alzheimer's disease (memantine),[57] and pulmonary tuberculosis (N-adamantan-2-yl-N′-((2E)-3,7-dimethyl-2, 6-octadien-1-yl)-1,2-ethanediamine (SQ109)).[58] Amanta-dine, rimantadine, and memantine are orally active and are generally well tolerated by patients. Among our target com-pounds, we included conjugates between **1** and (i) 4-methyl-phenoxyacetic acid, which mimics the internal fragment of the orally available compounds rosiglitazone and pro-pranolol, (ii) 3-hydroxy-2-methyl-4-oxo-1-pyridineacetic acid, which mimics deferiprone (**2**), and (iii) deferasirox (**3**) itself.

Chemistry. 3-Hydroxy-2-methyl-4-oxo-1-pyridineacetic acid (L$_{1D}$), which is the N-acetic acid derivative of **2**, was prepared according to literature methods,[59,60] and the purity of the compound was confirmed by ^{1}H and ^{13}C NMR spectro-scopy. Seven carboxylic acid derivatives, adamantane-1-carboxylic acid (AdA), 3-hydroxyadamantane-1-carboxylic acid (AdA$_{OH}$), 3,5-dimethyladamantane-1-carboxylic acid (AdA$_{dMe}$), adamantane-1-acetic acid (AdAc), 4-methylphenoxyacetic acid (MPOAc), L$_{1D}$, or 4-[3,5-bis(2-hydroxyphenyl)-1,2,4-triazol-1-yl]-benzoic acid (L$_{DX}$, **3**), were conjugated to **1** to yield **1**-AdA (**4**), **1**-AdA$_{OH}$ (**5**), **1**-AdA$_{dMe}$ (**6**), **1**-AdAc (**7**), **1**-MPOAc (**8**), **1**-L$_{1D}$ (**9**), or **1**-L$_{DX}$ (**10**), respectively (Figure 2). Initially, **4** was prepared via the conjugation of **1** with NHS-activated adamantane-1-carboxylic acid.[61] A more streamlined synthesis of **4−10** used HOBt-based, EDC-activated con-jugation[62] (Scheme 1) and the compounds were purified to >95% using preparative RP-HPLC. Conjugation in each of **4−10** was evident from the absence in the ^{1}H NMR spectra of the amine group signal ($\delta = 2.7$ ppm) of **1** and of the CO$_2$H signal in each of AdA, AdA$_{OH}$, AdA$_{dMe}$, AdAc, MPOAc, L$_{1D}$, or **3** ($\delta \sim 11.9$ ppm). Additionally, the appearance of the signal due to the amide peak ($\delta \sim 7.3$ ppm) and of the signals assigned to the ancillary ligands confirmed conjugation.
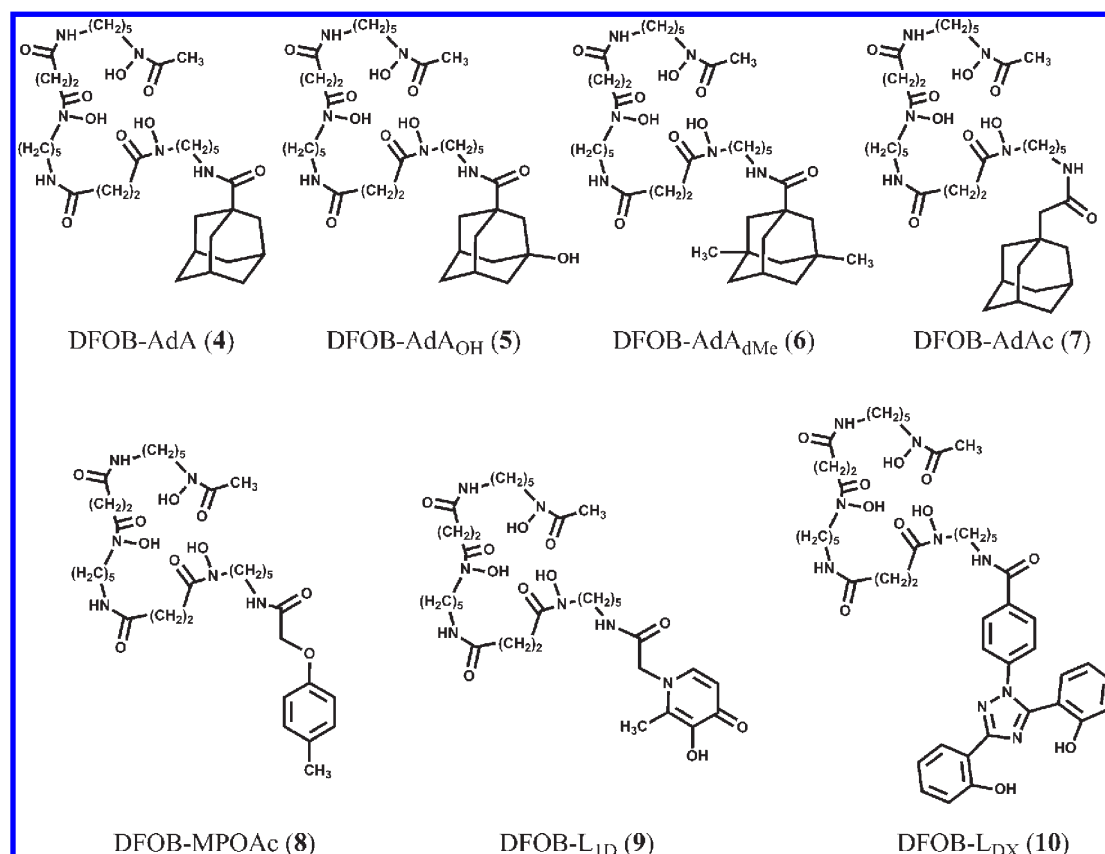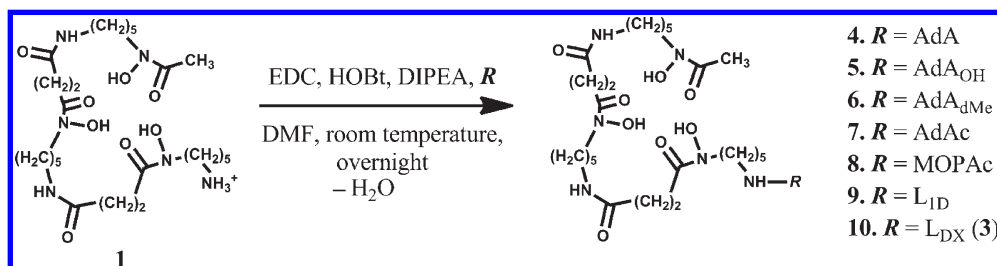
Figure 2. Schematic of the new DFOB conjugates prepared in this investigation: DFOB-AdA (**4**), DFOB-AdA$_{OH}$ (**5**), DFOB-AdA$_{dMe}$ (**6**), DFOB-AdAc (**7**), DFOB-MPOAc (**8**), DFOB-L$_{1D}$ (**9**), and DFOB-L$_{DX}$ (**10**).

Scheme 1. Synthesis of **4**−**10**

Charge of 4−10 in the Absence and Presence of Fe(III) and Fe(III)/(II) Redox Potentials. Upon the basis of the range of the pK_a values determined for the three hydroxamic acid-based protons of DFOB (pK_a 8.32−9.71)[63] and that compounds **4**−**8** have ancillary fragments with protons that will not ionize under biologically relevant conditions (as a reference point for **5**, 1-adamantanol pK_a = 18[64]), **4**−**8** will be neutral at physiological pH values. While compounds **9** and **10** have ancillary fragments with ionizable protons, the pK_a values of the hydroxyl group of **2** (pK_a = 9.75)[65,66] and of the phenolate groups of **3** (pK_a = 10.13 and 12.09)[67] prescribe that **9** and **10** will be neutral at physiological pH values. Therefore, **4**−**10** would be expected to be able to readily cross cell membranes as neutral species, which is likely to be favorable for accessing intracellular iron pools. The 1:1 complex formed between Fe(III) and the triple deprotonated DFOB fragment of **4**−**8** will also be neutral. Therefore, Fe(III)-loaded **4**−**8** are expected to exit the cell as neutral complexes. Depending upon metal:ligand stoichiometry, the charge of Fe(III)-loaded complexes of **9** and **10** may deviate

from neutral. Upon the basis of the established coordination chemistry of Fe(III) and **2**[68] or **3**,[67,69] it is likely that there will be more than one type of Fe(III)-loaded complex formed with **9** and **10**.

The negative Fe(III)/(II) redox potentials reported for [Fe(**1**(3−))]$^{+/0}$ ($E_{1/2}$ −0.48 V vs NHE at pH 7.5),[70,71] [Fe(**2**(1−))$_3$]$^{0/1−}$ ($E_{1/2}$ −0.62 to −0.54 V vs NHE)[72] and [Fe(**3**(3−))$_2$]$^{3−/4−}$ ($E_{1/2}$ −0.6 V vs NHE),[69] indicate that the Fe-loaded complexes of **4**−**10** will exist as redox stable Fe(III) complexes. Thus, it is unlikely that these complexes would engage in one-electron reduction reactions to yield the corresponding Fe(II) complexes under physiological conditions. Therefore, the possibility of the generation of ROS from Fe(II)-based Fenton reactions is unlikely for **4**−**10**. This enhances the potential for these compounds as Fe(III) chelators for iron overload rather than as iron chelators for cancer treatment.[32] The latter class of compounds, which includes di-2-pyridyl ketone 4,4-dimethyl-3-thiosemicarbazone (Dp44mT), are thought to depend upon Fe(III)/(II) redox cycling mechanisms for cytotoxicity.[32,33,36,37]

Table 1. ESI-MS Data (Positive Ion Mode) from **4−10** in the Absence and Presence of Fe(III)

compd	[M]	Fe(III) free			Fe(III) loaded		
		exp	calcd	species	exp	calcd	species
4	722.9	723.1	723.9	$[M + H^+]^+$	776.5	776.8	$[M - 3H^+ + Fe^{3+} + H^+]^+$
		745.3	745.9	$[M + Na^+]^+$	798.5	798.8	$[M - 3H^+ + Fe^{3+} + Na^+]^+$
		1467.5	1468.8	$[2 M + Na^+]^+$			
5	738.9	737.2	739.9	$[M + H^+]^+$	792.5	792.8	$[M - 3H^+ + Fe^{3+} + H^+]^+$
					814.5	814.8	$[M - 3H^+ + Fe^{3+} + Na^+]^+$
6	751.0	751.1	752.0	$[M + H^+]^+$	804.5	804.8	$[M - 3H^+ + Fe^{3+} + H^+]^+$
					826.6	826.8	$[M - 3H^+ + Fe^{3+} + Na^+]^+$
7	736.9	737.4	737.9	$[M + H^+]^+$	790.6	790.8	$[M - 3H^+ + Fe^{3+} + H^+]^+$
		759.6	759.9	$[M + Na^+]^+$	812.6	812.8	$[M - 3H^+ + Fe^{3+} + Na^+]^+$
		782.3	781.9	$[M - H^+ + 2Na^+]^+$			
8	708.8	710	709.8	$[M + H^+]^+$	762.3	762.7	$[M - 3H^+ + Fe^{3+} + H^+]^+$
		732	731.8	$[M + Na^+]^+$	784.3	784.7	$[M - 3H^+ + Fe^{3+} + Na^+]^+$
		1439.2	1440.6	$[2 M + Na^+]^+$	887.2	888.6	$[M - 3H^+ + Fe^{3+} + H^+]^+ \cdot 2NaCl \cdot 0.5H_2O$
9	725.8	727	726.8	$[M + H^+]^+$	868.1	868.9	$[M - 4H^+ + 2Fe^{3+} + Cl^-]^+$
		748.5	748.8	$[M + Na^+]^+$			
10	916.0	916.5	917.0	$[M + H^+]^+$	1022.2	1022.7	$[M - 5H^+ + 2Fe^{3+}]^+$
		938.7	939.0	$[M + Na^+]^+$			

Fe(III) Coordination. The Fe(III) coordination of **4−10** was examined using ESI-MS (Table 1), electronic absorption spectroscopy, and RP-HPLC measurements. For Fe(III)-loaded solutions of **4−7**, the dominant species in the positive ion ESI-MS formulated as the protonated ($[M - 3H^+ + Fe^{3+} + H^+]^+$) or sodiated ($[M - 3H^+ + Fe^{3+} + Na^+]^+$) form of the intrinsically uncharged species, $[M - 3H^+ + Fe^{3+}]$, in which Fe(III) was bound to the triple deprotonated **1** motif. For **8**, the $[M - 3H^+ + Fe^{3+} + H^+]^+$ and $[M - 3H^+ + Fe^{3+} + Na^+]^+$ ions were present in low abundance (both ~12%), with the major signal (100%) ascribed to $[M - 3H^+ + Fe^{3+} + H^+]^+ \cdot 2NaCl \cdot 0.5H_2O$. The Fe(III):ligand ratio of 1:1 for **4−8** determined from ESI-MS measurements was also established from Job's plots analyses. The isotope pattern of the signal at $m/z = 868.1$ for Fe(III)-loaded **9** simulated as $[M - 4H^+ + 2Fe^{3+} + Cl^-]^-$ ($[C_{33}H_{51}N_7O_{11}ClFe_2]^+$ requires 868.9). For Fe(III)-loaded **10**, the observed isotope pattern ($m/z = 1022.2$) was consistent with $[M - 5H^+ + 2Fe^{3+}]^+$ ($[C_{46}H_{56}N_9O_{11}Fe_2]^+$ requires 1022.7) (Figure 3). For **9** and **10**, which feature pendant groups with the capacity to bind iron, it is possible that species exist where the metal:ligand ratio is >1. This is evident from the ESI-MS analysis, with Fe(III):**9** or **10** = 2:1, indicating that **9** and **10** could potentially carry a greater than stoichiometric load of Fe.

Under iron saturation, Fe(III)-loaded **9** or **10** could yield $[Fe_4(9(4-))_3]$ or $[Fe_3(10(5-))_2]^-$, respectively (Figure 4). The argument against Fe(III)-saturated complexes of **9** and **10** as efficacious Fe mobilizing agents relates to the high molecular weights of each of these complexes, $[Fe_4(9(4-))_3]$ ($M_r = 2388.8$ g mol^{-1}) and $[Fe_3(10(5-))_2]^-$ ($M_r = 1989.6$ g mol^{-1}), which may impede cellular efflux. Models of Fe(III)-loaded complexes of **1−10** were built in HyperChem 7.5 using data from X-ray crystal structures of $[Fe(1(3-))]^+$,[17] 2,5-dioxo-pyrrolidin-1-yl adamantane-1-carboxylate,[61] $[Cr(2(1-))_3]$,[73] and $[Fe\{(3,5-bis(2-hydroxyphenyl)-1-phenyl-1,2,4-triazole)-(2-)\}_2]$.[69] The volumes of $[Fe_4(9(4-))_3]$ (5335 Å^3) and $[Fe_3(10(5-))_2]^-$ (4436 Å^3) were significantly greater than the volume of $[Fe(6(3-))]$ (1984 Å^3). The size and shape of the Fe(III) complex may be an important structure−activity relationship with regard to the ability of **9** and **10** to mobilize cellular Fe, although the variable stoichiometry of Fe(III):**9** or **10** complexes makes it difficult to establish such a relationship with certainty.

RP-HPLC of Compounds in the Absence and Presence of Fe(III). All compounds were purified by preparative scale RP-HPLC because the modest solubility of **4−10** in water or methanol prevented purification by recrystallization or flash chromatography. A single major peak was observed in the analytical RP-HPLC of **4−10**, which demonstrated that the purity of the compounds was >95% (Figure 5). In the presence of Fe(III), the values of the retention time (t_r) of the peaks attributable to Fe(III)-loaded **4−9** decrease (range of 0.5 min (**6**) to 2.1 min (**9**)), which indicates that the Fe(III)-loaded complexes are more water-soluble that the free ligand. This is consistent with the function of bacterial siderophores in nature to increase the aqueous solubility of Fe(III) under aerobic conditions[10] and with the decrease in log$D_{7.4}$ values for Fe(III)-loaded complexes of **1−3**, relative to the values of the respective free ligands.[74]

Two peaks eluted in the RP-HPLC trace of a solution of Fe(III)-loaded **9** (t_r 12.2 and 10.9 min). Analysis from RP-HPLC-MS (positive ion mode) showed a distribution of Fe(III)-loaded **9** species. The HPLC-MS trace from the fraction eluting at $t_r = 12.2$ min yielded signals at m/z: 390.32 (60), m/z 416.79 (1), 779.22 (100), and 1557.90 (5), corresponding to $[M - 3H^+ + Fe^{3+} + 2H^+]^{2+}$ (m/z_{calc} 390.34), $[M - 3H^+ + 2Fe^{3+} - H^+]^{2+}$ (m/z_{calc} 416.75), $[M - 3H^+ + Fe^{3+} + H^+]^+$ (m/z_{calc} 779.67), and $[M - 4H^+ + Fe^{3+} + M - H^+ + Fe^{3+}]^+$ or $[2(M - 3H^+ + Fe^{3+}) + H^+]^+$ (m/z_{calc} 1558.34), respectively. The major Fe(III)-**9** species present in the fraction eluting at $t_r = 12.2$ min occurred as 1:1 or 2:2 species. The HPLC-MS trace from the fraction eluting at $t_r = 10.9$ min yielded signals at m/z 390.32 (60), m/z 416.79 (100), 779.22 (75), 868.09 (25), and 946.04 (40). The latter two signals were unique to the peak eluting at $t_r = 10.9$ min and corresponded with $[M - 3H^+ + 2Fe^{3+} - H^+ + Cl^-]^+$ (m/z_{calc} 868.96) and $[M - 3H^+ + 2Fe^{3+} + SO_4^{2-} \cdot 0.5CH_3-OH]^+$ (m/z_{calc} 946.61). The three major Fe(III)-**9** species present in the peak eluting at $t_r = 10.9$ min occurred as 2:1 species. Therefore, the HPLC-MS analysis indicated that there was a distribution of Fe(III)-**9** species present with different Fe(III):ligand ratios with charges that may contribute a distribution coefficient (log$D$) based effect upon the t_r values in the RP-HPLC for the two groups of species. In support of this idea is the Job's plot analysis for **9**, which showed diffuse isosbestic points at 260, 310, and 370 nm,
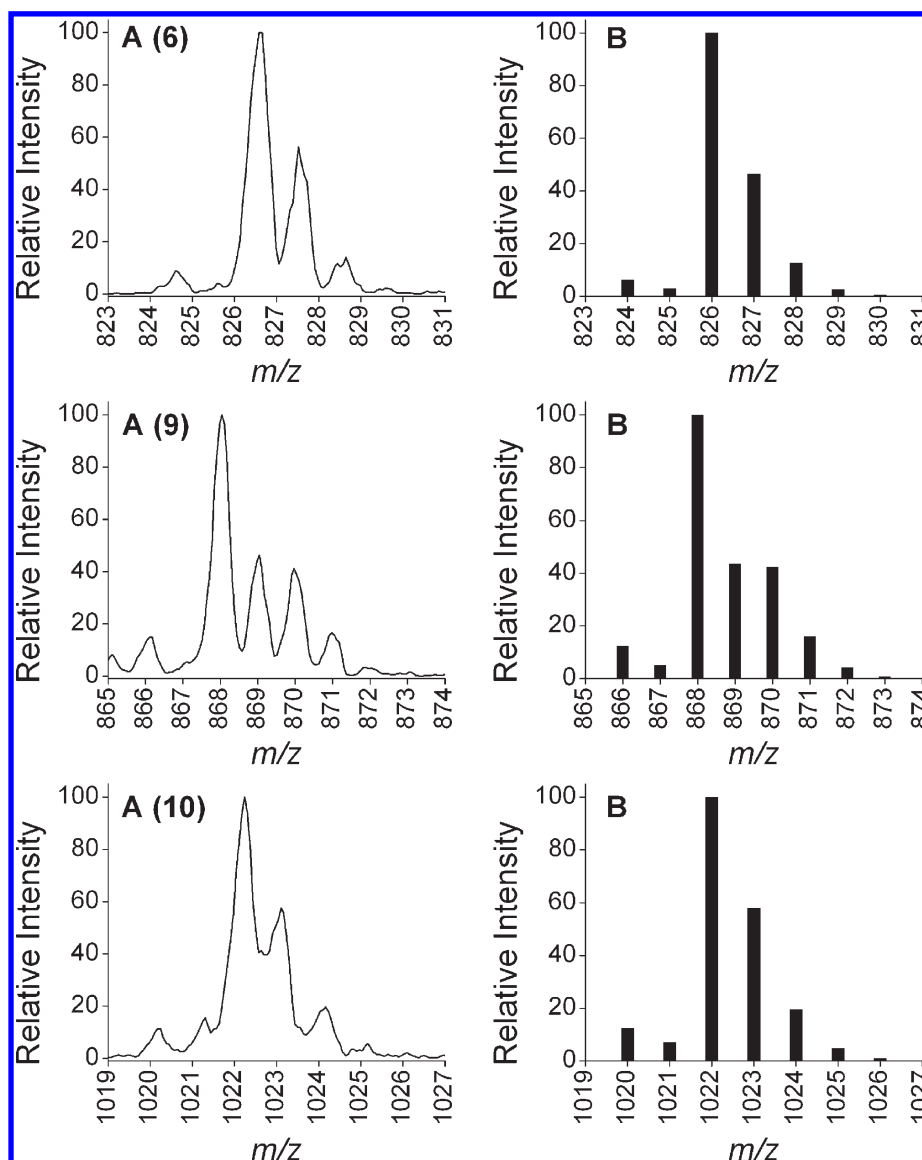
Figure 3. ESI-MS (positive ion) from Fe(III)-loaded solutions of **6**, **9**, or **10** as experiment (A) and (B) simulated. For **6**, m/z 826.6 (obs) $[M - 3H^+ + Fe^{3+} + Na^+]^+$ requires 826.8 (calcd) $[C_{38}H_{63}N_6O_9FeNa]^+$. For **9**, m/z 868.1 (obs) $[M - 4H^+ + 2Fe^{3+} + Cl^-]^+$ requires 868.9 (calcd) $[C_{33}H_{51}N_7O_{11}ClFe_2]^+$. For **10**, m/z 1022.2 (obsd) $[M - 5H^+ + 2Fe^{3+}]^+$ requires 1022.7 (calcd) $[C_{46}H_{56}N_9O_{11}Fe_2]^+$.

indicative of the presence of more than two species in solution. A distribution of species formed between Fe(III) and **2** has been detected within the limits of ESI-MS,[68] which further supports the presence of more than one species in solutions of Fe(III) and **9**.

For **10**, there was not a clear shift in the retention time of the peak ascribed to Fe(III)-loaded **10** compared to the free ligand. However, Fe(III) binding was evident from the significant change in the absorbance value of the peak of Fe(III)-loaded **10**. The absorbance value at 220 nm of an electronic absorption spectrum from a 1:1 Fe(III):**10** solution (0.1 mM) and **10** (0.1 mM) from the Job's plot analysis was 1.8 and 0.15, respectively. A similar fold difference in absorbance was observed in the RP-HPLC traces of **10** in the absence and presence of Fe(III). The phenomenon of a change in electronic absorption spectrum but not in RP-HPLC retention time for hydrophobic siderophores has been reported for those derived from bacteria.[75] The apex of the major peak from a solution of Fe(III)-loaded **10** analyzed by RP-HPLC-MS (positive-ion mode) gave a signal at

$m/z = 969.29$, which corresponded to $[M - 3H^+ + Fe^{3+} + H^+]^+$. The sloping front of the peak gave a signal at $m/z = 1022.13$, which corresponded to $[M - 5H^+ + 2Fe^{3+}]^+$, as observed in the ESI-MS experiments (Table 1). Therefore, similarly to Fe(III)-loaded **9**, there appeared to be a distribution of species of Fe(III)-loaded **10**, which accords with the complex pH-dependent species distribution previously observed for **3**.[69]

Determination of Log*P* Values of 4−10. The t_r values for **4−10** were greater than the t_r value of **1**, which is congruous with the predicted increase in the log*P* values of **4−10**, compared to **1**. The water solubility of **1** is attributable, in part, to the charged amine group at physiological pH values. The charge neutrality of **4−10**, in addition to the lipophilicity inherent to the ancillary fragments (Figure 2), would expect to yield compounds that are more lipophilic than the parent **1**. Previous work has shown this to be the case for alkylated adducts of **1**.[51]

The log*P* values of **4−10** in the absence and presence of Fe(III) were estimated using RP-HPLC (Table 2). This
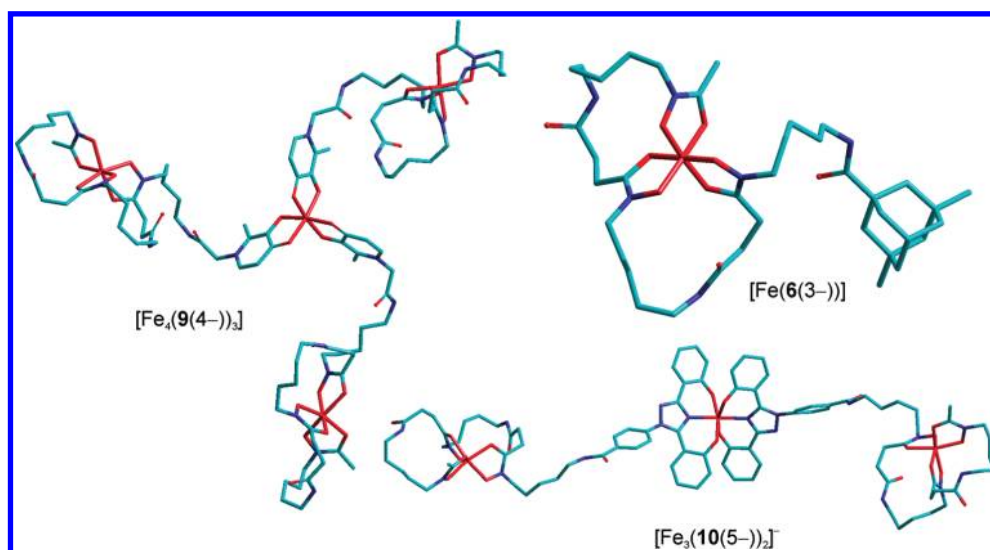
Figure 4. Models built using HyperChem 7.5 of [Fe(**6**(3−))], [Fe₄(**9**(4−))₃] and [Fe₃(**10**(5−))₂]⁻ based on data from X-ray crystal structures of related fragments.[17,61,69,73] Hydrogen atoms have been omitted for clarity.
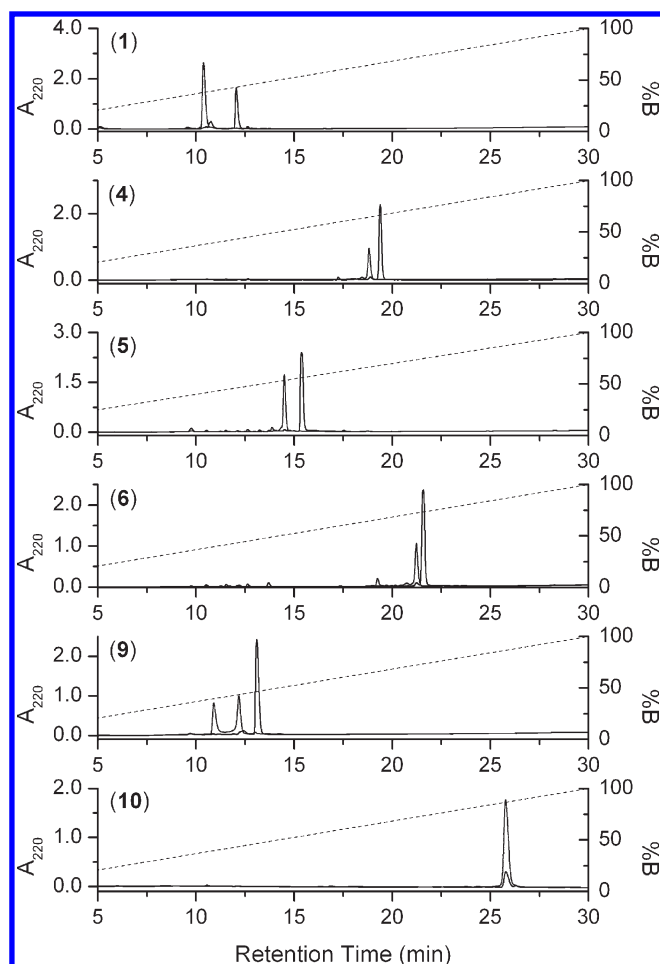

Figure 5. RP-HPLC traces of **1**, **4**, **5**, **6**, **9**, and **10** in the absence (black) or presence (gray) of Fe(III).

method is valid in this case because, under the conditions used for RP-HPLC measurements, **4−10** will be neutral and there will be no $\log D$ contribution to the $\log P$ values. For neutral, Fe(III)-loaded complexes of **4−8**, the $\log P$ values will also be valid, as determinable via RP-HPLC. However, due to the non-neutral charge on Fe(III)-loaded **9** and **10**,

$\log P$ values are not able to be calculated reliably using RP-HPLC, alongside values for **1−3** and for Fe(III)-loaded **1−3**. The t_r values for **4**, **6−8**, and **10** fell within or close to the t_r values of the four standard compounds used to generate the regression analysis.[76] For **5** and **9**, the t_r values fell outside the range of the standards, which prompted parallel determinations of $\log P$ values for **4−10** using the shake-flask method. The experimentally determined $\log P$ values for **4−10** using both RP-HPLC and shake-flask methods compared reasonably well (Table 2) and were also in broad agreement with $\log P$ values calculated using Advanced Chemistry Development Software V8.14 or for models of **4−10** that were built using HyperChem 7.5 (Table 2).

Cellular ⁵⁹Fe Mobilization. The ability of **1−10** and Dp44mT to mobilize intracellular ⁵⁹Fe from human SK-N-MC neuroepithelioma cells prelabeled with ⁵⁹Fe-Tf was examined (Figure 6A). The Fe metabolism of this cell type and the effect of a variety of chelators on this cell type is well characterized,[77,78] which underscores its choice for measuring Fe mobilization. The ability of **1** ($\log P_{(av)} = -2.1$) to induce the mobilization of intracellular ⁵⁹Fe is rather modest (12 ± 1%), relative to control medium alone (5 ± 1%; Figure 6A). This is consistent with our previous findings using this assay where DFOB·mesylate was unable to readily access intracellular iron stores over short incubation times.[77,78]

Of the four adamantane-1-carboxylic acid-based conjugates of **1**, three compounds (**4**, **6**, and **7**) were effective in increasing the mobilization of intracellular ⁵⁹Fe in comparison to free **1** by factors of 2.2, 3, and 2.8, respectively. Compound **6** increased ⁵⁹Fe release to an extent that was comparable ($p > 0.05$) to the positive controls, **3**, and Dp44mT (Figure 6A). Compound **7** showed ⁵⁹Fe mobilizing efficacy comparable ($p > 0.05$) to that of **3**. In contrast, **5** showed activity that was similar to control medium and was significantly ($p < 0.001$) less efficient as an ⁵⁹Fe mobilizing agent than **1**.

Because no major steric or electronic perturbations were made to the **1** motif of the monofunctional **1**-adamantyl adducts **4−7**, the affinities of **4−7** toward Fe(III) will be similar to the affinity between **1** and Fe(III) ($\log\beta_{110} = 30.5$).[16,17] These values, or the pFe(III) values (pFe(III) =

Table 2. LogP Values of **1−10** in the Absence and Presence of Fe(III) as Determined from RP-HPLC, the Shake-Flask Method, and from Calculation

compd	Fe(III) free						Fe(III) loaded		
	t_r (min)[b]	$LogP_{exp}$[c]	$LogP_{exp}$[d]	$LogP_{calc}$[e]	$LogP_{calc}$[f]	$LogP_{av}$	t_r (min)[b]	$LogP_{exp}$[c]	V (Å^3)
1	12.04	NC[g]	ND	−2.74	−1.45	−2.10 ± 0.91	10.40	NC	1470
2	ND[h]	ND	−1.02[i]	−0.22	−0.81	−0.68 ± 0.41	ND	ND	1155
3	25.43	NC	3.8[j]	6.43	5.18	5.14 ± 1.32	25.39	NC	1766
4	19.31	1.29	2.11	ND	1.35	1.58 ± 0.46	18.56	1.04	1903
5	15.39	−0.11	0.29	ND	0.11	0.10 ± 0.20	14.51	−0.48	1922
6	21.54	1.95	2.92	ND	2.22	2.36 ± 0.50	21.08	1.82	1984
7	19.92	1.47	2.21	ND	1.28	1.65 ± 0.49	19.38	1.31	2002
8	18.21	0.93	1.68	ND	0.80	1.14 ± 0.48	17.48	0.68	1918
9	13.04	−1.16	−1.29	ND	−0.66	−1.04 ± 0.33	10.93	NC	5335[k]
							12.23	NC	
10	25.8	3.02	2.17	ND	4.17	3.12 ± 1.00	25.8	NC	4436[l]
BDME[a]	20.02	ND	1.61[m]	1.64	1.51	1.59 ± 0.07	ND	ND	ND
BDEE[a]	24.09	ND	2.54[m]	2.70	2.19	2.48 ± 0.26	ND	ND	ND
NAPH[a]	26.99	ND	3.32	3.45	3.05	3.27 ± 0.20	ND	ND	ND
DBFN[a]	28.88	ND	4.04	4.12	3.11	3.76 ± 0.56	ND	ND	ND

[a] BDME = 1,2-benzenedicarboxylic acid 1,2-dimethyl ester; BDEE = 1,2-benzenedicarboxylic acid 1,2-diethyl ester; NAPH = naphthalene; DBFN = dibenzofuran. [b] t_o = 1.81 min. [c] Determined from RP-HPLC (multiple runs showed reproducibility; given data is from a single series of experiments). [d] Determined from shake-flask. [e] As reported as calculated using Advanced Chemistry Development Software V8.14.on SciFinder Scholar Database. [f] Calculated from models built using HyperChem 7.5. [g] NC = not calculable. [h] ND = not determined. [i] From ref 91. [j] From ref 92. [k] Modeled for Fe(III) saturated 9:Fe(III) = 3:4 complex (Figure 4). [l] Modeled for Fe(III) saturated 10:Fe(III) = 2:3 complex (Figure 4). [m] From ref 93.

$-\log[Fe(III)]$ when $[Fe(III)]_{total} = 10^{-6}$ M and $[ligand]_{total} = 10^{-5}$ M at pH 7.4; for **1**, pFe(III) = 26),[79] are not expected to differ significantly among this subgroup of compounds. Therefore, the decreased release of ^{59}Fe mediated by **5**, compared to the ^{59}Fe mobilization mediated by **4**, **6**, and **7**, suggests the efficacy of a chelator is not solely determined by the affinity toward Fe(III). In fact, multiple factors are involved in terms of optimal Fe chelation efficacy, as found for other types of ligands.[80]

Of the remaining **1** conjugates (**8**, **9**, and **10**), **8** and **10** showed significantly ($p < 0.001$) greater ^{59}Fe cellular efflux activity than **1**. The conjugate between L_{1D} and **1** (**9**) demonstrated little activity, not being significantly ($p > 0.05$) more active that control medium at mobilizing ^{59}Fe from cells. Compared to the control, the clinically used orally active chelator, L1 (**2**), also showed little ability to mobilize ^{59}Fe (Figure 6A) and was less effective than the other positive controls (**1**, **3** and Dp44mT). Previous studies using a similar protocol have demonstrated that relatively high concentrations of L1 (i.e., 0.5 mM) are necessary to induce only moderate ^{59}Fe mobilization from cells.[81] Hence, in terms of structure−activity relationships, conjugates between **1** and **2** do not appear optimal. The conjugate between **1** and **3** (**10**) showed ^{59}Fe mobilization efficacy that was significantly ($p < 0.001$) less effective than **3** alone.

An ideal iron chelating molecule for iron overload treatment should have properties that allow the compound to: (i) cross the cell membrane to access intracellular iron stores, (ii) selectively form a redox-inactive Fe(III) complex, and (iii) exit the cell as a stable, Fe(III)-loaded complex for excretion.[7,32] Criteria (i) and (iii) are described in part by the charge and the partition coefficient of the free compound and of the Fe(III)-loaded complex, respectively, and criterion (ii) is described by the thermodynamics and kinetics of Fe(III) coordination. In the case of some of the **1** conjugates (namely, **4**, **6−8**), these properties have been favorably altered in comparison to **1**. In contrast, for other conjugates such as **5** and **9**, structure−activity relationships involving properties such as relatively low logP values and/or the high molecular weight of Fe(III)-loaded complexes may explain the hindered membrane permeability and, thus, Fe chelation efficacy.

Inhibition of Cellular ^{59}Fe Uptake from ^{59}Fe-Transferrin. The ability of **1−10** or Dp44mT to prevent the internalization of ^{59}Fe from ^{59}Fe-Tf was analyzed in the human SK-N-MC neuroepithelioma cell line (Figure 6B). Generally, these results reflected those of the intracellular ^{59}Fe mobilization study (Figure 6A), demonstrating that compounds with high ^{59}Fe mobilization efficacy were also efficient at preventing the uptake of ^{59}Fe from ^{59}Fe-Tf. The ability of **1** to prevent ^{59}Fe uptake from ^{59}Fe-Tf was poor, inhibiting ^{59}Fe uptake to 87% of the control (Figure 6B), as shown in previous studies.[77,78] Of the compounds in this work, **4**, **6−8**, and **10** were significantly ($p < 0.01$) more active than **1**. Compound **6** was the most efficient compound, inhibiting ^{59}Fe uptake from ^{59}Fe-Tf to 18 ± 2% of the untreated control. This efficiency was significantly ($p < 0.001$) greater than the positive control **3**, which reduced ^{59}Fe uptake to 39 ± 2% of the control and was slightly less effective than the highly potent antitumor chelator, Dp44mT, which inhibited ^{59}Fe uptake to 12 ± 1% of the control.

In summary, examining both the Fe efflux and Fe uptake studies (Figure 6A,B), the most effective **1** conjugates in terms of Fe chelation efficacy were **4**, **6**, **7**, and **10**, with activities that are at least twice that of **1**.

Structure−Activity Relationship between LogP Values and ^{59}Fe Mobilization. A parabolic relationship is evident between the logP values of **4−10** and the cellular efflux of ^{59}Fe (Figure 7A), giving an optimal logP value of 2.3 for maximal Fe efflux. The data from **1**, **2**, and Dp44mT[36] also fit well onto this parabola, with data for **3** an outlier. Because the descending parabola is described by only one data point with a broad error margin (**10**), there is some uncertainty as to whether the relationship between the logP values and ^{59}Fe efflux is truly parabolic. However, the ascending data is populated by sufficient data points to claim at least a sigmoidal relationship between ^{59}Fe efflux and logP values < 2.3. This optimal logP value for Fe mobilization is also supported by the parabolic, or at a minimum, sigmoidal relationship, between logP and ^{59}Fe uptake from ^{59}Fe-Tf (Figure 7B). Thus, the lipophilicity of the chelator appears to be an important factor in determining the ability of the ligand to mobilize cellular Fe.
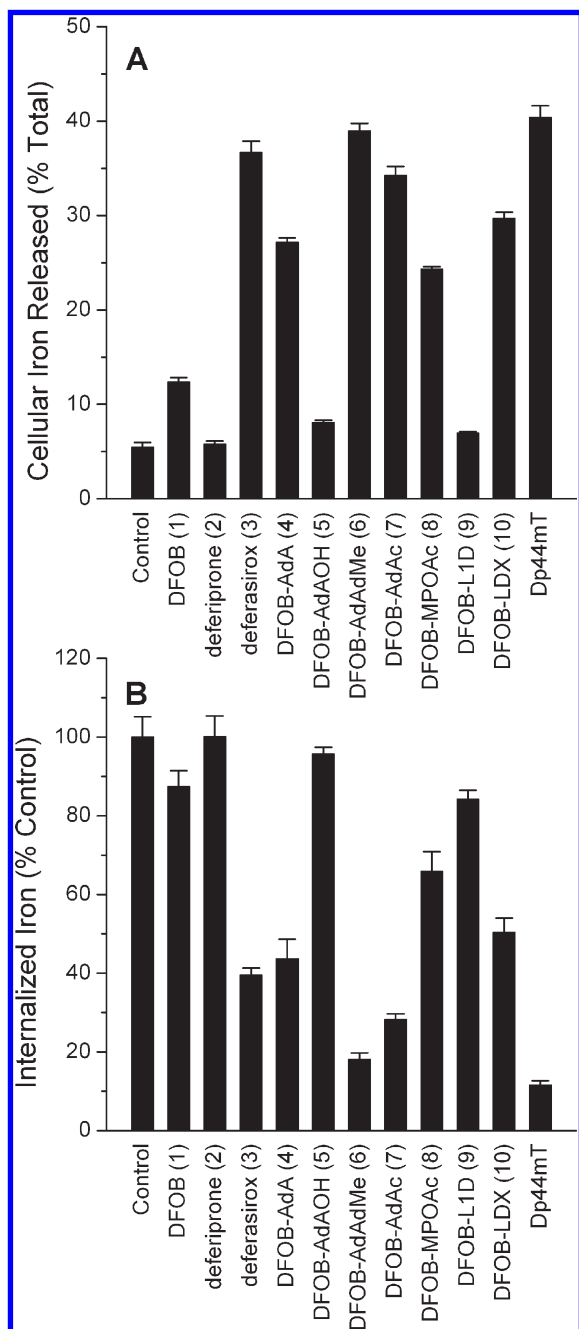
Figure 6. The effect of the new DFOB conjugates (**4−10**) in comparison with the clinically used chelators DFOB (**1**), deferiprone (**2**), deferasirox (**3**), or Dp44mT on: (A) cellular ^{59}Fe released (%) from human SK-N-MC neuroepithelioma cells prelabeled with ^{59}Fe-transferrin (^{59}Fe-Tf), or (B) ^{59}Fe uptake (% of control) from ^{59}Fe-transferrin (^{59}Fe-Tf) by SK-N-MC neuroepithelioma cells. Results are mean ± SD of three experiments with three determinations in each experiment.

Cell Viability. The ability of selected compounds from **1−10** and Dp44mT to inhibit cellular proliferation of Madin−Darby canine kidney type II (MDCK II) cells and human SK-N-MC neuroepithelioma cells was assessed using the [3-(4,5-dimethylthiazol-2-yl)-2,5-diphenyltetrazolium bromide] (MTT) assay[82] (Table 3). Compounds that are well tolerated by cells will not affect regular cellular proliferation or growth and will have high IC$_{50}$ (or LD$_{50}$) values relative to more cytotoxic compounds. The cell viability data using the human SK-N-MC neuroepithelioma cell type reflects similar
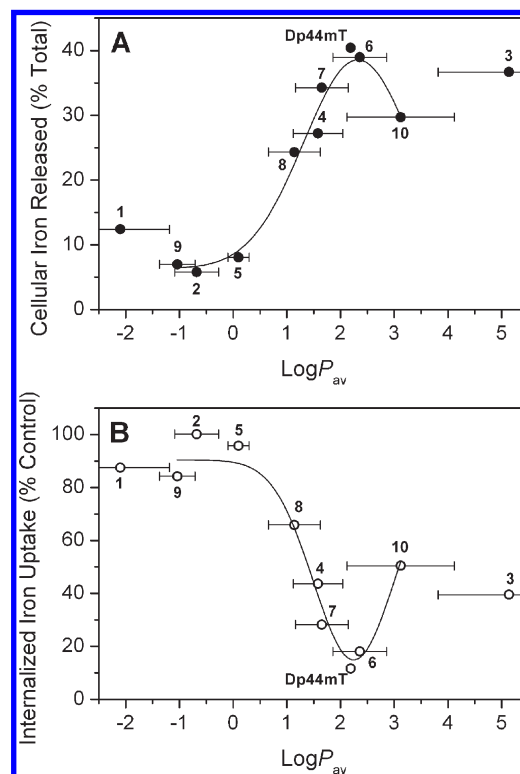

Figure 7. Log$P$ values (average of values determined by RP-HPLC, shake-flask, and calculation) of **1−10** and Dp44mT as a function of (A) cellular ^{59}Fe released (%) from human SK-N-MC neuroepithelioma cells prelabeled with ^{59}Fe-transferrin (^{59}Fe-Tf) or (B) ^{59}Fe uptake (% of control) from ^{59}Fe-transferrin (^{59}Fe-Tf) by SK-N-MC neuroepithelioma cells.

Table 3. IC$_{50}$ Values (μM) of **1−10** and Dp44mT in Madin−Darby Canine Kidney Type II (MDCK II) or in SK-N-MC Neuroepithelioma cell types

		IC$_{50}$ (μM)	
	compd	MDCK II canine kidney	SK-N-MC neuro-epithelioma
1	DFOB	9.49 ± 1.24	16.04 ± 0.47
2	deferiprone	ND^a	165.88 ± 1.90
3	deferasirox	ND^a	20.54 ± 0.56
4	DFOB-AdA	118.86 ± 1.16	174.04 ± 1.61
5	DFOB-AdA$_{OH}$	>100	>200
6	DFOB-AdA$_{dMe}$	163.37 ± 1.52	92.36 ± 1.66
7	DFOB-AdAc	225.56 ± 1.28	167.14 ± 2.82
8	DFOB-MPOAc	>150	>200
9	DFOB-L$_{1D}$	>300	>200
10	DFOB-L$_{DX}$	23.41 ± 1.53	20.62 ± 1.79
	Dp44mT	ND^a	0.01 ± 0.01

^{a} ND = not determined.

trends as observed in the MDCK II cell line. Importantly, in both cell types, all of the **1** conjugates (**4−10**) showed less cytotoxicity than **1**. Moreover, the most active **1** conjugates at mobilizing ^{59}Fe from cells and reducing cellular ^{59}Fe uptake from ^{59}Fe-Tf, namely **4**, **6**, **7**, and **10**, were significantly ($p < 0.005$) less cytotoxic than **1**, demonstrating that these compounds are highly tolerated and do not remove cellular Fe pools vital for cellular proliferation. This low antiproliferative activity is vital in the design of an iron chelator for the treatment of iron overload. The antiproliferative activity of all of the **1** conjugates are 1600 to >20000 times less effective than the known cytotoxic iron chelator, Dp44mT (IC$_{50}$ 0.01 μM; Table 3).[40] Hence, this analysis

suggests that the **1** conjugates are more appropriate for the treatment of iron overload disease rather than cancer. Finally, a recent study showed a positive correlation between the log$P$ value and toxicity of desferrithiocin analogues.[27] For **4−10**, no structure−activity relationships were evident between log$P$ and toxicity.

Conclusions

The high solubility of **1** in water, which impacts negatively on its biological activity, can be significantly reduced by conjugating an ancillary fragment to the amine group of **1** without adversely affecting the Fe(III) coordinating ability of the conjugate. This is a crucial structure−activity relationship that may be useful to exploit in the future. We conjugated to **1**: (i) polycyclic-cage based compounds (adamantane-based derivatives), which have analogues in the clinic (amantadine, rimantadine, and memantine) that are orally active and that are generally well-tolerated by patients, (ii) 4-methylphenoxyacetic acid, and (iii) a deferiprone mimic (3-hydroxy-2-methyl-4-oxo-1-pyridineacetic acid), and deferasirox itself. Given that the affinity toward Fe(III) will not vary significantly among **4−8**, the relatively poor Fe mobilization ability of **5** illustrates that Fe(III) affinity is not the sole determinant of Fe chelating efficacy. From Fe efflux and Fe uptake studies, **4**, **6**, **7**, and **10** were at least twice as active as **1** with regard to Fe chelation efficacy and were significantly less cytotoxic than **1**, as determined using two different cell types. Therefore, these compounds may have promise as compounds for the treatment of iron overload disease rather than as anticancer agents. Neurological conditions that have been associated with transition metal ion dys-homeostasis, such as Parkinson's disease, Alzheimer's disease, and Huntington's disease,[83] or other conditions that have shown benefits from treatment via Fe chelation, such as malaria,[41,84] could also be potentially targeted by this class of compounds.

Experimental Section

Chemical Studies. Chemicals. Desferrioxamine B·mesylate (DFOB, 95%), 3-hydroxy-2-methyl-4-pyrone (maltol, 99%), glycine (>99%) adamantane-1-carboxylic acid (AdA, >99%), 3-hydroxyadamantane-1-carboxylic acid (AdA$_{OH}$, 97%), 3,5-dimethyladamantane-1-carboxylic acid (AdA$_{dMe}$, 97%), adamantane-1-acetic acid (AdAc, 98%), 4-methylphenoxyacetic acid (MPOAc, 98%), N-(3-dimethylaminopropyl)-N'-ethylcarbodiimide·HCl (EDC, protein sequence grade), Fe(ClO$_4$)$_3$·H$_2$O, dimethylformamide (DMF, biotech grade), and acetonitrile (CH$_3$CN, biotech grade) were obtained from Sigma-Aldrich (St. Louis, MO). 1-Octanol (99.5% GC grade) was from Fluka (Buchs, Switzerland). N-Hydroxybenzotriazole (HOBt) was obtained from Auspep (Parkville, VIC, Australia), and 4-[3,5-bis-(2-hydroxyphenyl)-1,2,4-triazol-1-yl]benzoic acid (L$_{DX}$, deferasirox) was obtained from AmplaChem (Carmel, IN). N,N-Diisopropylethylamine (DIPEA) (99%) was purchased from Lancaster Synthesis, Inc. (Pelham, NH), and methanol (99%) was obtained from Mallinckrodt Chemicals (Phillipsburg, NJ). All chemicals and solvents were used as received.

General Instrumentation. [1]H Nuclear magnetic resonance spectra were recorded using a Bruker Avance DPX 200 (Rheinstetten, Germany) at a frequency of 200.13 MHz or a Bruker Avance DPX 300 at a frequency of 300.10 MHz. Chemical shifts are reported as parts per million (ppm) with DMSO-d_6 (δ_H = 2.50) or CD$_3$OD (δ_H 3.31) used as an internal reference. [13]C Nuclear magnetic resonance spectra were recorded using a Bruker Avance DPX 200 spectrometer at a frequency of 50.3 MHz or a Bruker Avance DPX 300 at a frequency of 75.5 MHz. Electron spray ionization mass spectra

(ESI-MS) were recorded using positive ionization on a Finnigan LCQ or a Finnigan MAT 900 XL ion trap mass spectrometer (San Jose, CA) with the following parameters. Mobile phase, methanol; flow rate, 0.30 mL min^{-1}; injection volume, 25 μL, spray voltage, 4.50 kV; capillary voltage, 35 V; capillary temperature, 210 °C; tube lens-offset, 10 V. Analytical thin layer chromatography (TLC) was performed using precoated silica gel plates (Sigma-Aldrich), which were eluted with MeOH: CHCl$_3$ = 1:3 and visualized using solid iodine or by dipping the plate into an ethanolic solution of FeCl$_3$ (60 mM). Reversed-phase high pressure liquid chromatography (RP-HPLC) used a Waters system (Milford, MA) consisting of a GBC 1460 degasser, a Rheodyne 7725i injector (analytical 20 μL loop, preparative 1700 μL loop) (Apple Valley, MN), a Waters 486 tunable absorbance detector, and a Waters Empower 2 software with Waters Sunfire C18 columns (particle size 5 μm, column dimension 4.6 mm × 150 mm i.d. (analytical), or particle size 5 μm, column dimension 19 mm × 150 mm i.d. (preparative)) and a flow rate of 0.2 mL/min (analytical) or 7.0 mL/min (preparative), with a mobile phase of water (0.1% TFA, solvent A) and acetonitrile (0.1% TFA, solvent B). HPLC-MS was conducted on a Thermo Separation system with a ThermoQuest Finnigan LCQ Deca mass spectrometer (San Jose, CA, USA).

General Procedure. 3-Hydroxy-2-methyl-4-oxo-1-pyridineacetic acid (L$_{1D}$) was synthesized according to the literature[59,60] from an aqueous solution (75 mL) of glycine (30 g, 400 mmol), maltol (12.7 g, 100 mmol), and NaOH (11 g, 275 mmol), which was reacted at 35 °C for 5 d. The solution was acidifed with 5 M HCl (4 mL) and was refrigerated for 2 h to yield a cream colored residue, which was filtered and washed with cold water. The solid product was redissolved in basic aqueous solution (pH 10.8) using 2 M NaOH (20 mL) and was acidified with 5 M HCl (4 mL) to give L$_{1D}$ as a pale-white solid (3.28 g, 18%). ^{1}H NMR (300 MHz, DMSO-d_6) δ_H: 7.3 (1H, s, OH), 2.1 (3H, s, CH), 1.9 (6H, s, CH$_2$), 1.7 (6H, s, CH$_2$).

Compounds **4−10** were prepared based upon a literature bioconjugation method[62] from a solution of DMF (10 mL) containing AdA, AdA$_{OH}$, AdA$_{dMe}$, AdAc, MPOAc, L$_{1D}$, or **3** (1 mmol), EDC (1.5 mmol), **1** (1 mmol), and HOBt (0.19 g, 1.5 mmol), which was heated to 45 °C. After the reagents had dissolved, DIPEA (2 mmol) was added to the solution and the mixture was stirred overnight at room temperature under nitrogen. The solution was evaporated to dryness in vacuo and the solid residue was washed with diethylether (3 mL) and distilled water (3 mL) before redissolving the solid in methanol and removing the solvent under reduced pressure. The progress of all syntheses was monitored using TLC. Compounds **4−10** were not sufficiently soluble in water or methanol to enable purification using either recrystallization or flash chromatography and were, therefore, purified to >95% purity, using preparative RP-HPLC. This level of purity was confirmed by CHN microanalysis.

DFOB-AdA (4). The residue was triturated with diethylether (5 × 5 mL), recrystallized from methanol and purified by preparative RP-HPLC (90:10 (A:B) to 25:75 (A:B) over 30 min) to give **4** as a off-white solid (0.56 g, 70%). Solubility in ethanol (25 °C): 28 mg mL^{-1} (~38 mM). ^{1}H NMR (300 MHz, DMSO-d_6) δ_H: 9.6 (2H, m, NH), 7.7 (3H, s, OH), 7.3 (1H, s, NH), 3.4 (6H, t, J = 9 Hz, CH$_2$), 3.0 (4H, q, J = 6 Hz, CH$_2$), 2.6 (4H, t, J = 6 Hz, CH$_2$), 2.3 (4H, t, J = 6 Hz, CH$_2$), 1.9 (3H, s, CH$_3$), 1.7 (3H, s, CH), 1.6 (12H, m, CH$_2$), 1.1−1.5 (18H, m, CH$_2$). ^{13}C NMR (300 MHz, DMSO-d_6) δ_C: 177.1, 172.3, 171.6, 47.5, 47.2, 36.5, 30.3, 29.2, 28.0, 27.9, 26.4, 23.9, 23.8, 20.7. MS: m/z ESI (positive ion). Found [M + H$^+$]$^+$ 723.07 (98), [M + Na$^+$]$^+$ 745.27 (100), [C$_{36}$H$_{62}$N$_6$O$_9$Na]$^+$ requires 745.91. MeOH (320 nm), ε = 18.27 M^{-1} cm^{-1}. Anal. Calcd for C$_{36}$H$_{62}$N$_6$O$_9$: C, 59.81% H; 8.64%; N, 11.63%. Found: C, 57.44% H; 7.50%; N, 11.15%.

DFOB-AdA$_{OH}$ (5). The residue was triturated with diethylether (5 × 5 mL), recrystallized from methanol and purified by RP-HPLC (90:10 (A:B) to 25:75 (A:B) over 30 min) to give **5** as

an off-white solid (0.45 g, 61%). Solubility in ethanol (25 °C): 15.2 mg mL^{-1} (~20 mM). Solubility in water (25 °C): 5 mg mL^{-1} (~6.5 mM). ^{1}H NMR (300 MHz, DMSO-d_6) δ_H: 9.6 (2H, m, NH), 7.7 (3H, s, OH), 7.3 (1H, s, NH), 3.4 (6H, t, J = 9 Hz, CH$_2$), 3.2 (1H, s, OH), 3.0 (4H, q, J = 6 Hz, CH$_2$), 2.6 (4H, t, J = 6 Hz, CH$_2$), 2.3 (4H, t, J = 6 Hz, CH$_2$), 1.9 (3H, s, CH$_3$), 1.7 (2H, s, CH), 1.5–1.6 (12H, m, CH$_2$), 1.2–1.5 (18H, m, CH$_2$). ^{13}C NMR (300 MHz, DMSO-d_6) δ_C: 176.3, 171.7, 67.0, 56.4, 47.2, 44.7, 38.2, 31.0, 30.3, 29.2, 27.9, 26.4, 23.9, 23.8, 20.7. MS: m/z ESI (positive ion). Found [M + H$^+$]$^+$ 737.20 (100), [C$_{36}$H$_{63}$N$_6$O$_{10}$]$^+$ requires 739.92. MeOH (320 nm), ε = 49.74 M^{-1} cm^{-1}. Anal. Calcd for C$_{36}$H$_{62}$N$_6$O$_{10}$: C, 58.51% H; 8.46%; N, 11.38%. Found: C, 56.88% H; 8.21%; N, 10.92%.

DFOB-AdA$_{dMe}$ (6). The residue was triturated with diethylether (5 × 5 mL), recrystallized from methanol, and purified by RP-HPLC (90:10 (A:B) to 40:60 (A:B) over 30 min) to give **6** as an off-white solid (0.57 g, 80%). Solubility in ethanol (25 °C): 15 mg mL^{-1} (~20 mM). ^{1}H NMR (300 MHz, DMSO-d_6) δ_H: 9.6 (2H, m, NH), 7.7 (3H, s, OH), 7.3 (1H, s, NH), 3.4 (6H, t, J = 15 Hz, CH$_2$), 3.0 (4H, q, J = 6 Hz, CH$_2$), 2.6 (4H, t, J = 9 Hz, CH$_2$), 2.3 (4H, t, J = 6 Hz, CH$_2$), 1.9 (3H, s, CH$_3$), 1.6–1.1 (31H, m, CH$_2$, CH), 0.8 (6H, s, CH$_3$). ^{13}C NMR (300 MHz, d_6-DMSO) δ_C: 176.8, 172.3, 171.7, 50.7, 45.4, 42.8, 37.8, 31.1, 28.2, 27.9, 26.4, 23.9, 23.8, 20.7. MS: m/z ESI (positive ion). Found [M + H$^+$]$^+$ 751.13 (100), [C$_{38}$H$_{67}$N$_6$O$_9$]$^+$ requires 751.98. MeOH (320 nm), ε = 32.17 M^{-1} cm^{-1}. Anal. Calcd for C$_{38}$H$_{66}$N$_6$O$_9$: C, 60.77% H; 8.86%; N, 11.19%. Found: C, 58.85% H; 8.04%; N, 10.71%.

DFOB-AdAc (7). The residue was triturated with diethylether (5 × 5 mL), recrystallized from methanol, and purified by RP-HPLC (90:10 (A:B) to 25:75 (A:B) over 30 min) to give **7** as an off-white solid (0.55 g, 80%). Solubility in ethanol (25 °C): 15 mg mL^{-1} (~20 mM). ^{1}H NMR (300 MHz, DMSO-d_6) δ_H: 9.6 (2H, m, NH), 7.7 (3H, s, OH), 7.3 (1H, s, NH), 3.4 (6H, t, J = 6 Hz, CH$_2$), 3.0 (4H, q, J = 6 Hz, CH$_2$), 2.6 (4H, t, J = 6 Hz, CH$_2$), 2.3 (4H, t, J = 6 Hz, CH$_2$), 1.9 (3H, s, CH$_3$), 1.8 (2H, s, CH$_2$), 1.7 (3H, s, CH), 1.5–1.6 (12H, m, CH$_2$), 1.0–1.5 (18H, m, CH$_2$). ^{13}C NMR (300 MHz, d_6-DMSO) δ_C: 171.6, 170.1, 50.4, 42.5, 36.8, 30.2, 29.2, 28.4, 27.9, 26.4, 23.9, 20.7. MS: m/z ESI (positive ion). Found [M + H$^+$]$^+$ 737.44 (100), [C$_{37}$H$_{65}$N$_6$O$_9$]$^+$ requires 737.95. MeOH (320 nm), ε = 16.53 M^{-1} cm^{-1}. Anal. Calcd for C$_{37}$H$_{64}$N$_6$O$_9$: C, 60.30% H; 8.75%; N, 11.41%. Found: C, 58.37% H; 8.53%; N, 11.72%.

DFOB-MPOAc (8). The residue was triturated with diethylether (5 × 5 mL), recrystallized from methanol, and purified by RP-HPLC (90:10 (A:B) to 40:60 (A:B) over 30 min) to give **8** as an off-white solid (0.23 g, 73%). ^{1}H NMR (200 MHz, DMSO-d_6) δ_H: 7.1 (2H, d, J = 7.1 Hz, CH), 6.8 (2H, d, J = 7.0 Hz, CH), 4.4 (2H, s, CH$_2$), 3.5 (6H, t, J = 6.8 Hz, CH$_2$), 3.0 (4H, m, CH$_2$), 2.5 (4H, m, CH$_2$), 2.3 (4H, m, CH$_2$), 2.2 (3H, s, CH$_3$), 1.9 (3H, s, CH$_3$), 1.3–1.5 (12H, m, CH$_2$), 1.2 (6H, m, CH$_2$). ^{13}C NMR (200 MHz, DMSO-d_6) δ_C: 21.1, 21.4, 24.5, 27.1, 28.5, 29.8, 31.0, 47.8, 48.2, 68.2, 115.6, 130.8, 156.7, 168.6, 172.3, 173.0. MS: m/z ESI (positive ion). Found [M + Na$^+$]$^+$ 731.7 (100), [C$_{34}$H$_{56}$N$_6$O$_{10}$Na]$^+$ requires 731.40. MeOH (320 nm), ε = 101.63 M^{-1} cm^{-1}. Anal. Calcd for C$_{34}$H$_{56}$N$_6$O$_{10}$: C, 57.61% H; 7.96%; N, 11.86%. Found: C, 56.60% H; 7.31%; N, 11.73%.

DFOB-L$_{1D}$ (9). The residue was triturated with diethylether (5 × 5 mL), recrystallized from methanol, and purified by RP-HPLC (95:5 (A:B) to 40:60 (A:B) over 30 min) to give **9** as a very pale-pink solid (0.11 g, 70%). ^{1}H NMR (300 MHz, CD$_3$OD) δ_H: 8.2 (1H, d, J = 7.0 Hz, CH), 7.2 (1H, d, J = 7.0 Hz, CH), 5.2 (2H, s, CH$_2$), 3.6 (6H, t, J = 5.6 Hz, CH$_2$), 3.2 (4H, t, J = 6.9 Hz, CH$_2$), 2.8 (4H, t, J = 6.8 Hz, CH$_2$), 2.5 (4H, t, J = 7.0 Hz, CH$_2$), 2.1 (3H, s, CH$_3$), 1.5–1.7 (12H, m, CH$_2$), 1.3–1.4 (6H, m, CH$_2$), (OH not observed). ^{13}C NMR (300 MHz, CD$_3$OD) δ_C: 19.2, 23.$\overline{9}$, 26.2, 26.3, 27.9, 28.8, 28.9, 30.4, 39.3, 39.7, 48.9, 58.0, 113.1, 139.8, 142.8, 143.9, 159.7, 165.6, 172.5, 173.5, 173.9. MS: m/z ESI (positive ion). Found [M + H$^+$]$^+$ 726.6 (65), [M + Na$^+$]$^+$ 748.7 (100), [C$_{46}$H$_{61}$N$_9$O$_{11}$Na]$^+$ requires 748.8. MeOH

(320 nm), ε = 99.6 M^{-1} cm^{-1}. Anal. Calcd for C$_{33}$H$_{55}$N$_7$O$_{11}$·2H$_2$O: C, 52.02% H; 7.81%; N, 12.87%. Found: C, 49.69% H; 6.42%; N, 11.93%.

DFOB-L$_{DX}$ (10). The residue was triturated with diethylether (5 × 5 mL), recrystallized from methanol, and purified by RP-HPLC (95:5 (A:B) to 45:55 (A:B) over 30 min) to give **10** as an off-white solid (0.14 g, 65%). ^{1}H NMR (200 MHz, CD$_3$OD) δ_H: 8.2 (2H, d, J = 6.9 Hz, CH), 7.9 (2H, d, J = 6.5 Hz, CH), 7.6 (2H, d, J = 6.8 Hz, CH), 7.4 (2H, m, CH), 6.9–7.0 (4H, m, CH), 3.6 (6H, t, J = 6.8 Hz, CH$_2$), 3.2 (4H, m, CH$_2$), 2.8 (4H, m, CH$_2$), 2.4 (4H, m, CH$_2$), 2.1 (3H, s, CH$_3$), 1.6–1.7 (8H, m, CH$_2$), 1.5 (4H, m, CH$_2$), 1.3 (6H, m, CH$_2$), (OH not observed). ^{13}C NMR (200 MHz, CD$_3$OD) δ_C: 19.2, 23.7, $\overline{2}$3.9, 26.3, 27.9, 29.0, 30.5, 39.2, 39.9, 44.7, 116.3, 119.6, 119.8, 123.8, 127.2, 128.3, 130.9, 131.4, 133.5, 141.5, 157.2, 160.1, 173.2, 173.5. MS: m/z ESI (positive ion). Found [M + H$^+$]$^+$ 916.5 (85), [M + Na$^+$]$^+$ 938.7 (100), [C$_{46}$H$_{61}$N$_9$O$_{11}$Na]$^+$ requires 939.03. MeOH (320 nm), ε = 3.127 × 10^3 M^{-1} cm^{-1}. Anal. Calcd for C$_{46}$H$_{61}$N$_9$O$_{11}$: C, 60.31% H; 6.91%; N, 13.76%. Found: C, 59.40% H; 5.63%; N, 13.38%.

Extinction Coefficients and Job's Plot Analysis. A plot of absorbance/path length (cm^{-1}) at 320 nm vs concentration (M) in methanol of **4**−**10** was measured using a SpectraMax M5/M5^e UV−vis (Molecular Devices, Sunnyvale, CA) and the slope of the line determined as ε (M^{-1} cm^{-1}). Job's Plots analyses were carried out for **4**−**10**, as detailed in the literature,[85] with compounds (0.1 mM) dissolved in a solution of 20% (v/v) MeOH in Tris·HCl (100 mM, pH 7.4) and the pH value of the solution adjusted to pH 7.4 prior to making the solution to volume. A stock solution of Fe(III) (0.1 mM) was prepared from FeCl$_3$·6H$_2$O in a similar fashion to the compounds (20% v/v MeOH in 100 mM Tris, pH 7.4). Molar ratios of Fe:compound were 0, 0.1, 0.2, 0.3, 0.4, 0.5, 0.6, 0.7, 0.8, 0.9, and 1, with 0 containing no iron and 1 containing no ligand. All samples had a final concentration ([Fe(III)] + [ligand]) of 0.1 mM and electronic absorption spectra were acquired from 200 to 800 nm, with the absorbance value of 450 nm absorbance used to construct the Job's plot.

Fe(III)-Loading of 4−10 for ESI-MS and RP-HPLC. An aliquot of a freshly prepared methanolic solution of FeCl$_3$·6H$_2$O (100 μL of 10 mM) was added to an aliquot (100 μL of 10 mM) of **4**−**8** in methanol. For **9** and **10**, the volume ratio of FeCl$_3$·6H$_2$O:compound was 150:50 μL.

Partition Coefficients. Analytical RP-HPLC was used to estimate the log of the partition coefficients (log$P$) of **4**−**10**. Samples (5 mM) of **4**−**10** in MeOH (HPLC grade) were filtered (0.22 μm) and analyzed by analytical RP-HPLC, together with a set of compounds with known log$P$ values (1,2-benzenedicarboxylic acid dimethylester (log$P$ = 1.59), 1,2-benzenedicarboxylic acid diethylester (log$P$ = 2.48), naphthalene (log$P$ = 3.27), and dibenzofuran (log$P$ = 3.76)). The capacity factor (k) was determined for the samples using eq 1, where t_r was the retention time of the compound and t_o was the deadtime (t_o = 1.81 min). The log of the partition coefficient (log$P$) was calculated according to eq 2.[76]

$$k = (t_r - t_o)/t_o \qquad (1)$$

$$\log k = a + b \log P \qquad (2)$$

Partition coefficients were also determined using the shake-flask method with presaturated 1-octanol and water solutions as follows. An aliquot (1 mL) of water was added to an aliquot of 1-octanol containing dissolved **4**−**10** (1 or 2 mg) in a glass vial, and the mixture was shaken overnight at RT. Aliquots (20 μL) of each phase were analyzed by analytical RP-HPLC using the conditions described above.

Molecular Modeling. Models were built in HyperChem 7.5 using data from X-ray crystal structures of [Fe(**1**(3−))]$^+$,[17] 2,5-dioxopyrrolidin-1-yl adamantane-1-carboxylate,[61] [Cr(**2**(1−))$_3$],[73] and [Fe{(3,5-bis(2-hydroxyphenyl)-1-phenyl-1,2,4-triazole)(2−)}$_2$].[69] The structure of the organic ancillary fragment was minimized

using the Polak-Ribiere algorithm and the MM+ force field and the structure of the Fe(III)-loaded ligand was frozen. No conformational searching procedure was used.

Biological Studies. Cell Culture. The human SK-N-MC neuroepithelioma and Madin−Darby canine kidney type II (MDCK II) cell lines were obtained from the American Type Culture Collection (ATCC; Manassas, VA). The SK-N-MC cell type was grown as described previously,[77] while MDCK II cells were cultured by standard procedures.[86]

^{59}Fe-Transferrin Labeling. Human transferrin (Tf) was labeled with ^{59}Fe (Dupont NEN, MA) to produced ^{59}Fe$_2$-Tf (^{59}Fe-Tf), as previously described.[87,88]

^{59}Fe Efflux from SK-N-MC Neuroepithelioma Cells. Efflux of ^{59}Fe from SK-N-MC neuroepithelioma cells were measured for **1−10** and for Dp44mT at concentrations of 50 μM using established techniques.[38,77,89] Briefly, following prelabeling of cells with ^{59}Fe-Tf (0.75 μM) for 3 h at 37 °C, the cell cultures were washed four times with ice-cold PBS and then subsequently incubated with each chelator (50 μM) for 3 h at 37 °C. The overlying media containing released ^{59}Fe was then separated from the cells using a Pasteur pipet. Radioactivity was measured in both the cell pellet and supernatant using a γ-scintillation counter (Wallac Wizard 3, Turku, Finland). In these studies, the new ligands were compared to the previously characterized chelators, **1, 2, 3**, and Dp44mT.

Effect of 1−10 at Preventing ^{59}Fe Uptake from Transferrin by SK-N-MC Neuroepithelioma Cells. The uptake of ^{59}Fe from ^{59}Fe-labeled transferrin was measured for **1−10** and for Dp44mT at concentrations of 50 μM in SK-N-MC neuroepithelioma cells using standard techniques.[38,77,89] Briefly, cells were incubated with ^{59}Fe-Tf (0.75 μM) for 3 h at 37 °C in the presence of each of the chelators (50 μM). The cells were then washed four times with ice-cold PBS and internalized ^{59}Fe was determined by standard techniques by incubating the cell monolayer for 30 min at 4 °C with the general protease Pronase (1 mg/mL; Sigma).[87,88] The cells were removed from the monolayer using a plastic spatula and centrifuged for 1 min at 14000 rpm. The supernatant represents membrane-bound, Pronase-sensitive ^{59}Fe that was released by the protease, while the Pronase-insensitive fraction represents internalized ^{59}Fe. The new ligands were compared to the previously characterized chelators, **1, 2, 3**, and Dp44mT.

Effect of 1−10 on Cell Viability. This was examined in Madin−Darby canine kidney type II (MDCK II) cells and in human SK-N-MC neuroepithelioma cells using the MTT assay by standard methods.[77,82,90] MTT color formation was directly proportional to the number of viable cells measured by Trypan blue staining (SK-N-MC)[77] or total cell protein (MDCK II).[86]

Statistical Analysis. Experimental data were compared using Student's *t*-test. Results were expressed as mean or mean ± SD (number of experiments) and considered to be statistically significant when $p < 0.05$.

References

(1) Weatherall, D.; Akinyanju, O.; Fucharoen, S.; Olivieri, N.; Musgrove, P. Inherited Disorders of Hemoglobin. In *Disease Control Priorities in Developing Countries*, 2nd ed.; Jamison, D. T., Breman, J. G., Measham, A. R., Alleyne, G., Claeson, M., Evans, D. B., Jha, P., Mills, A., Musgrove, P., Eds.; Oxford University Press: New York, 2006; pp 663−680.

(2) Weatherall, D. J.; Clegg, J. B. Inherited Haemoglobin Disorders: An Increasing Global Health Problem. *Bull. WHO* **2001**, *79*, 704–712.

(3) Nick, H. Iron Chelation, Quo Vadis? *Curr. Opin. Chem. Biol.* **2007**, *11*, 419–423.

(4) Hershko, C.; Link, G.; Konijn, A. M. Iron Chelation. In *Molecular and Cellular Iron Transport*; Templeton, D. M., Ed.; Marcel Dekker, Inc.: New York, 2002; pp 787−816.

(5) Barton, J. C. Chelation Therapy for Iron Overload. *Curr. Gastroenterol. Rep.* **2007**, *9*, 74–82.

(6) Bernhardt, P. V. Coordination Chemistry and Biology of Chelators for the Treatment of Iron Overload Disorders. *Dalton Trans.* **2007**, 3214–3220.

(7) Kalinowski, D. S.; Richardson, D. R. The Evolution of Iron Chelators for the Treatment of Iron Overload Disease and Cancer. *Pharmacol. Rev.* **2005**, *57*, 547–583.

(8) Bickel, H.; Bosshardt, R.; Gäumann, E.; Reusser, P.; Vischer, E.; Voser, W.; Wettstein, A.; Zähner, H. Metabolic Products of Actinomycetaceae. XXVI. Isolation and Properties of Ferrioxamines A to F, Representing New Sideramine Compounds. *Helv. Chim. Acta* **1960**, *43*, 2118–2128.

(9) Stintzi, A.; Barnes, C.; Xu, J.; Raymond, K. N. Microbial Iron Transport via a Siderophore Shuttle: A Membrane Ion Transport Paradigm. *Proc. Natl. Acad. Sci. U.S.A.* **2000**, *97*, 10691–10696.

(10) Butler, A. Marine Siderophores and Microbial Iron Mobilization. *BioMetals* **2005**, *18*, 369–374.

(11) Drechsel, H.; Winkelmann, G. Iron Chelation and Siderophores. In *Transition Metals in Microbial Metabolism*; Winkelmann, G., Carrano, C. J., Eds.; Harwood Academic: Amsterdam, 1997; pp 1−49.

(12) Braich, N.; Codd, R. Immobilized Metal Affinity Chromatography for the Capture of Hydroxamate-Containing Siderophores and Other Fe(III)-binding Metabolites from Bacterial Culture Supernatants. *Analyst* **2008**, *133*, 877–880.

(13) Porter, J. B.; Rafique, R.; Srichairatanakool, S.; Davis, B. A.; Shah, F. T.; Hair, T.; Evans, P. Recent Insights into Interactions of Deferoxamine with Cellular and Plasma Iron Pools: Implications for Clinical Use. *Ann. N.Y. Acad. Sci.* **2005**, *1054*, 155–168.

(14) Glickstein, H.; Ben El, R.; Link, G.; Breuer, W.; Konjin, A. M.; Hershko, C.; Nick, H.; Cabantchik, Z. Action of Chelators in Iron-Loaded Cardiac Cells: Accessibility to Intracellular Labile Iron and Functional Consequences. *Blood* **2006**, *108*, 3195–3203.

(15) Olivieri, N. F.; Brittenham, G. M. Iron-Chelating Therapy and the Treatment of Thalassemia. *Blood* **1997**, *89*, 739–761.

(16) Konetschny-Rapp, S.; Jung, G.; Raymond, K. N.; Meiwes, J.; Zaehner, H. Solution Thermodynamics of The Ferric Complexes of New Desferrioxamine Siderophores Obtained by Directed Fermentation. *J. Am. Chem. Soc.* **1992**, *114*, 2224–2230.

(17) Dhungana, S.; White, P. S.; Crumbliss, A. L. Crystal Structure of Ferrioxamine B: A Comparative Analysis and Implications for Molecular Recognition. *J. Biol. Inorg. Chem.* **2001**, *6*, 810–818.

(18) Codd, R. Traversing the Coordination Chemistry and Chemical Biology of Hydroxamic Acids. *Coord. Chem. Rev.* **2008**, *252*, 1387–1408.

(19) Cappellini, M. D.; Pattoneri, P. Oral Iron Chelators. *Annu. Rev. Med.* **2009**, *60*, 25–38.

(20) Scott, L. E.; Orvig, C. Medicinal Inorganic Chemistry Approaches to Passivation and Removal of Aberrant Metal Ions in Disease. *Chem. Rev.* **2009**, *109*, 4885–4910.

(21) Kontoghiorghes, G. J.; Pattichis, K.; Neocleous, K.; Kolnagou, A. The Design and Development of Deferiprone (L1) and Other Iron Chelators for Clinical Use: Targeting Methods and Application Prospects. *Curr. Med. Chem.* **2004**, *11*, 2161–2183.

(22) Olivieri, N. F.; Brittenham, G. M.; McLaren, C. E.; Templeton, D. M.; Cameron, R. G.; McClelland, R. A.; Burt, A. D.; Fleming, K. A. Long-Term Safety and Effectiveness of Iron-Chelation Therapy with Deferiprone for Thalassemia Major. *N. Engl. J. Med.* **1998**, *339*, 417–423.

(23) Hoffbrand, A. V.; Al-Refaie, F.; Davis, B.; Siritanakatkul, N.; Jackson, B. F. A.; Cochrane, J.; Prescott, E.; Wonke, B. Long-term Trial of Deferiprone in 51 Transfusion-Dependent Iron Overloaded Patients. *Blood* **1998**, *91*, 295–300.

(24) Hershko, C. Oral Iron Chelators: New Opportunities and New Dilemmas. *Haematologica* **2006**, *91*, 1307–1312.

(25) Hershko, C.; Konijn, A. M.; Nick, H. P.; Breuer, W.; Cabantchik, Z. I.; Link, G. ICL670A: A New Synthetic Oral Chelator: Evaluation in Hypertransfused Rats with Selective Radioiron Probes of Hepatocellular and Reticuloendothelial Iron Stores and in Iron-Loaded Rat Heart Cells in Culture. *Blood* **2001**, *97*, 1115–1122.

(26) Bergeron, R. J.; Streiff, R. R.; Creary, E. A.; Daniels, R. D., Jr.; King, W.; Luchetta, G.; Wiegand, J.; Moerker, T.; Peter, H. H. A. A Comparative Study of the Iron-Clearing Properties of Desferrithiocin Analogues with Desferrioxamine B in a *Cebus* Monkey Model. *Blood* **1993**, *81*, 2166–2173.

(27) Bergeron, R. J.; Wiegand, J.; McManis, J. S.; Vinson, J. R. T.; Yao, H.; Bharti, N.; Rocca, J. R. (*S*)-4,5-Dihydro-2-(2-hydroxy-4-hydroxyphenyl)-4-methyl-4-thiazolecarboxylic Acid Polyethers: A Solution to Nephrotoxicity. *J. Med. Chem.* **2006**, *49*, 2772–2783.

(28) Donovan, J. M.; Plone, M.; Dagher, R.; Bree, M.; Marquis, J. Preclinical and Clinical Development of Deferitrin, A Novel, Orally Available Iron Chelator. *Ann. N.Y. Acad. Sci.* **2005**, *1054*, 492–494.

(29) Brosnahan, G.; Gokden, N.; Swaminathan, S. Acute Interstitial Nephritis due to Deferasirox: A Case Report. *Nephrol. Dial. Transplant.* **2008**, *23*, 3356–3358.

(30) Kontoghiorghes, G. J. Deferasirox: Uncertain Future Following Renal Failure Fatalities, Agranulocytosis and Other Toxicities. *Expert Opin. Drug Saf.* **2007**, *6*, 235–239.

(31) Turcot, I.; Stintzi, A.; Xu, J.; Raymond, K. N. Fast Biological Iron Chelators: Kinetics of Iron Removal from Human Diferric Transferrin by Multidentate Hydroxypyridonate. *J. Biol. Inorg. Chem.* **2000**, *5*, 634–641.

(32) Kalinowski, D. S.; Richardson, D. R. Future of Toxicology—Iron Chelators and Differing Modes of Action and Toxicity: The Changing Face of Iron Chelation Therapy. *Chem. Res. Toxicol.* **2007**, *20*, 715–720.

(33) Kalinowski, D. S.; Sharpe, P. C.; Bernhardt, P. V.; Richardson, D. R. Structure—Activity Relationships of Novel Iron Chelators for the Treatment of Iron Overload Disease: The Methyl Pyrazinylketone Isonicotinoyl Hydrazone Series. *J. Med. Chem.* **2008**, *51*, 331–344.

(34) Bernhardt, P. V.; Chin, P.; Sharpe, P. C.; Richardson, D. R. Hydrazone Chelators for the Treatment of Iron Overload Disorders: Iron Coordination Chemistry and Biological Activity. *Dalton Trans.* **2007**, 3232–3244.

(35) Bernhardt, P. V.; Wilson, G. J.; Sharpe, P. C.; Kalinowski, D. S.; Richardson, D. R. Tuning the Antiproliferative Activity of Biologically Active Iron Chelators: Characterization of the Coordination Chemistry and Biological Efficacy of 2-Acetylpyridine and 2-Benzoylpyridine Hydrazone Ligands. *J. Biol. Inorg. Chem.* **2008**, *13*, 107–119.

(36) Richardson, D. R.; Sharpe, P. C.; Lovejoy, D. B.; Senaratne, D.; Kalinowski, D. S.; Islam, M.; Bernhardt, P. V. Dipyridyl Thiosemicarbazone Chelators with Potent and Selective Antitumor Activity Form Iron Complexes with Redox Activity. *J. Med. Chem.* **2006**, *49*, 6510–6521.

(37) Bernhardt, P. V.; Sharpe, P. C.; Islam, M.; Lovejoy, D. B.; Kalinowski, D. S.; Richardson, D. R. Iron Chelators of the Dipyridylketone Thiosemicarbazone Class: Precomplexation and Transmetalation Effects on Anticancer Activity. *J. Med. Chem.* **2009**, *52*, 407–415.

(38) Kalinowski, D. S.; Sharpe, P. C.; Bernhardt, P. V.; Richardson, D. R. Design, Synthesis, and Characterization of New Iron Chelators with Anti-Proliferative Activity: Structure—Activity Relationships of Novel Thiohydrazone Analogues. *J. Med. Chem.* **2007**, *50*, 6212–6225.

(39) Richardson, D. R.; Kalinowski, D. S.; Richardson, V.; Sharpe, P. C.; Lovejoy, D. B.; Islam, M.; Bernhardt, P. V. 2-Acetylpyridine Thiosemicarbazones are Potent Iron Chelators and Antiproliferatuve Agents: Redox Activity, Iron Complexation and Characterization of their Antitumor Activity. *J. Med. Chem.* **2009**, *52*, 1459–1470.

(40) Whitnall, M.; Howard, J. B.; Ponka, P.; Richardson, D. R. A Class of Iron Chelators with a Wide Spectrum of Potent Antitumor Activity that Overcomes Resistance to Chemotherapeutics. *Proc. Natl. Acad. Sci. U.S.A.* **2006**, *103*, 14901–14906.

(41) Loyevsky, M.; Lytton, S. D.; Mester, B.; Libman, J.; Shanzer, A.; Cabantchik, Z. I. The Antimalarial Action of Desferal Involves a Direct Access Route to Erythrocytic (*Plasmodium falciparum*) Parasites. *J. Clin. Invest.* **1993**, *91*, 218–224.

(42) Palanché, T.; Marmolle, F.; Abdallah, M. A.; Shanzer, A.; Albrecht-Gary, A.-M. Fluorescent Siderophore-Based Chemosensors: Iron(III) Quantitiative Determinations. *J. Biol. Inorg. Chem.* **1999**, *4*, 188–198.

(43) Ghosh, M.; Lambert, L. J.; Huber, P. W.; Miller, M. J. Synthesis, Bioactivity, and DNA-Cleaving Ability of Desferrioxamine B-Nalidixic Acid and Anthraquinone Carboxylic Acid Conjugates. *Bioorg. Med. Chem. Lett.* **1995**, *5*, 2337–2340.

(44) Diarra, M. S.; Lavoie, M. C.; Jacques, M.; Darwish, I.; Dolence, E. K.; Dolence, J. A.; Ghosh, A.; Ghosh, M.; Miller, M. J.; Malouin, F. Species Selectivity of New Siderophore-Drug Conjugates that use Specific Iron Uptake for Entry into Bacteria. *Antimicrob. Agents Chemother.* **1996**, *40*, 2610–2617.

(45) Moggia, F.; Brisset, H.; Fages, F.; Chaix, C.; Mandrand, B.; Dias, M.; Levillain, E. Design, Synthesis and Redox Properties of Two Ferrocene-Containing Iron Chelators. *Tetrahedron Lett.* **2006**, *47*, 3371–3374.

(46) Hou, Z.; Whisenhunt, D. W. J.; Xu, J.; Raymond, K. N. Potentiometric, Spectrophotometric, and ¹H NMR Study or Four Desferrioxamine B Derivatives and Their Ferric Complexes. *J. Am. Chem. Soc.* **1994**, *116*, 840–846.

(47) Rodgers, S. J.; Raymond, K. N. Ferric Ion Sequestering Agents. 11. Synthesis and Kinetics of Iron Removal from Transferrin of Catechoyl Derivatives of Desferrioxamine B. *J. Med. Chem.* **1983**, *26*, 439–442.

(48) White, D. L.; Durbin, P. W.; Jeung, N.; Raymond, K. N. Specific Sequestering Agents from the Actinites. 16. Synthesis and Initial Biological Testing of Polydentate Oxohydroxypyridinecarboxylate Ligands. *J. Med. Chem.* **1988**, *31*, 11–18.

(49) Laub, R.; Schneider, Y. J.; Octave, J. N.; Trouet, A.; Crichton, R. R. Cellular Pharmacology of Deferrioxamine B and Derivatives in Cultured Rat Hepatocytes in Relation to Iron Mobilization. *Biochem. Pharmacol.* **1985**, *34*, 1175–1183.

(50) Rosebrough, S. F. Plasma Stability and Pharmacokinetics of Radiolabeled Deferoxamine-Biotin Derivatives. *J. Pharmacol. Exp. Ther.* **1993**, *265*, 408–415.

(51) Ihnat, P. M.; Vennerstrom, J. L.; Robinson, D. H. Synthesis and Solution Properties of Deferoxamine Amides. *J. Pharmaceut. Sci.* **2000**, *89*, 1525–1536.

(52) Hallaway, P. E.; Eaton, J. W.; Panter, S. S.; Hedlund, B. E. Modulation of Deferoxamine Toxicity and Clearance by Covalent Attachment to Biocompatible Polymers. *Proc. Natl. Acad. Sci. U.S.A.* **1989**, *86*, 10108–10112.

(53) Miller, M. J.; Zhu, H.; Xu, Y.; Wu, C.; Walz, A. J.; Vergne, A.; Roosenberg, J. M.; Moraski, G.; Minnick, A. A.; McKee-Dolence, J.; Hu, J.; Fennell, K.; Dolence, E. K.; Dong, L.; Franzblau, S.; Malouin, F.; Mollmann, U. Utilization of Microbial Iron Assimilation Processes for the Development of New Antibiotics and Inspiration for the Design of New Anticancer Agents. *BioMetals* **2009**, *22*, 61–75.

(54) Roosenberg, J. M. I.; Lin, Y.-M.; Lu, Y.; Miller, M. J. Studies and Syntheses of Siderophores, Microbial Iron Chelators, and Analogs as Potential Drug Delivery Agents. *Curr. Med. Chem.* **2000**, *7*, 159–197.

(55) Stouffer, A. L.; Acharya, R.; Salom, D.; Levine, A. S.; Di Costanzo, L.; Soto, C. S.; Tereshko, V.; Nanda, V.; Stayrook, S.; De Grado, W. F. Structural Basis for the Function and Inhibition of an Influenza Virus Proton Channel. *Nature* **2008**, *451*, 596–599.

(56) Moresco, R. M.; Volonte, M. A.; Messa, C.; Gobbo, C.; Galli, L.; Carpinelli, A.; Rizzo, G.; Panzacchi, A.; Franceschi, M.; Fazio, F. New Perspectives on Neurochemical Effects of Amantadine in the Brain of Parkinsonian Patients: A PET—[¹¹C]Raclopride Study. *J. Neural Transm.* **2002**, *109*, 1265–1274.

(57) De Felice, F. G.; Velasco, P. T.; Lambert, M. P.; Viola, K.; Fernandez, S. J.; Ferreira, S. T.; Klein, W. L. Aβ Oligomers Induce Neuronal Oxidative Stress through an *N*-Methyl-D-aspartate Receptor-dependent Mechanism That Is Blocked by the Alzheimer Drug Memantine. *J. Biol. Chem.* **2007**, *282*, 11590–11601.

(58) Jia, L.; Tomaszewski, J. E.; Hanrahan, C.; Coward, L.; Noker, P.; Gorman, G.; Nikonenko, B.; Protopopova, M. Pharmacodynamics and Pharmacokinetics of SQ109, a New Diamine-Based Antitubercular Drug. *Br. J. Pharmacol.* **2005**, *144*, 80–87.

(59) Zhang, Z.; Rettig, S. J.; Orvig, C. Physical and Structural Studies of *N*-Carboxymethyl- and *N*-(*p*-Methoxyphenyl)-3-hydroxy-2-methyl-4-pyridinone. *Can. J. Chem.* **1992**, *70*, 763–770.

(60) Kruck, T. P. A.; Burrow, T. E. Synthesis of Feralex A Novel Aluminum/Iron Chelating Compound. *J. Inorg. Biochem.* **2002**, *88*, 19–24.

(61) Liu, J.; Clegg, J. K.; Codd, R. 2,5-Dioxopyrrolidin-1-yl Adamantane-1-carboxylate. *Acta Crystallogr., Sect. E: Struct. Rep. Online* **2009**, *65*, o1740–o1741.

(62) Lau, J.; Behrens, C.; Sidelmann, U. G.; Knudsen, L. B.; Lundt, B.; Sams, C.; Ynddal, L.; Brand, C. L.; Pridal, L.; Ling, A.; Kiel, D.; Plewe, M.; Shi, S.; Madsen, P. New β-Alanine Derivatives are Orally Available Glucagon Receptor Antagonists. *J. Med. Chem.* **2007**, *50*, 113–128.

(63) Boukhalfa, H.; Reilly, S. D.; Neu, M. P. Complexation of Pu(IV) with the Natural Siderophore Desferrioxamine B and the Redox Properties of Pu(IV)(siderophore) Complexes. *Inorg. Chem.* **2007**, *46*, 1018–1026.

(64) Sinha, A.; Lopez, L. P. H.; Schrock, R. R.; Hock, A. S.; Müller, P. Reactions of M(*N*-2—6-*i*-Pr₂C₆H₃)(CHR)(CH₂R')₂ (M = Mo, W) Complexes with Alcohols To Give Olefin Metathesis Catalysts of

the Type M(*N*-2,6-*i*-Pr$_2$C$_6$H$_3$)(CHR)(CH2R')(OR"). *Organometallics* **2006**, *25*, 1412–1423.

(65) Clarke, E. T.; Martell, A. E. Stabilities of 1,2-Dimethyl-3-hydroxy-4-pyridinone Chelates of Divalent and Trivalent Metal Ions. *Inorg. Chim. Acta* **1992**, *191*, 57–63.

(66) Santos, M. A.; Gama, S.; Pessoa, J. C.; Oliveira, M. C.; Toth, I.; Farkas, E. Complexation of Molybdenum(VI) with Bis(3-hydroxy-4-pyridinone)amino Acid Derivatives. *Eur. J. Inorg. Chem.* **2007**, 1728–1737.

(67) Heinz, U.; Hegetschweiler, K.; Acklin, P.; Faller, B.; Lattmann, R.; Schnebli, H. P. 4-[3,5-Bis(2-hydroxyphenyl)-1,2,4-triazole-1-yl]-benzoic Acid: A Novel Efficient and Selective Iron(III) Complexing Agent. *Angew. Chem., Int. Ed.* **1999**, *38*, 2568–2570.

(68) Devanur, L. D.; Neubert, H.; Hider, R. C. The Fenton Activity of Iron(III) in the Presence of Deferiprone. *J. Pharm. Sci.* **2008**, *97*, 1454–1467.

(69) Steinhauser, S.; Heinz, U.; Bartholomä, M.; Weyhermüller, T.; Nick, H.; Hegetschweiler, K. Complex Formation of ICL670 and Related Ligands with Fe^{III} and Fe^{II}. *Eur. J. Inorg. Chem.* **2004**, 4177–4192.

(70) Fontecave, M.; Pierre, J. L. Activation and Toxicity of Oxygen. 2. Iron and Hydrogen Peroxide: Biochemical Aspects. *Bull. Soc. Chim. Fr.* **1993**, *130*, 77–85.

(71) Spasojevic, I.; Armstrong, S. K.; Brickman, T. J.; Crumbliss, A. L. Electrochemical Behavior of the Fe(III) Complexes of the Cyclic Hydroxamate Siderophores Alcaligin and Desferrioxamine E. *Inorg. Chem.* **1999**, *38*, 449–454.

(72) Merkofer, M.; Kissner, R.; Hider, R. C.; Koppenol, W. H. Redox Properties of the Iron Complexes of Orally Active Iron Chelators CP20, CP502, CP509, and ICL670. *Helv. Chim. Acta* **2004**, *87*, 3021–3034.

(73) Hsieh, W.-Y.; Liu, S. Synthesis and Characterization of Cr(III) Complexes with 3-Hydroxy-4-Pyrones and 1,2-Dimethyl-3-Hydroxy-4-Pyridinone (DMHP): X-Ray Crystal Structures of Cr(DMHP)$_3$·12H$_2$O and Cr(ma)$_3$. *Synth. React. Inorg., Met.-Org., Nano-Met. Chem.* **2005**, *35*, 61–70.

(74) Huang, X.-P.; Spino, M.; Thiessen, J. J. Transport Kinetics of Iron Chelators and Their Chelates in Caco-2 Cells. *Pharm. Res.* **2006**, *23*, 280–290.

(75) Pakchung, A. A. H.; Soe, C. Z.; Codd, R. Studies of Iron-Uptake Mechanisms in Two Bacterial Species of the *Shewanella* Genus Adapted to Middle-Range (*Shewanella putrefaciens*) or Antarctic (*Shewanella gelidimarina*) Temperatures. *Chem. Biodiversity* **2008**, *5*, 2113–2123.

(76) Yamagami, C.; Ogura, T.; Takao, N. Hydrophobicity Parameters Determined by Reversed-phase Liquid Chromatography. *J. Chromatogr.* **1990**, *514*, 123–136.

(77) Richardson, D. R.; Tran, E. H.; Ponka, P. The Potential of Iron Chelators of the Pyridoxal Isonicotinoyl Hydrazone Class as Effective Antiproliferative Agents. *Blood* **1995**, *86*, 4295–4306.

(78) Richardson, D. R.; Ponka, P. The Iron Metabolism of the Human Neuroblastoma Cell: Lack of Relationship Between the Efficacy of Iron Chelation and the Inhibition of DNA Synthesis. *J. Lab. Clin. Med.* **1994**, *124*, 660–671.

(79) Liu, Z. D.; Hider, R. C. Design of Clinically Useful Iron(III)-Selective Chelators. *Med. Res. Rev.* **2001**, *22*, 26–64.

(80) Baker, E.; Richardson, D.; Gross, S.; Ponka, P. Evaluation of the Iron Chelation Potential of Hydrazones of Pyridoxal, Salicylaldehyde and 2-Hydroxy-1-naphthylaldehyde Using the Hepatocyte in Culture. *Hepatology* **1992**, *15*, 492–501.

(81) Richardson, D. R.; Baker, E. Two Saturable Mechanisms of Iron Uptake From Transferrin in Human Melanoma Cells: The Effects of Transferrin Concentration, Chelators, and Metabolic Probes on Transferrin and Iron Uptake. *J. Cell. Physiol.* **1994**, *161*, 160–168.

(82) Mosmann, T. Rapid Colorimetric Assay for Cellular Growth and Survival: Application to Proliferation and Cytotoxicity Assays. *J. Immunol. Methods* **1983**, *65*, 55–63.

(83) Zecca, L.; Youdim, M. B.; Riederer, P.; Connor, J. R.; Crichton, R. R. Iron, Brain Ageing and Neurodegenerative Disorders. *Nat. Rev. Neurochem.* **2004**, *5*, 863–873.

(84) Mabeza, G. F.; Loyevsky, M.; Gordeuk, V. R.; Weiss, G. Iron Chelation Therapy for Malaria: A Review. *Pharmacol. Ther.* **1999**, *81*, 53–75.

(85) Bergeron, R. J.; Weigand, J.; Weimar, W. R.; Vinson, J. R. T.; Bussenius, J.; Yao, G. W.; McManis, J. S. Desazadesmethyldesferrithiocin Analogues as Orally Effective Iron Chelators. *J. Med. Chem.* **1999**, *42*, 95–108.

(86) Parry, S. N.; Ellis, N.; Li, Z.; Maitz, P.; Witting, P. K. Myoglobin Induces Oxidative Stress and Decreases Endocytosis and Monolayer Permissiveness in Cultured Kidney Epithelial Cells without Affecting Viability. *Kidney Blood Press. Res.* **2008**, *31*, 16–28.

(87) Richardson, D. R.; Baker, E. The Uptake of Iron and Transferrin by the Human Malignant Melanoma Cell. *Biochim. Biophys. Acta* **1990**, *1053*, 1–12.

(88) Richardson, D. R.; Baker, E. Intermediate Steps in Cellular Iron Uptake from Transferrin. Detection of a Cytoplasmic Pool of Iron, Free of Transferrin. *J. Biol. Chem.* **1992**, *267*, 21384–21389.

(89) Kalinowski, D. S.; Yu, Y.; Sharpe, P. C.; Islam, M.; Liao, Y.-T.; Lovejoy, D. B.; Kumar, N.; Bernhardt, P. V.; Richardson, D. R. Design, Synthesis, and Characterization of Novel Iron Chelators: Structure−Activity Relationships of the 2-Benzoylpyridine Thiosemicarbazone Series and Their 3-Nitrobenzoyl Analogues as Potent Antitumor Agents. *J. Med. Chem.* **2007**, *50*, 3716–3729.

(90) Richardson, D. R.; Milnes, K. The Potential of Iron Chelators of the Pyridoxal Isonicotinoyl Hydrazone Class as Effective Antiproliferative Agents II: The Mechanism of Action of Ligands Derived from Salicylaldehyde Benzoyl Hydrazone and 2-Hydroxy-1-Naphthylaldehyde Benzoyl Hydrazone. *Blood* **1997**, *89*, 3025–3038.

(91) Yokel, R. A.; Datta, A. K.; Jackson, E. G. Evaluation of Potential Aluminum Chelators in Vitro by Aluminum Solubilization Ability, Aluminum Mobilization from Transferrin and the Octanol/Aqueous Distribution of the Chelators and Their Complexes with Aluminum. *J. Pharmacol. Exp. Ther.* **1991**, *257*, 100–106.

(92) Nick, H. P.; Acklin, P.; Faller, B.; Jin, Y.; Lattman, R.; Rouan, M.-C.; Sergejew, T.; Thomas, H.; Wiegand, H.; Schnebli, H. P. A New, Potent, Orally Active Iron Chelator. In *Iron Chelators: New Development Strategies*; Badman, D. G., Bergeron, R. J., Brittenham, G. M., Eds.; The Saratoga Group: Ponte Vedra Beach, FL, 2000; pp 311−331.

(93) Kotowska, U.; Garbowska, K.; Isidorov, V. A. Distribution Coefficients of Phthalates Between Absorption Fiber and Water and its Use in Quantitative Analysis. *Anal. Chim. Acta* **2006**, *560*, 110–117.

4   Publication 2

Comparing the potential renal protective activity of desferrioxamine B and the novel chelator desferrioxamine B-N-(3-hydroxyadamant-1-yl)carboxamide in a cell model of myoglobinuria

Der Vergleich der Wirkung von Desferrioxamin B und dem neuen Eisenchelator Desferrioxamin B-N-(3-hydroxyadamant-1-yl)carboxamid zum Schutz der Niere in einem *in vitro*-Modell von Myoglobinurie

4.1   Abstract (German Translation)

Die Akkumulation von Mb (Myoglobin) in der Niere als Folge schwerer Verbrennung fördert oxidativen Schaden und Entzündung, was zu akutem Nierenversagen führt. Die Vermutung, dass Häm-Eisen oxidativen Schaden verursacht, hat dazu geführt, Eisenchelatoren [z.B. DFOB (desferrioxamin B)] auf ihre Wirkung zu testen, die Niere vor diesem Schaden zu schützen. Es wurde die Eigenschaft von DFOB und einem DFOB-Derivat {DFOB-AdA$_{OH}$ [DFOB-*N*-(3-hydroxyadamant-1-yl)carboxamid]} verglichen, Nierenepithelzellen vor Mb zu schützen. Epithelzellen aus dem Nierentubulus wurden mit Dihydrorhodamin-123 geladen und mit 100 µM Mb inkubiert. Mb erhöhte die Rhodamin-123-Fluoreszenz im Vergleich zur Kontrolle (kein Mb), was auf erhöhten oxidativen Stress hindeutet. Extrazelluläres Mb führte zu einer Reorganisation des Transferrinrezeptors, was durch Verwendung von markiertem Transferrin und mit Hilfe der Durchflusszytometrie und Fluoreszensmikroskopie gezeigt werden konnte. Mb stimulierte die Genexpression von HO-1 (Hämoxygenase-1), TNFα (Tumornekrosefaktor α), und sowohl ICAM (intrazelluläres Adhäsionsmolekül) als auch VCAM (vaskuläres Adhäsionsmolekül) und verringerte die Permeabilität von einschichtigem Epithel. Die Inkubation mit DFOB oder DFOB-AdA$_{OH}$ verminderte die Mb-vermittelte Rhodamine-123-Fluoreszenz, Genexpression von HO-1, ICAM und TNFα und stellte die Permeabilität des einschichtigen Epithels wieder her. Die Sekretion des entzündungsfördernen Chemokins MCP-1 erhöhte sich in Zellen, die Mb ausgesetzt waren und dies wurde von

DFOB und DFOB-AdA$_{OH}$ aufgehoben. Zellen, die nur mit DFOB oder DFOB-AdA$_{OH}$ behandelt wurden zeigten keine Veränderung in der Permeabilität, MCP-1-Sekretion oder Genexpression von HO-1, TNFα, ICAM oder VCAM. Ähnlich wie bei DFOB konnten nach Inkubation von DFOB-AdA$_{OH}$ mit Mb und H$_2$O$_2$ mittels EPR-Spektroskopie Nitroxidradikale ermittelt werden, was auf eine potentielle antioxidative Aktivität zusätzlich zur Eisenchelation hindeutet: mit Fe(III) geladenes DFOB-AdA$_{OH}$ zeigte keine Formation eines Nitroxidradikals. Zusammengefasst verringerten die Chelatoren Mb-induzierten oxidativen Stress, hemmten Entzündungsprozesse und verbesserten die Funktion von Epithelzellen. DFOB-AdA$_{OH}$ zeigte ähnliche Eigenschaften wie DFOB, womit dieser neue, geringtoxische Chelator die Niere vor akutem Nierenversagen nach Verbrennungen schützen könnte.

4.2   Original Publication
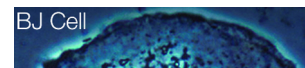
Comparing the potential renal protective activity of desferrioxamine B and the novel chelator desferrioxamine B-*N*-(3-hydroxyadamant-1-yl)carboxamide in a cell model of myoglobinuria

Ludwig K. GROEBLER*, Joe LIU†, Anu SHANU*, Rachel CODD† and Paul K. WITTING*[1]

*Discipline of Pathology, Redox Biology Group and Bosch Institute, The University of Sydney, Sydney, NSW 2006, Australia, and †Discipline of Pharmacology and Bosch Institute, The University of Sydney, Sydney, NSW 2006, Australia

Accumulating Mb (myoglobin) in the kidney following severe burns promotes oxidative damage and inflammation, which leads to acute renal failure. The potential for haem–iron to induce oxidative damage has prompted testing of iron chelators [e.g. DFOB (desferrioxamine B)] as renal protective agents. We compared the ability of DFOB and a DFOB-derivative {DFOB-AdA$_{OH}$ [DFOB-*N*-(3-hydroxyadamant-1-yl)carboxamide]} to protect renal epithelial cells from Mb insult. Loading kidney-tubule epithelial cells with dihydrorhodamine-123 before exposure to 100 μM Mb increased rhodamine-123 fluorescence relative to controls (absence of Mb), indicating increased oxidative stress. Extracellular Mb elicited a reorganization of the transferrin receptor as assessed by monitoring labelled transferrin uptake with flow cytometry and inverted fluorescence microscopy. Mb stimulated *HO-1* (haem oxygenase-1), *TNFα* (tumour necrosis factor α), and both *ICAM* (intercellular adhesion molecule) and *VCAM* (vascular cell adhesion molecule) gene expression and inhibited epithelial monolayer permeability. Pre-treatment with DFOB or DFOB-AdA$_{OH}$ decreased Mb-

mediated rhodamine-123 fluorescence, *HO-1*, *ICAM* and *TNFα* gene expression and restored monolayer permeability. MCP-1 (monocyte chemotactic protein 1) secretion increased in cells exposed to Mb-insult and this was abrogated by DFOB or DFOB-AdA$_{OH}$. Cells treated with DFOB or DFOB-AdA$_{OH}$ alone showed no change in permeability, MCP-1 secretion or *HO-1*, *TNFα*, *ICAM* or *VCAM* gene expression. Similarly to DFOB, incubation of DFOB-AdA$_{OH}$ with Mb plus H$_2$O$_2$ yielded nitroxide radicals as detected by EPR spectroscopy, indicating a potential antioxidant activity in addition to metal chelation; Fe(III)-loaded DFOB-AdA$_{OH}$ showed no nitroxide radical formation. Overall, the chelators inhibited Mb-induced oxidative stress and inflammation and improved epithelial cell function. DFOB-AdA$_{OH}$ showed similar activity to DFOB, indicating that this novel low-toxicity chelator may protect the kidney after severe burns.

Key words: acute renal failure, antioxidant, burn, metal chelation therapy, myoglobinuria, oxidative stress.

INTRODUCTION

In the event of skeletal muscle breakdown, which occurs subsequent to severe burns, the affected muscle mass can undergo a process termed RM (rhabdomyolysis) [1]. This leads to the release of toxic factors including skeletal Mb (myoglobin) into the circulation, where the protein is rapidly cleared and accumulates in the kidney (termed myoglobinuria) [2]. Myoglobinuria has been linked to ARF (acute renal failure) [3], and research in this field has demonstrated that accumulating Mb promotes both oxidative damage [4] and inflammation [5] within the kidney. Although the proportion of burns patients developing ARF is relatively low, mortality rates for these patients consistently remain above 80 % [6]. Therefore development of therapeutic strategies to limit the extent of ARF following severe burns would be advantageous.

The molecular mechanisms that underlie Mb toxicity have been studied previously and include renal vasoconstriction, intraluminal cast formation and haem-induced cytotoxicity [7]. It is not clear whether renal tubular cast formation is causally related or rather a consequence of the pathology associated with ARF [8]. In addition, degradation of the accumulating Mb probably results in the release of free haem and its catabolism by HOs (haem oxygenases) [9] coupled with release of iron and carbon

monoxide [10] and the concomitant formation of the antioxidant bilirubin [11]. Accumulating ferrous iron (Fe^{2+}) can generate hydroxyl radicals via the Fenton reaction, which can then damage cellular targets, including lipids, protein and DNA, and contribute to enhanced oxidative stress [12].

Several studies have also linked oxidative stress and inflammatory responses in renal tissues and cells following RM [13,14]. The potential for iron to be involved in these responses has prompted research aimed at testing whether iron chelators such as DFOB (desferrioxamine B) can provide protection for renal tissues. For example, DFOB provides renal protection in an animal model of RM [15,16], indicating that the supplemented chelator preserves kidney function in the presence of extracellular Mb. Studies in cell models also implicate DFOB in preserving mitochondrial function in renal cells [17], although this may not be due to iron chelation alone, since DFOB also inhibits Mb pro-oxidative activity [18]. However, the corresponding therapeutic drug Desferal® is limited by its hydrophilic nature and short plasma half-life [19], low oral activity [20], an inability to cross cell membranes and modest nephrotoxicity [21]. Other orally available chelating agents are not as effective as DFOB in the primary goal of sequestering iron and show adverse side effects or increased nephrotoxicity [22,23].
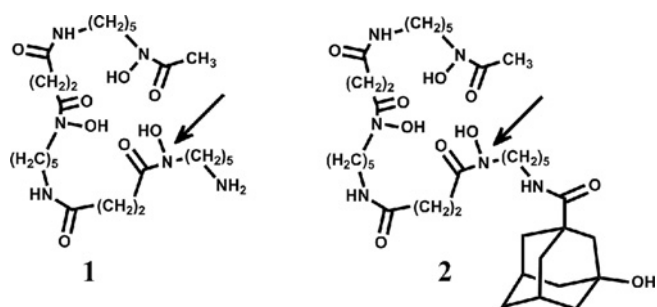

Figure 1   Chemical structures of the therapeutic iron chelator DFOB (1) and DFOB-AdA$_{OH}$ (2)

Arrows indicate the hydroxamic acid moiety adjacent to the terminal amine group in each compound.

Recently, a number of lipophilic low toxicity iron-chelating compounds were synthesized by conjugating DFOB to adamantyl derivatives [24]. Characteristically, these compounds showed similar iron-chelating properties to DFOB, but with decreased cytotoxicity towards cultured renal epithelial cells. Notably, in terms of toxicity, the conjugates of DFOB exhibit 6–15-fold greater IC$_{50}$ values than DFOB under the same culture conditions [24]. The conjugates also exhibited subtle differences in their ability to efflux iron from cells, suggesting that structural elements and/or physical properties modulate their uptake and secretion from different cell types. It is envisaged that this novel class of iron chelator may potentially overcome the selected therapeutic limitations of Desferal® and show improved renal tolerance, as well as still maintaining a high iron-binding efficacy.

In the present study, we compared the ability of DFOB-AdA$_{OH}$ [DFOB-N-(3-hydroxyadamant-1-yl)carboxamide; structure shown in Figure 1] and its parent compound DFOB to protect cultured kidney epithelial cells in an established cell model of RM that mimics urinary Mb levels detected in severe electrical-burn-induced muscle myolysis [25].

EXPERIMENTAL

Materials

Chemicals were of the highest quality available. DFOB mesylate (95 %) and cell culture materials were from Sigma–Aldrich. The DFOB–adamantane conjugate DFOB-AdA$_{OH}$ was synthesized and purified by HPLC as described previously [24]. Chelators were analytically pure as defined by HPLC. Fresh stock solutions of DFOB and DFOB-AdA$_{OH}$ (final concentration 1 mM) were prepared in DMSO. Experiments were carried out with chelators present at a final concentration 100 μM, as this was within the IC$_{50}$ toxic level for each agent [24].

Cell culture

Kidney epithelial cells [MDCK II (Madin–Darby canine kidney II); A.T.C.C.] were cultured as described previously [25]. Plates of cells were randomly allocated for control or iron chelator pre-treatment. Cells were washed twice in PBS (pH 7.4) and treated with vehicle (DMSO, control) or 100 μM iron chelator diluted in HPSS (Hepes-buffered physiological salt solution; 22 mM Hepes, pH 7.4, 124 mM NaCl, 5 mM KCl, 1 mM MgCl$_2$, 1.5 mM CaCl$_2$, 0.16 mM H$_3$PO$_4$, 5 mM NaHCO$_3$ and 5.6 mM D-glucose). After 2 h at 37 °C, cells were washed and then treated with 100 μM Mb or vehicle (as a control). In rats

with glycerol-induced ARF, urinary Mb can reach ∼2 mM [26]. However, despite significant myolysis of skeletal muscle in cases of severe electrical burns, urinary Mb is only within the range of ∼50–60 μM [25]. Therefore in the present study we chose to employ a dose of 100 μM Mb as an insult to the cultured epithelial cells to mimic the renal pathology induced by severe burns. Under these conditions, cell viability in control and Mb-treated cells remained unchanged after 24 h [25] and this time point was judged as suitable to make the biochemical and molecular comparisons described below.

Cell model of RM

Equine heart ferric Mb (Sigma) was used to establish the cell model of RM. Mb solutions were freshly prepared in PBS, sterilized by passage through 0.2 μm pore-size filters (Millipore) and then standardized using $\varepsilon_{409} = 188$ mM^{-1}·cm^{-1} [27]. All solutions prepared in this way displayed a Soret band at 409 nm assigned as ferric haem with no other absorbance in the range 410–425 nm, indicative of the absence of ferrous-oxy-Mb. The stock solution of Mb was then diluted in culture medium to a final concentration of 100 μM for use in cell studies. After 24 h, cells were washed twice with PBS and harvested for the assays outlined below. Where required, cells were harvested with 0.1 % trypsin and pellets were isolated by centrifugation (358 g for 4 min, 4 °C).

Oxidative stress response

To determine oxidative stress during experimental RM, cells were pre-treated with iron chelator or vehicle alone and incubated with Mb for 24 h as described above. Prior to harvest (∼4 h), cells were exposed to 50 μg/ml non-fluorescent DHR-123 (dihydrorhodamine-123; Invitrogen). In some experiments, Mb was removed prior to incubation with DHR-123. Oxidation of DHR-123 yields the fluorescent product R-123 (rhodamine-123). The cellular probe DHR-123 reacts non-specifically with intracellular ROS (reactive oxygen species) in a reaction mediated by peroxidase, cytochrome c or Fe^{2+} and thus is a useful fluorigenic probe for detecting enhanced oxidative stress in cells and tissues [28]. Mean fluorescence intensity was measured by flow cytometry (FACSCalibur; BD Biosciences) with excitation at 488 nm and emission at 540 nm. For each experiment conducted, 10 000 events were recorded before assessment of the data using standard FACSCalibur software.

Gene regulation

Isolation of total mRNA and assessment of gene regulation was determined by quantitative real-time RT (reverse transcription)–PCR. Briefly, MDCK II cells were lysed and total RNA was isolated with a commercial kit according to the manufacturer's instructions (GenElute; Sigma). Equal amounts (1 μg) of RNA were primed with oligo(dT)$_{15}$ primers and reverse-transcribed using a cDNA synthesis kit (Bioline). Amplification of cDNA was performed in a total volume of 15 μl of SYBR Green I Mastermix (Quantace; Bioline) containing appropriate primers using a Roche LightCycler 480. After initial denaturation (95 °C for 10 min), 40 PCR cycles were performed using the following conditions: 95 °C, 15 s; 60 °C, 15 s; and 72 °C, 15 s followed by a melt-step (55–95 °C). Primer pairs used for the assessment of β-actin, *HO-1*, *TNFα* (tumour necrosis factor α), *NF-κB* (nuclear factor κB), *VCAM-1* (vascular cell adhesion molecule 1) and *ICAM-1* (intercellular adhesion molecule 1) levels are shown in Table 1. Relative gene expression was assessed using the second

Table 1   Forward and reverse primer sequences used in gene analysis

Primers were obtained from Sigma and diluted to 10 μM before use. Annealing temperature was 60°C for all primer sets employed.

Gene	Sense	Anti-sense
β-Actin	5′-AGCCATGTACGTAGCCATCC-3′	5′-CTCTCAGCTGTGGTGGTGAA-3′
HO-1	5′-GCGTCGACTTCTTCACCTTC-3′	5′-GGTCCTCAGTGTCCTTGCTC-3′
TNFα	5′-GAGCCGACGTGCCAATG-3′	5′-CAACCCATCTGACGGCACTA-3′
NF-κB	5′-AACCCGTAGTGTCAGATGCC-3′	5′-GGACGAACACAGAGGTTGGT-3′
VCAM-1	5′-CAACTGAGTGGCCCCCTAG-3′	5′-GAGATCATTGCCATTCAGCA-3′
ICAM-1	5′-AGAGAGGCTGCACTCCACAG-3′	5′-GCTCACTCAGGGTCAGGTTG-3′

derivative maximum method and normalized to the corresponding β-actin response for the same sample. Gene expression in the control sample was arbitrarily assigned a unitary value and gene response was expressed as a fold change relative to the control.

Endocytosis of fluorescently labelled transferrin

Preparations of MDCK II cells were supplemented with 100 μM iron chelator or vehicle (DMSO) alone and then either exposed to Mb or vehicle (PBS) as indicated in the Figure legends. After 24 h, the cells were harvested and the cell pellets that were either exposed to Mb treatment or not (control) were resuspended in 1 ml of PBS and treated with transferrin conjugated to Alexa Fluor® 488 (5 μg/ml; Invitrogen). After 15 min, the cells were analysed by flow cytometry (FACSCalibur; BD Biosciences) as described previously [29].

In separate experiments, cells were grown on to sterile coverslips, treated as described above and then washed with 0.2 M acetic acid containing 0.5 M NaCl (pH 2.8), then fixed in 4% (w/v) paraformaldehyde (pH 7.5) for 15 min at 20°C. Coverslips were then mounted with Fluorescent Mounting Medium (Dako) and examined with an inverted fluorescent microscope using identical microscope settings (Axiovert 200; Zeiss) and then saved as tagged image files for further manipulation (AxioVision v4.5; Carl Zeiss).

Evaluation of monolayer permeability

Cells were seeded (1×10^5 cells/ml) on to six-well, 0.4 μm pore size, transparent transwells (Greiner) and cultured to 90% confluence. Following supplementation with 100 μM iron chelator or vehicle alone, cells were exposed to 100 μM Mb or vehicle as a further control (to assess the impact of the chelators alone on monolayer permeability). After 24 h, cells were treated with 2.5 μCi of [^{3}H]inulin/ml of complete medium (Sigma) and the amount of [^{3}H]inulin present in the upper or lower chamber was assayed with a scintillation counter (Packard-Bell) as described previously [25]. Finally, monolayer permeability was expressed as a percentage of [^{3}H]inulin passing through the monolayer of cells.

Expression of MCP-1 (monocyte chemotactic protein 1)

For quantitative determination of CCL2 (CC chemokine ligand 2)/MCP1, adherent cells were pre-treated with iron chelator or vehicle alone and incubated in the presence or absence of Mb as described above. After 24 h of incubation, samples of cell culture medium were taken and analysed using an AlphaLISA assay (PerkinElmer). Briefly, cell supernatants were centrifuged, diluted and incubated with anti-m/rCCL2/MCP-1 acceptor beads and the corresponding biotinylated antibody anti-m/rCCL2/MCP-1

for 60 min. Then, streptavidin donor beads were added and the absorbance was measured after a 30 min incubation on an Enspire plate reader (PerkinElmer).

Oxidation of chelators DFOB and DFOB-AdA$_{OH}$ by peroxidases

Solutions of the individual chelators (final concentration 500 μM) were incubated with either 250 μM HRP (horseradish peroxidase, Sigma) or Mb (Sigma), dissolved in phosphate buffer (50 mM phosphate, pH 7.4) and oxidation was initiated by the addition of 500 μM H_2O_2 or buffer (as a negative control). Mixing the chelator with 500 μM H_2O_2 alone served as a further control. After a 5 min incubation at 20°C, a sample of the reaction mixture was taken and transferred into a quartz flat cell (Wilmad) for measurement with a Bruker EMX EPR spectrometer at 293 K; with parameters of: power 100 mW, microwave frequency 9.8 GHz, modulation amplitude 1 mT and sweep 84 s. EPR spectra were recorded as an average of four cumulative scans. Hyperfine couplings were obtained by spectral simulation using the simplex algorithm [30] provided in the WINSIM program (http://www.niehs.nih.gov/research/resources/software/tools/index.cfm). All hyperfine couplings are expressed in units of mT. Simulations were considered acceptable if they produced correlation factors of $R = 0.98$. The detection limit of the stable nitroxide (TEMPO) radical was $\sim$50 nM. The remaining sample was frozen for analysis by reversed-phase HPLC with DFOB and DFOB-AdA$_{OH}$ eluting at $\sim$10 and 13 min respectively, as described previously [24]. Where required, Fe(III) was added to DFOB-AdA$_{OH}$ at a 1:1 molar ratio and the Fe(III)–DFOB-AdA$_{OH}$ complex was purified by HPLC as described previously [24]. The purified Fe(III) complex was verified by ESI-MS yielding a molecular mass of 792.5 Da (spray voltage 4.5kV, capillary voltage 35V, carrier N_2 gas) and was used in further EPR studies to assess the impact of iron loading on nitroxide radical formation.

Statistical analyses

Statistical analyses were performed with Prism (GraphPad). Results are presented as means $\pm$ S.D. of replicate analyses from at least three independent experiments (or as indicated in the Figure legends). Differences between data sets were assessed with one-way ANOVA using Bonferroni's multiple comparisons post-hoc test. Significance was accepted at the 95% level; $P < 0.05$.

RESULTS

Oxidative stress in MDCK II cells exposed to Mb

Treating cultured MDCK II cells with 100 μM Mb for 24 h resulted in a 2.3-fold increase in R-123 fluorescence relative to the controls (Figure 2), whereas removal of Mb prior to addition of DHR-123 completely diminished R-123 fluorescence, indicating that added Mb promoted DHR-123 oxidation (results not shown). Pre-treatment of cells with DFOB-AdA$_{OH}$ significantly decreased the mean fluorescence intensity, although this did not reach baseline levels in the control. Similarly, pre-treatment of cells with DFOB before addition of Mb diminished the mean fluorescence intensity; however, this did not reach statistical significance.

Gene regulation in MDCK II cells treated with Mb

The gene response for the antioxidant response element HO-1, and the inflammatory markers TNFα, NF-κB, ICAM-1 and VCAM-1,

Table 2   Gene expression in cultured kidney epithelial cells

Confluent MDCK II cells were pre-incubated with the iron chelator indicated (final chelator concentration 100 μM) or vehicle (control) in the absence or presence of 100 μM Mb. After 24 h, cells were harvested, mRNA isolated and the corresponding cDNA was probed for gene regulation as described in the Experimental section. Gene expression levels in the control were arbitrarily assigned a value of 1 and the other results were expressed relative to this level in the controls. The results represent the means ($\pm$ S.D.) from three to six different cell preparations. *Significantly different to the control; $P < 0.05$. †Significantly different to the corresponding Mb-treated group; $P < 0.05$.
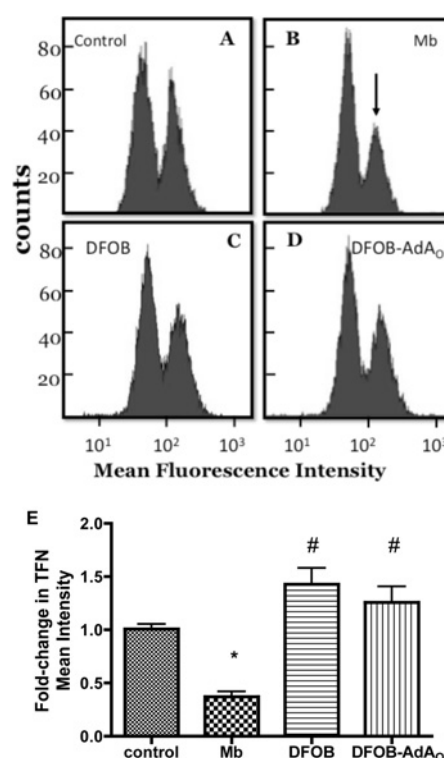
Gene	Control	Mb	Mb + DFOB	Mb + DFOB-AdA$_{OH}$	DFOB	DFOB-AdA$_{OH}$
HO-1	1.0 (0.0)	3.0 (0.7)*	1.5 (1.1)†	1.2 (0.6)†	1.2 (0.4)	0.9 (0.3)
TNFα	1.0 (0.0)	5.3 (2.3)*	1.7 (0.9)†	1.8 (0.9)†	1.3 (0.9)	1.2 (0.3)
NF-κB	1.0 (0.0)	1.5 (0.7)	0.9 (0.2)	0.7 (0.6)	0.4 (0.2)*	0.6 (0.3)*
ICAM-1	1.0 (0.0)	2.6 (1.5)	1.2 (0.5)	1.1 (0.5)	1.0 (0.5)	0.9 (0.0)
VCAM-1	1.0 (0.0)	3.3 (4.8)	7.6 (13.8)	7.6 (0.9)*	1.6 (0.9)	1.4 (0.2)
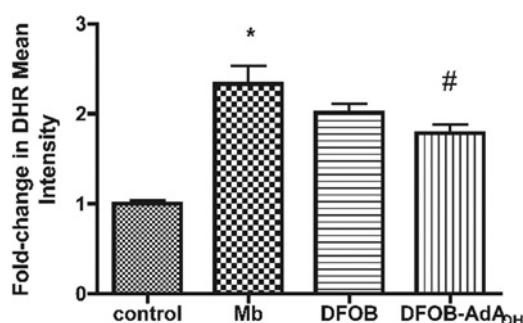
Figure 2   Mb-stimulated oxidative stress in MDCK II cells

Cells were treated in the absence or presence of 100 μM iron chelator and subsequently exposed to extracellular Mb for 24 h. Prior to harvest, cells were loaded with 50 μg/ml DHR-123 and the extent of R-123 fluorescence was monitored. The results represent the means $\pm$ S.D. from three independent studies each performed in triplicate. *Significantly different to the control; $P < 0.001$. #Significantly different to the corresponding Mb-treated group; $P < 0.05$.

Figure 3   Endocytosis of labelled transferrin in cultured MDCK II cells assessed by flow cytometry

Mb-treated cells were incubated with fluorescently labelled transferrin (5 μg/ml) for 15 min at 37°C prior to analysis. Data shown represent histograms of MDCK II cells in the (**A**) absence (control) or (**B**) presence of Mb (100 μM) both without chelator treatment, or samples pre-treated with 100 μM (**C**) DFOB or with (**D**) DFOB-AdA$_{OH}$ before addition of extracellular Mb. The arrow in (**B**) indicates the declining peak response that was inhibited by the presence of the chelators. (**E**) Endocytosis of labelled transferrin (TFN) was monitored and re-expressed as a proportion of the total cell population for each of the treatment groups. The results represent the means $\pm$ S.D. from three experiments. *Significantly different to the control; $P < 0.001$. #Significantly different to the corresponding Mb-treated group; $P < 0.001$.

were monitored by quantitative real-time RT–PCR and are shown in Table 2. Consistent with extracellular Mb eliciting a heightened oxidative stress 24 h after insult (Figure 2), *HO-1* expression increased significantly in response to the same Mb insult, with expression reaching 3-fold higher levels than in the control. Addition of the iron chelators DFOB and DFOB-AdA$_{OH}$ muted *HO-1* gene expression, suggesting that the chelators inhibited the cellular oxidative response that promotes *HO-1* expression [9]. Notably, no change in *HO-1* gene expression was evident in cells pre-treated with the iron chelators in the absence of Mb insult.

The pro-inflammatory genes *TNFα*, *NF-κB* and *ICAM-1* all showed a trend to increased expression in the presence of extracellular Mb, but only *TNFα* reached statistical significance (Table 2). Interestingly, gene expression of *VCAM-1* was increased in renal epithelial cells exposed to Mb and greater increases were evident in cells pre-loaded with chelators, suggesting that the chelators DFOB and DFOB-AdA$_{OH}$ acted in concert with Mb to induce some pro-inflammatory responses in cultured renal epithelial cells as well as down-regulating others. Importantly, pre-treatment of the cells with DFOB or DFOB-AdA$_{OH}$ in the absence of extracellular Mb had no material impact on the genes monitored in the present study, with the exception of *NF-κB*, which was decreased in response to incubation with the chelators (Table 2). The latter is interpreted as depletion of the intracellular pool of iron leading to decreased (oxidative) activation of the transcription factor.

Receptor-mediated endocytosis in cultured MDCK II cells

The receptor-mediated endocytosis of fluorescently labelled transferrin in the absence or presence of added Mb and with or without DFOB or DFOB-AdA$_{OH}$ supplementation was quantified by flow cytometry as shown in Figure 3. The presence of two sub-populations of cells was indicative of two distinct intracellular pools of transferrin in the MDCK II cells [29]. These pools were assigned previously as a slow-cycling population of transferrin receptor complex that is mobilized to the Golgi apparatus and a pool of fast-cycling transferrin receptor complex that releases transferrin in the cytoplasm [31]. The latter mechanism leads to a rapid recycling of the receptor to the plasma membrane without translocation to the Golgi [31]. Assessment of the population scatter plots in the absence of added Mb indicated that the chelators had no material impact on the distribution of cells (results not shown).

Exposure of the cells to extracellular Mb induced a selective reorganization of these intracellular transferrin pools, with the left-hand peak remaining largely unaffected and the right-hand peak decreasing markedly (compare Figures 3A and 3B). By contrast, pre-treatment of the cells with DFOB or DFOB-AdA$_{OH}$ somewhat restored the distribution of transferrin endocytosis (Figures 3C and 3D). Quantitative analysis (accounting for both peak populations) showed a distinct Mb-dependent loss in mean
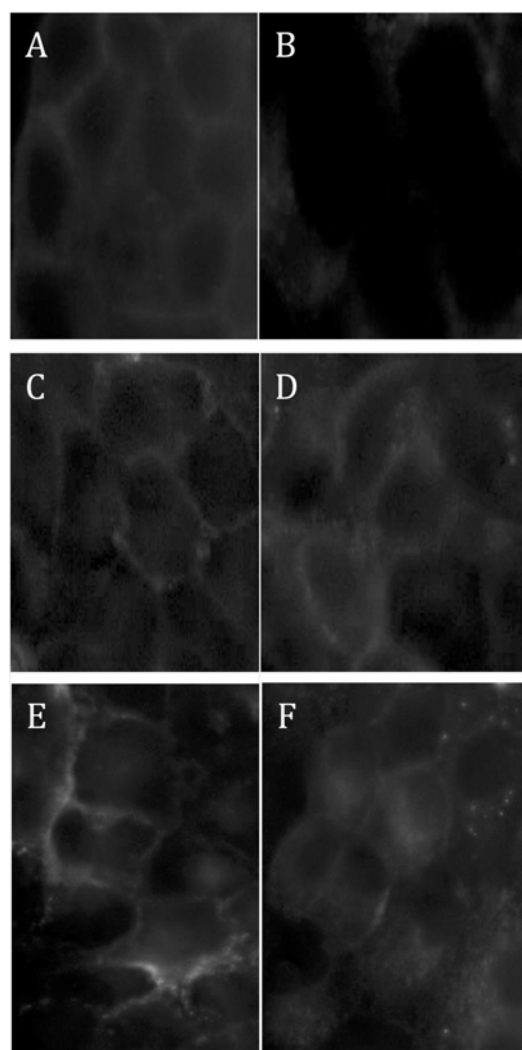
Figure 4   Inhibition of endocytosis by added Mb is reversed by pre-treatment of cells with iron chelators as judged by fluorescent microscopy

MDCK II cells were seeded (1×10^5 cells/ml) on to glass coverslips, sub-cultured at 37°C in a 5% $CO_{2(g)}$ atmosphere and then incubated with fluorescently labelled transferrin (5 μg/ml) for 15 min at 37°C prior to analysis. Representative micrographs show MDCK II cells in the (**A**) absence (control) or (**B**) presence of Mb (100 μM) both without chelator pre-treatment, or samples pre-treated with 100 μM (**C**) DFOB or with (**D**) DFOB-AdA$_{OH}$ before addition of extracellular Mb. The chelators (**E**) DFOB and (**F**) DFOB-AdA$_{OH}$ marginally enhance the uptake of labelled transferrin in the absence of added Mb. Images were taken using an inverted fluorescence microscope (63× oil objective) fitted with a high-resolution colour digital imaging camera and then transformed to tagged image files and downloaded into Microsoft PowerPoint (2007) for further manipulation.

fluorescence intensity that was sensitive to pre-treatment of the cells with the chelators DFOB or DFOB-AdA$_{OH}$ (Figure 3E).

The ability of DFOB or DFOB-AdA$_{OH}$ to enhance transferrin uptake in the presence of Mb was verified by monitoring the receptor-mediated binding of labelled transferrin in MDCK II cells with fluorescent microscopy (Figure 4). As anticipated, exposure of cells to Mb down-regulated the endocytosis of labelled transferrin (compare Figures 4A and 4B), whereas pre-incubation with the chelators restored transferrin receptor-mediated endocytosis as judged by the increased membrane fluorescence (compare Figures 4A, 4C and 4D). Pre-treatment with the chelators alone showed a marginal increase in transferrin endocytosis relative to the control in the absence of chelators
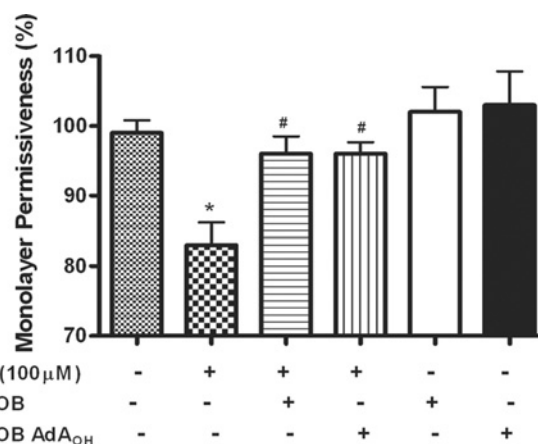

Figure 5   Monolayer permissiveness decreases in MDCK II cells after exposure to extracellular Mb and added chelators inhibit this activity

Non-specific [^{3}H]inulin transport was monitored in the absence or presence of 100 μM iron chelator in both the presence and absence of extracellular Mb (final concentration 100 μM). Monolayer permissiveness improves in the presence of iron-chelating drugs, whereas the chelators alone have no material effect on monolayer permeability. The results represent the means $\pm$ S.D. from nine experiments. *Significantly different to the control; $P < 0.001$. #Significantly different to the corresponding Mb-treated group; $P < 0.05$.

and added Mb (compare Figures 4A, 4E and 4F), consistent with repletion of the iron stores after chelator treatment.

Evaluation of monolayer permeability

Monitoring the transport of [^{3}H]inulin across a confluent monolayer of epithelial cells provides an indication of the bulk epithelial monolayer integrity as described previously [32]. Overall, non-specific monolayer permeability decreased significantly upon Mb challenge yielding ∼15% lower permeability than the control (Figure 5). Pre-treatment of the cells with the iron chelators reversed this decrease in permissiveness and restored monolayer permeability to the control levels in the absence of extracellular Mb. Notably, pre-treatment of the cells with DFOB or DFOB-AdA$_{OH}$ alone had no impact on monolayer permeability in the absence of an Mb insult, consistent with the low toxicity of the chelators at the selected dose.

Expression of MCP-1

The secreted protein MCP-1 displays chemotactic activity for monocytes and basophils and is considered as a biomarker of inflammation [33]. Renal cells produce MCP-1 upon stimulation through activation of the NF-κB pathway [34]. Notably, secretion of MCP-1 from MDCK II cells significantly increased (1.3-fold) in the presence of Mb compared with cells cultured in Mb-free medium. Pre-treatment of cells for 2 h with DFOB or DFOB-AdA$_{OH}$ inhibited these inflammatory responses and decreased MCP-1 levels to below baseline (Figure 6). Pre-treatment of the cells with DFOB or DFOB-AdA$_{OH}$ in the absence of Mb insult had no effect on MCP-1 levels in cultured MDCK II cells, which was consistent with the unchanged level of *TNFα* gene expression recorded under identical conditions (see Table 2).

Formation of stable nitroxide radicals

Enzymatic oxidation of DFOB by HRP is known to yield a stable nitroxide radical through hydrogen atom extraction from
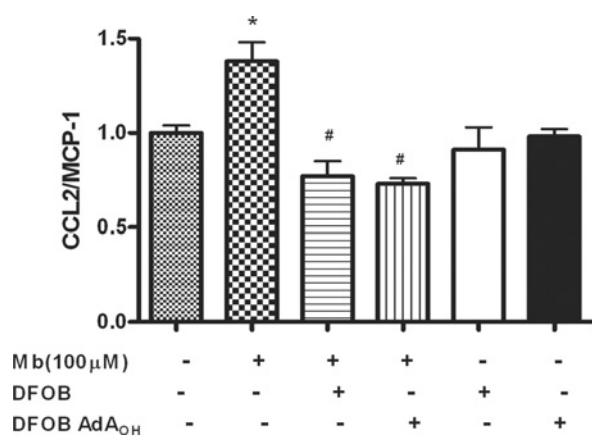
Figure 6   Monocyte chemoattractant protein 1 expression in MDCK II cells after exposure to extracellular Mb

Upon exposure to Mb for 24 h, cell supernatant was collected and the AlphaLISA assay was performed to determine the MCP-1 concentration. Mb increases the expression of MCP-1, whereas pre-treatment with DFOB or DFOB-AdA$_{OH}$ suppressed MCP-1 expression. In the absence of extracellular Mb, the iron-chelating drugs showed no material effect on MCP-1 secreted into the medium. The results represent the means $\pm$ S.D. from three experiments. *Significantly different to the control; $P < 0.01$. #Significantly different to the corresponding Mb-treated group; $P < 0.001$.

the hydroxamic acid moiety closest to the terminal amine group [35] (indicated by arrows in Figure 1). We recapitulated the generation of this radical using the HRP/H_2O_2 oxidizing system (results not shown) and demonstrated that a similar radical was formed in the reactions between DFOB-AdA$_{OH}$ and HRP/H_2O_2 as determined by EPR spectroscopy (Figure 7A). Simulation of the EPR spectrum indicated hyperfine couplings (aN 0.78 and aH 0.62 mT, obtained by spectral simulation to high correlations; $r = 0.98$) (Figure 7B). The identical radical was formed in reactions of DFOB-AdA$_{OH}$ and Mb/H_2O_2 (Figure 7C). Consistent with HRP exhibiting greater peroxidase activity than Mb, the steady-state concentration of nitroxide radical was increased in mixtures containing HRP (compare Figures 7A and 7C). Notably, binding of Fe(III) to DFOB-AdA$_{OH}$ completely inhibited the formation of the nitroxide radical by Mb/H_2O_2 (Figure 7D), indicating that binding of iron regulated the availability of the hydroxamic acid moiety for enzymic oxidation. No radical products were detected in the absence of H_2O_2 or in mixtures of chelator and peroxide alone, indicating that an enzymatic reaction is required to yield the radical (results not shown).

Addition of peroxide to mixtures containing Mb and DFOB-AdA$_{OH}$ resulted in near complete depletion of the chelator (99.0 $\pm$ 3%: mean $\pm$ S.D.; $n = 5$) (Figure 8). No product peaks were detected in the period monitored by HPLC (up to 40 min) (results not shown). A similar extent of chelator depletion occurred with reaction mixtures containing Mb/H_2O_2 and DFOB (results not shown). Taken together, these results indicate that both DFOB-AdA$_{OH}$ and parental DFOB scavenge oxidants produced by peroxidase enzymes (including Mb, which has limited peroxidase ability [27]) in a redox reaction that involves generation of a free nitroxide radical.

DISCUSSION

Multiple mechanisms have been suggested to explain the role of Mb in promoting acute renal injury following RM [13]. However, the exact link between the presence of extracellular Mb in the vascular system and acute kidney injury is not yet clear. The

Figure 7   Peroxidase enzymes oxidize DFOB or DFOB-AdA$_{OH}$ to yield a stable nitroxide radical

Solutions of HRP (**A**) or Mb (**C** and **D**), both at a final concentration of 250 μM, were mixed with the chelator DFOB-AdA$_{OH}$ (final concentration 250 μM) either without (**A** and **C**) or with (**D**) ligation to Fe(III). Next, the reaction mixtures were treated with 500 μM H_2O_2 and incubated at 20 °C for 2 min before transfer to a flat cell for EPR spectroscopy as described in the Experimental section. Spectrometer settings: power 100 mW, modulation amplitude 1 mT and sweep time 84 s. EPR spectra were recorded as an average of four cumulative scans. The spectrum shown in (**B**) represents EPR simulation of the spectrum in (**A**). Simulations were performed using WIMSIM software as described in the Experimental section. The results are representative of three independent experiments.

protective effect of DFOB in animal models of RM [15,16] has led to the notion that free iron plays a critical role in this acute pathology by participating in reactions that generate free radicals that cause an increase in cellular oxidative stress. Consequently, chelators that effectively bind and export iron from within cells have the potential to diminish intracellular oxidative stress and thereby protect renal cells from the effects of extracellular Mb and improve kidney function.

To attenuate the production of Fe(II)-dependent Fenton-based ROS, an ideal chelator will bind Fe as a stable Fe(III)–chelator complex that does not redox cycle to the Fe(II)–complex, since the dissociation of the latter could add to the Fe(II) burden. The thermodynamic stability of Fe(III)-loaded DFOB manifests as a negative Fe(III)/Fe(II) redox potential [$E_{1/2} = -0.48$ V compared with NHE (normal hydrogen electrode) at pH 7.5] [36,37]. Since the structural modification in DFOB-AdA$_{OH}$ occurs in a region distal to that of Fe(III) co-ordination, the stability of Fe(III)-loaded DFOB-AdA$_{OH}$ will reflect closely that of Fe(III)-loaded DFOB. Indeed, previous work that studied the co-ordination chemistry of DFOB-AdA$_{OH}$ and analogues found that all complexes were formed as Fe(III) complexes and there was no evidence of Fe(II) co-ordination [24]. The potential value of DFOB-AdA$_{OH}$ above DFOB as a stable Fe(III)-based chelator lies in its reduced toxicity and its improved membrane partition properties, as reflected by log$P$ values (DFOB-AdA$_{OH}$, log$P = 0.11$; DFOB, log$P = -2.10$) [24].
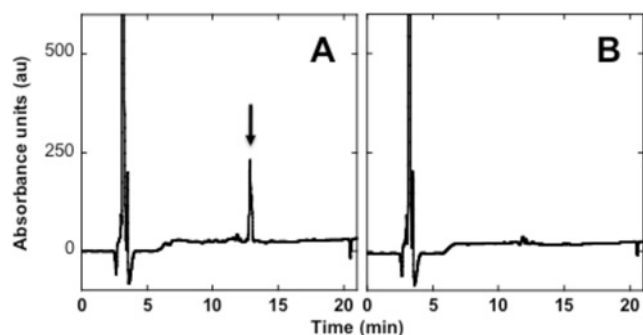
Figure 8　Oxidation of DFOB-AdA$_{OH}$ with Mb completely depletes the chelator from solution

Solutions of Mb (final concentration 250 μM) were mixed with DFOB-AdA$_{OH}$ (final concentration 250 μM) in the absence (**A**) or presence (**B**) of H$_2$O$_2$ (final concentration 500 μM). Next, the mixtures were incubated at 20 °C for 5 min before analysis with reversed-phase HPLC. The arrow in (**A**) denotes the retention time for DFOB-AdA$_{OH}$. Chromatograms shown are representative of two independent experiments each performed in triplicate.

Consistent with the notion that extracellular Mb promotes renal epithelial dysfunction through enhancing oxidative stress [25,29], exposure of MDCK II cells to Mb in the presence of DHR-123 increased ROS production. This resulted in a parallel increase in the gene response for *HO-1* and *TNFα*, implying an oxidative activation of the cells upon exposure to extracellular Mb. Pre-treatment of the cells with iron chelators decreased R-123 mean fluorescence intensity, indicating that the chelating agents diminished oxidative stress induced by Mb. Completely congruent with a decrease in oxidative stress, the gene response for *HO-1* and pro-inflammatory *TNFα* also diminished to baseline levels upon pre-treatment with the chelators, with similar activities noted for both DFOB or DFOB-AdA$_{OH}$.

On the basis of the results shown in the present study, it is clear that the chelators ameliorate Mb-induced oxidative stress in cultured kidney epithelial cells to similar extents. Gene expression of *HO-1* can be dependent on antioxidant response elements in the promoter region of the gene encoding HO-1 [38], and the redox-sensitive transcription factor NF-κB is also linked to TNFα expression [39]. Whether this potential renal protective activity is due to the direct chelation of intracellular iron or the ability of the chelators to act as antioxidants, which inhibit Mb-oxidant production independent of iron chelation in the extracellular milieu [35,40], or alternatively a combination of these mechanisms, is not clear.

The unregulated pro-oxidant activity of extracellular Mb can lead to indiscriminate damage to lipids [41] and proteins [42], whereas redox cycling of Mb has been implicated in the pathogenesis of RM-induced renal failure [43]. We have shown previously that haptoglobin efficiently binds extracellular Mb and inhibits Mb-mediated renal cell dysfunction [25]. This renal-protective action can also be recapitulated by supplementing cells with a phenolic antioxidant [29]. Our results from the present study demonstrating that peroxidase enzymes are able to oxidize the iron-free chelators to yield a nitroxide radical indicate a potential for the chelators to inhibit the peroxidase activity of Mb by an oxidant-scavenging mechanism in addition to decreasing the impact of intracellular iron (over)load, effectively expanding their spectrum of biological activity.

Previous studies have suggested that free radicals can injure the renal tubular epithelium by initiating a cascade of pro-inflammatory mediators such as cytokines and chemokines [44]. For example, activation of the NF-κB pathway stimulates

TNFα expression that in turn enhances apoptosis [45], increases glomerular damage and cytotoxicity and decreases renal cell viability [45]. In the case of renal epithelial cells, extracellular Mb elicits an inflammatory response through activation of the c-Src kinase-activator protein-1 and NF-κB pathways [14]. As a consequence, the activated or injured kidney cells secrete selectins, integrins and adhesion proteins [46]. Consistent with DFOB or DFOB-AdA$_{OH}$ exhibiting an anti-inflammatory action, both chelators down-regulated the expression of *TNFα* and subsequent secretion of MCP-1 in the presence of Mb, whereas in the absence of Mb the chelators had no impact on *TNFα* or MCP-1.

This anti-inflammatory activity may be beneficial to renal tissues during ARF. Secreted CCL2/MCP-1 plays a key role in acute and chronic renal diseases and leads to the infiltration and activation of monocytes [47], a hallmark of renal injury, and fibrosis in diabetic nephropathy [48]. The ability of iron chelators to decrease pro-inflammatory signalling in the kidney following RM probably results in a suppression of monocyte-macrophage activation driven by CCL2/MCP-1 as demonstrated in atherosclerosis [49].

Receptor-mediated endocytosis plays a crucial role in membranous transport function within kidney tubules. The decrease in transferrin uptake (shown in Figures 3 and 4) highlights the potential for extracellular Mb to promote the renal insufficiency that underlies ARF [50]. Transferrin receptors at the cell surface are sensitive to oxidative stress, presumably induced by thiol oxidation [31]. Humans do not have an active mechanism for iron excretion and the balance of intracellular iron is tightly regulated by the rate of erythropoiesis and distribution between intracellular iron stores by specialized proteins [51]. Therefore, a decrease in transferrin receptors can be interpreted as an overload of cellular iron, reflecting iron dysregulation. Importantly, both iron chelators increased transferrin uptake primarily through restoring the recycling of transferrin receptors to the cell surface. Whether this is due to an inhibition in oxidative stress as suggested previously [31] or whether chelation and removal of cellular iron plays a primary role in maintaining intracellular homoeostasis is presently unclear and further studies are warranted to elucidate which pathway is responsible for maintaining receptor-mediated endocytosis in this cell model of RM.

As well as receptor-specific transport via endocytosis, passive flow of ions/solutes following a concentration gradient is one of the major transport pathways in tubular epithelium [52]. Oxidative stress is known to impair epithelial function, potentially via damaging of tight junctions by free radicals and hydrogen peroxide acting as a protein tyrosine phosphatase inhibitor [53]. The supplementation of iron chelators significantly enhanced monolayer permeability in the presence of extracellular Mb, indicating a sustained tight junction function in the presence of Mb insult.

In this *in vitro* model of RM, supplementation with the iron chelator DFOB and the novel derivative DFOB-AdA$_{OH}$ resulted in overall enhanced cell function. We were able to demonstrate that iron chelators ameliorate oxidative stress and restore receptor-mediated transport as well as passive transport by maintaining epithelial monolayer permissiveness. Pre-treatment with the chelators also decreased the pro-inflammatory response elicited by extracellular Mb, and the pseudo-peroxidase was able to oxidize the chelators to yield the identical nitroxide radical. DFOB-AdA$_{OH}$ shows similar properties to DFOB. However, due to the decreased renal toxicity of this class of chelator [24], DFOB-AdA$_{OH}$ and other conjugated analogues show significant promise in the treatment of iron overload disease as well as a potential therapeutic strategy to combat ARF after RM.

AUTHOR CONTRIBUTION

Ludwig Groebler is a Visiting Research Trainee from Germany who is completing a doctorate while working in Paul Witting's laboratory. He was responsible for carrying out the majority of the work in the present study with guidance from the senior researcher. Together with Paul Witting, Ludwig Groebler was involved in formulating a draft manuscript. Anu Shanu is a Ph.D. student under the supervision of Paul Witting. She performed additional studies requested by the reviewers following assessment of the first submission of the manuscript. Her work investigated the impact of chelator supplementation on monolayer permissiveness and cellular production of MCP-1. Joe Liu is a Ph.D. student under the supervision of Rachel Codd. He was responsible for the preparation and purification of the chelator DFOB-AdA$_{OH}$ and its iron-bound form, and performing mass analyses. Joe Lui and Rachel Codd advised the research team on the use of the chelators and reviewed the results generated. All authors were involved in reviewing and updating the text associated with the revised manuscript.

FUNDING

REFERENCES

1 Lazarus, D. and Hudson, D. (1997) Fatal rhabdomyolysis in a flame burn patient. Burns **23**, 446–450
2 Bywaters, E. and Stead, J. (1944) The production of renal failure following injection of solutions containing myohaemoglobin. Exp. Physiol. **33**, 53–70
3 Holt, S. and Moore, K. (2001) Pathogenesis and treatment of renal dysfunction in rhabdomyolysis. Int. Care Med. **27**, 803–811
4 Holt, S., Reeder, B., Wilson, M., Harvey, S., Morrow, J. and Roberts, I. (1999) Increased lipid peroxidation in patients with rhabdomyolysis. Lancet **353**, 1241
5 Shulman, L., Yuhus, Y., Frolkis, I. and Gavendo, S. (1993) Glycerol induced ARF in rats is mediated by tumor necrosis factor-α. Kidney Int. **43**, 1397–1397
6 Holm, C., Hörbrand, F., Henckel von Donnersmarck, G. and Mühlbauer, W. (1999) Acute renal failure in severely burned patients. Burns **25**, 171–178
7 Zager, R. (1992) Heme protein-ischemic interactions at the vascular, intraluminal, and renal tubular cell levels: implications for therapy of myoglobin-induced renal injury. Renal Failure **14**, 341–344
8 Oken, D., Arce, M. and Wilson, D. (1966) Glycerol-induced hemoglobinuric acute renal failure in the rat. I. Micropuncture study of the development of oliguria. J. Clin. Invest. **45**, 724–735
9 Li, C., Hossieny, P., Wu, B., Qawasmeh, A., Beck, K. and Stocker, R. (2007) Pharmacologic induction of heme oxygenase-1. Antioxid. Redox Signal. **9**, 2227–2240
10 Hill-Kapturczak, N., Chang, S. and Agarwal, A. (2002) Heme oxygenase and the kidney. DNA Cell Biol. **21**, 307–321
11 Stocker, R. (2004) Antioxidant activities of bile pigments. Antioxid. Redox Signal. **6**, 841–849
12 Paller, M. (1988) Hemoglobin- and myoglobin-induced acute renal failure in rats: role of iron in nephrotoxicity. Am. J. Physiol. **255**, 539–544
13 Bosch, X., Poch, E. and Grau, J. (2009) Rhabdomyolysis and acute kidney injury. New Eng. J. Med. **361**, 62–72
14 Kim, S., Chang, J., Kim, S., Park, S., Park, J. and Lee, S. (2009) Myoglobin induces vascular cell adhesion molecule-1 expression through c-Src kinase-activator protein-1/nuclear factor-κB pathways. Nephron Exp. Nephrol. **114**, e48–e60
15 Shah, S. and Walker, P. (1988) Evidence suggesting a role for hydroxyl radical in glycerol-induced acute renal failure. Am. J. Physiol. **255**, 438–443
16 Zager, R. (1992) Combined mannitol and deferoxamine therapy for myohemoglobinuric renal injury and oxidant tubular stress. Mechanistic and therapeutic implications. J. Clin. Invest. **90**, 711–719
17 Plotnikov, E. Y., Chupyrkina, A. A., Pevzner, I. B., Isaev, N. K. and Zorov, D. D. (2009) Myoglobin causes oxidative stress, increase of NO production and dysfunction of kidney's mitochondria. Biochim. Biophys. Acta **1792**, 796–803
18 Reeder, B. J. and Wilson, M. T. (2005) Desferroxamine inhibits production of cytotoxic heme to protein crosslinked myoglobin: a mechanism to protect against oxidative stress without iron chelation. Chem. Res. Toxicol. **18**, 1004–1011
19 Porter, J., Rafique, R., Srichairatanakool, S., Davis, B., Shah, F., Hair, T. and Evans, P. (2006) Recent insights into interactions of deferoxamine with cellular and plasma iron pools: implications for clinical use. Ann. N. Y. Acad. Sci. **1054**, 155–68

20 Nick, H. (2007) Iron chelation, quo vadis? Curr. Opin. Chem. Biol. **11**, 419–423
21 Olivieri, N. and Brittenham, G. (1997) Iron-chelating therapy and the treatment of thalassemia. Blood **89**, 739–761
22 Kontoghiorghes, G., Pattichis, K., Neocleous, K. and Kolnagou, A. (2004) The design and development of deferiprone (L1) and other iron chelators for clinical use: targeting methods and application prospects. Curr. Med. Chem. **11**, 2161–2183
23 Olivieri, N., Brittenham, G., McLaren, C., Templeton, D., Cameron, R., McClelland, R., Burt, A. and Fleming, K. (1998) Long-term safety and effectiveness of iron-chelation therapy with deferiprone for thalassemia major. New Engl. J. Med. **339**, 417–423
24 Liu, J., Obando, D., Schipanski, L., Groebler, L. K., Witting, P. K., Kalinowski, D., Richardson, D. and Codd, R. (2010) Conjugates of desferrioxamine B (DFOB) with derivatives of adamantane or with orally available chelators as potential agents for treating iron overload. J. Med. Chem. **53**, 1370–1382
25 Parry, S. N., Ellis, N., Li, Z., Maitz, P. and Witting, P. (2008) Myoglobin induces oxidative stress and decreases endocytosis and monolayer permissiveness in cultured kidney epithelial cells without affecting viability. Kidney Blood Press. Res. **31**, 16–28
26 Zager, R. A., Foerder, C. and Bredl, C. (1991) The influence of mannitol on myoglobinuric acute renal failure: functional, biochemical, and morphological assessments. J. Am. Soc. Nephrol. **2**, 848–855
27 Witting, P. K. and Mauk, A. G. (2001) Reaction of human myoglobin and H_2O_2. J. Biol. Chem. **276**, 16540–16547
28 Wardman, P. (2007) Fluorescent and luminescent probes for measurement of oxidative and nitrosative species in cells and tissues: progress, pitfalls, and prospects. Free Radical Biol. Med. **43**, 995–1022
29 Shanu, A., Parry, S. N., Wood, S., Rodas, E. and Witting, P. K. (2010) The synthetic polyphenol tert-butyl-bisphenol inhibits myoglobin-induced dysfunction in cultured kidney epithelial cells. Free Radical Res. **44**, 843–853
30 Duling, D. R. (1994) Simulation of multiple isotropic spin-trap EPR spectra. J. Mag. Res. **104B**, 105–110
31 Malorni, W., Testa, U., Rainaldi, G., Tritarelli, E. and Peschle, C. (1998) Oxidative stress leads to a rapid alteration of transferrin receptor intravesicular trafficking. Exp. Cell Res. **241**, 102–116
32 Von Bonsdorff, C., Fuller, S. and Simons, K. (1985) Apical and basolateral endocytosis in Madin-Darby canine kidney (MDCK) cells grown on nitrocellulose filters. EMBO J. **4**, 2781–2792
33 Leonard, E. and Yoshimura, T. (1990) Human monocyte chemoattractant protein-1 (MCP-1). Immunol. Today **11**, 97–101
34 Donadelli, R., Abbate, M., Zanchi, C., Corna, D., Tomasoni, S., Benigni, A., Remuzzi, G. and Zoja, C. (2000) Protein traffic activates NF-κB gene signaling and promotes MCP-1-dependent interstitial inflammation. Am. J. Kidney Dis. **36**, 1226–1241
35 Morehouse, K. M., Flitter, W. D. and Mason, R. P. (1987) The enzymatic oxidation of Desferal to a nitroxide free radical. FEBS Lett. **222**, 246–250
36 Fontecave, M. and Pierre, J. L. (1993) Fer et peroxyde d'hydrogène: aspects chimiques d'un problème fondamental. Bull. Soc. Chim. Fr. **130**, 77–85
37 Spasojevic, I., Armstrong, S., Brickman, T. and Crumbliss, A. (1999) Electrochemical behavior of the Fe(III) complexes of the cyclic hydroxamate siderophores alcaligin and desferrioxamine E. Inorg. Chem. **38**, 449–454
38 Ryter, S. and Choi, A. (2005) Heme oxygenase-1: redox regulation of a stress protein in lung and cell culture models. Antioxid. Redox Signal. **7**, 80–91
39 Neuzil, J., Witting, P. K., Kontush, A. and Headrick, J. P. (2006) Role of vitamins E and C in nuclear factor-κB and nitric oxide signaling. In Encyclopedia of Vitamin E (Preedy, V. and Watson, R., eds), pp. 339–353, CABI Publishing, London
40 Reeder, B., Hider, R. and Wilson, M. (2008) Iron chelators can protect against oxidative stress through ferryl heme reduction. Free Radical Biol. Med. **44**, 264–273
41 Witting, P. K., Willhite, C. A., Davies, M. J. and Stocker, R. (1999) Lipid oxidation in human low-density lipoprotein induced by metmyoglobin/H_2O_2: involvement of α-tocopheroxyl and phosphatidylcholine alkoxyl radicals. Chem. Res. Toxicol. **12**, 1173–1181
42 Irwin, J. A., Ostdal, H. and Davies, M. J. (1999) Myoglobin-induced oxidative damage: evidence for radical transfer from oxidized myoglobin to other proteins and antioxidants. Arch. Biochem. Biophys. **362**, 94–104
43 Moore, K. P., Holt, S. G., Patel, R. P., Svistunenko, D. A., Zackert, W., Goodier, D., Reeder, B. J., Clozel, M., Anand, R., Cooper, C. E. et al. (1998) A causative role for redox cycling of myoglobin and its inhibition by alkalinization in the pathogenesis and treatment of rhabdomyolysis-induced renal failure. J. Biol. Chem. **48**, 31731–31737
44 Akcay, A., Nguyen, Q. and Edelstein, C. (2009) Mediators of inflammation in acute kidney injury. Mediators Inflamm. **2009**, 137072
45 Wajant, H., Pfizenmaier, K. and Scheurich, P. (2003) Tumor necrosis factor signaling. Cell Death Differ. **10**, 45–65

46 Ramesh, G. and Reeves, W. (2004) Inflammatory cytokines in acute renal failure. Kidney Int. **66**, S56–S61

47 Furuichi, K., Wada, T., Iwata, Y., Kitagawa, K., Kobayashi, K., Hashimoto, H., Ishiwata, Y., Asano, M., Wang, H. and Matsushima, K. (2003) CCR2 signaling contributes to ischemia-reperfusion injury in kidney. J. Am. Soc. Nephrol. **14**, 2503–2515

48 Tesch, G. (2008) MCP-1/CCL2: a new diagnostic marker and therapeutic target for progressive renal injury in diabetic nephropathy. Am. J. Physiol. **294**, F697

49 Zhang, W., Wei, H. and Frei, B. (2010) The iron chelator, desferrioxamine, reduces inflammation and atherosclerotic lesion development in experimental mice. Exp. Biol. Med. **235**, 633–641

50 Braun, S., Weiss, F., Keller, A., Ciccone, J. and Preuss, H. (1970) Evaluation of the renal toxicity of heme proteins and their derivatives: a role in the genesis of acute tubule necrosis. J. Exp. Med. **131**, 443–460

51 Finch, C. (1994) Regulators of iron balance in humans. Blood **84**, 1697–1699

52 Cho, M., Thompson, D., Cramer, C., Vidmar, T. and Scieszka, J. (1989) The Madin Darby canine kidney (MDCK) epithelial cell monolayer as a model cellular transport barrier. Pharm. Res. **6**, 71–77

53 Meyer, T., Schwesinger, C., Ye, J., Denker, B. and Nigam, S. (2001) Reassembly of the tight junction after oxidative stress depends on tyrosine kinase activity. J. Biol. Chem. **276**, 22048–22051

5   Publication 3

Co-supplementation with a synthetic polyphenol and vitamin C inhibits oxidative damage and improves vascular function yet does not inhibit acute renal injury in an animal model of rhabdomyolysis

Die parallele Verabreichung von einem synthetischem Polyphenol und Vitamin C verhindert oxidative Gewebeschäden und verbessert die Gefäßfunktion in einem Tiermodell der Rhabdomyolyse ohne dabei akutes Nierenversagen zu verhindern

5.1   Abstract (German Translation)

In einem *in vivo*-Modell für Rhabdomyolyse wurde untersucht, ob die gemeinsame Verabreichung von synthetischem tetra-*tert*-butyl Bisphenol (BP) und Vitamin C (Vit C) oxidativen Stress und akutes Nierenversagen (AKI) günstig beeinflusst. Ratten wurden in vier Gruppen unterteilt: Sham und Kontrolle (Standardfutter), BP mit Vitamin C (BP+) und BP ohne Vitamin C (BP-). Rhabdomyolyse wurde durch die intramuskuläre Injektion von Glycerol induziert. Vor Induktion der Rhabdomyolyse erhielten die Tiere der BP+ und BP- Gruppen für 4 Wochen eine Diät, die 0.12% w/w BP enthielt. Die BP+-Gruppe wurde parallel mit Vitamin C behandelt (100 mg/kg Ascorbat in PBS *i.p.* bei 72, 48 und 24 h vor Rhabdomyolyse-Induktion). Anschließend wurde bei allen Tieren, ausgenommen der Sham-Gruppe, durch die intramuskuläre Injektion einer Glycerollösung (50% v/v Glycerol/PBS; 6 ml/kg) in die Oberschenkel eine Rhabdomyolyse induziert. Nach 24 h wurden die Tiere euthanasiert und Urin, Plasma, Nieren und Aorten asserviert. Im Nierengewebe und Plasma war die Konzentration von Cholesterylesterhydroperoxid, Cholesterylesterhydroxyd und F_2-Isoprostan erhöht, was auf eine gesteigerte Oxidation von Lipiden hinweist. Weiterhin war in der Aorta der Gehalt an zyklischem Guanylylmonophosphat (cGMP) vermindert. Im Nierengewebe verursachte die experimentelle Rhabdomyolyse eine Stimulation der Genexpression von Glutathionperoxidase (GPx-4), Superoxiddismutase (SOD-1/2) und nukleärem Faktor kappa-beta (NFκB). Darüber hinaus entwickelten die Tiere akutes Nierenversagen, was durch die Bildung von tubulären Zylindern, geschädigtem Epithel und Proteinurie und erhöhten Urinkonzentrationen von Kidney Injury Molecule-1 (KIM-1) und Clusterin im

Urin gezeigt werden konnte. Die parallele Supplementierung mit BP und Vit C unterdrückte die Oxidation von Lipiden und ging mit einer verringerten Genexpression der gegenregulatorischen Enzyme GPx-4 und SOD-1/2 einher. Ebenso wurden NFκB und cGMP im Aortengewebe günstig beeinflusst. Die renale Dysfunktion und die morphologischen Veränderungen der Niere blieben allerdings bestehen. Im Gegensatz dazu reduzierte die alleinige Supplementierung mit Vit C die Entstehung von oxidativem Stress und verminderte die Bildung von Zylindern und Proteinurie, andere Plasma- und Urinmarker des akuten Nierenversagens blieben jedoch erhöht.

Diese Daten legen nahe, dass lipid- und wasserlösliche Antioxidantien variable therapeutische Effekte auf Rhabdomyolyse-bedingte Nierenfunktionsstörungen haben.

5.2   Original Publication

Original Contribution

Cosupplementation with a synthetic, lipid-soluble polyphenol and vitamin C inhibits oxidative damage and improves vascular function yet does not inhibit acute renal injury in an animal model of rhabdomyolysis

Ludwig K. Groebler [a], Xiao Suo Wang [a], Hyun Bo Kim [a], Anu Shanu [a], Farjaneh Hossain [a], Aisling C. McMahon [b], Paul K. Witting [a],*

[a] Discipline of Pathology, Redox Biology Group and Bosch Institute, The University of Sydney, Sydney, New South Wales 2006, Australia
[b] Biogerontology Group, ANZAC Research Institute, Concord Repatriation General Hospital, Concord NSW 2139, Australia

ARTICLE INFO

ABSTRACT

We investigated whether cosupplementation with synthetic tetra-*tert*-butyl bisphenol (BP) and vitamin C (Vit C) ameliorated oxidative stress and acute kidney injury (AKI) in an animal model of acute rhabdomyolysis (RM). Rats were divided into groups: Sham and Control (normal chow), and BP (receiving 0.12% w/w BP in the diet; 4 weeks) with or without Vit C (100 mg/kg ascorbate in PBS ip at 72, 48, and 24 h before RM induction). All animals (except the Sham) were treated with 50% v/v glycerol/PBS (6 mL/kg injected into the hind leg) to induce RM. After 24 h, urine, plasma, kidneys, and aortae were harvested. Lipid oxidation (assessed as cholesteryl ester hydroperoxides and hydroxides and F_2-isoprostanes accumulation) increased in the kidney and plasma and this was coupled with decreased aortic levels of cyclic guanylylmonophosphate (cGMP). In renal tissues, RM stimulated glutathione peroxidase (GPx)-4, superoxide dismutase (SOD)-1/2 and nuclear factor kappa-beta (NFκβ) gene expression and promoted AKI as judged by formation of tubular casts, damaged epithelia, and increased urinary levels of total protein, kidney-injury molecule-1 (KIM-1), and clusterin. Supplementation with BP ± Vit C inhibited the two indices of lipid oxidation, down-regulated GPx-4, SOD1/2, and NF-κβ gene responses and restored aortic cGMP, yet renal dysfunction and altered kidney morphology persisted. By contrast, supplementation with Vit C alone inhibited oxidative stress and diminished cast formation and proteinuria, while other plasma and urinary markers of AKI remained elevated. These data indicate that lipid- and water-soluble antioxidants may differ in terms of their therapeutic impact on RM-induced renal dysfunction.

© 2012 Elsevier Inc. All rights reserved.

In the event of skeletal muscle breakdown subsequent to severe burns (termed rhabdomyolysis; RM [1]), the affected muscle releases toxic factors into the extracellular milieu including skeletal myoglobin (Mb). Extracellular Mb accumulates in the blood where the protein is rapidly filtered by the kidney into the urine (a process termed myoglobinuria). Accumulation of extracellular Mb in the kidney has been linked to acute kidney injury (AKI), which is a clinical complication of severe burns [2]. Numerous studies have demonstrated that accumulating Mb promotes both oxidative damage [3] and inflammation [4] within the kidney, which is associated with the clinical progression of AKI toward renal insufficiency/failure. While the proportion of burn patients developing AKI is relatively low ranging 8–39% [5], mortality rates for these patients consistently remain above 80% [6]. Therefore, the development of therapeutic strategies to limit the extent of AKI and improve renal function following severe burn may impact positively on both morbidity and mortality.

The underlying molecular mechanism for extracellular Mb toxicity in the kidney have been studied and includes renal vasoconstriction, intraluminal cast formation within the renal tubular network, and heme protein-induced cytotoxicity affecting various renal cells [7]. The contribution of vasoconstriction to AKI is mediated by several factors including scavenging and/or oxidation of vasodilating NO by (oxy)Mb [8] and radical-mediated lipid oxidation, which yields isoprostane products that impact on vascular tone and kidney function [9,10]. Currently, it is unclear whether the presence of renal tubular casts can be causally related or rather a consequence of AKI [11]. In addition, degradation of accumulating Mb likely results in the release

of free heme and its catabolism by hemeoxygenases [12,13], which liberate iron and carbon monoxide [14] with concomitant formation of the antioxidant bilirubin in the intracellular compartment [13,15].

It is debated whether antioxidants may play a role in the prevention or therapy for AKI [13,16]. Employing antioxidants in the inhibition of RM-induced acute renal failure has yielded renal protection [17–20], although not all antioxidant supplementation studies [13,21,22] report improved renal function in this model of AKI. Such conflicting outcomes may arise from different biological activities of the test agents or compartmentalization of the antioxidant [13]. Antioxidants can exhibit additional functions including anti-inflammatory and cell signaling regulation independent of their antioxidant activity, e.g., vitamin E [23].

Phenolic compounds are a class of lipid-soluble chain-breaking antioxidants [24] that readily synergize with vitamin C (Vit C), the highly effective water-soluble antioxidant in living organisms [25]. Vitamin C is able to regenerate phenolic antioxidants to enhance their potency *in vivo*. We have demonstrated that the low-molecular-weight polyphenol 3,3′,5,5′-tetra-*tert*-butyl-biphenyl-4,4′-diol (BP) protects cultured kidney epithelial cells from Mb-mediated oxidative damage [26]. Similarly, rats supplemented with BP prior to experimental RM showed enhanced resistance to oxidative stress resulting in decreased kidney lipid oxidation and expression of antioxidant response genes [13]. Despite enhancing antioxidant capacity, rats supplemented with synthetic BP showed the same degree of AKI and loss of renal function. This lack of renal protection may be related to the compartmentalization of the lipophilic polyphenol that limits its effectiveness *in vivo*. Through synergizing with water-soluble antioxidants such as Vit C phenols can enhance their antioxidant action. Herein we have compared the renal protection of a synthetic phenolic antioxidant BP in an experimental model of RM with or without Vit C cosupplementation.

Experimental

Materials

Chemicals were of the highest quality available, and all solutions were freshly prepared using MilliQ Water or high quality analytical grade organic solvents and, where appropriate, sterilized prior to use. Unless otherwise indicated, materials were obtained from Sigma (Sydney, Australia). The synthetic polyphenol 3,3′,5,5′-tetra-*t*-butyl-biphenyl-4,4′-diol (referred to here as BP) was obtained from Maybridge (Cornwall, UK).

Electron paramagnetic spectroscopy

Ethanolic samples of BP (100 μM) were dispersed into 100 mM cetyltrimethylammonium chloride micelles and either irradiated with white light or incubated in the dark for 5 min as described previously [24]. Next, micelle solutions were transferred into a standard quartz flat cell (Wilmad, Buena, NJ) and the formation of phenoxyl radicals was monitored by EPR spectroscopy with an X-band Bruker EMX EPR spectrometer as described previously [27]. EPR spectra were acquired as an average of 3 scans with modulation frequency 100 kHz, sweep time 84 s, microwave power 63 mW, and modulation amplitude 0.1 mT. Where required, a solution of 200 μM ascorbic acid or PBS alone (control) was added to the micelle solutions before measurement. The limit of detection of a stable nitroxide (TEMPO) under identical spectrometer conditions was ~50 nM.

Animals

Male Wistar rats (0.4–0.6 kg) were obtained from the ARC facility (Western Australia) and acclimatized to the local environment. After 1 week, animals were fed a standard rodent chow, or chow supplemented with BP at 0.12% w/w, which yielded ~50 μM of the polyphenol in the circulating blood [13]. Thus, BP was dissolved in ethylalcohol, mixed

with the diet, and left in a fume hood to completely evaporate the alcoholic vehicle. Animals designated to the Control group received vehicle-treated chow. Food and water were available ad libitum. Animals designated to the Vit C and Vit C/BP cosupplemented groups were administered Vit C (100 mg/kg body weight ip) 72, 48, and 24 h before induction of experimental RM as described previously [28]. In parallel, animals designated to the Sham, Control, and BP groups received sterile saline solution (administered ip). Experimental procedures were approved by Sydney South West Animal Welfare Committee and adhered to the Australian Code of Practice for the care and use of animals for scientific purposes.

For the induction of RM animals were initially dehydrated for 18 h and anesthetized with isoflurane (2% v/v in $O_{2(g)}$, 1.5 L/min) and a baseline blood sample was collected through the tail vein. Next, animals were injected with a total of 6 mL/kg of freshly prepared hypertonic glycerol (50% v/v in sterile PBS), with equal volume administered into each hind limb. Animals assigned to the Sham group received an identical volume of sterile PBS. All animals were then housed in metabolic cages for 24 h (respective chow and water provided ad libitum) and the total urine output was collected and stored at 4 °C. Urinary globin concentrations (combined Mb and hemoglobin monitored at absorbance 405 nm [13]) were similar in animals administered hypertonic glycerol (53.4 ± 4.5 μM; mean $\pm$ SD; $n = 52$). Consistent with our previous report [13], urinary pH did not vary significantly between Control and antioxidant treatment groups (pH 7.2 ± 0.3 across all groups; mean $\pm$ SD; $n = 44$), although this was marginally lower than urinary pH measured in the Sham group (pH 7.4 ± 0.4). These data indicated that the extent of RM was similar among glycerol-treated animals and that antioxidant supplementation had no marked impact on the extent of muscle myolysis or urinary pH value.

Harvest of blood and organs

After 24 h, animals were anesthetized with isofluorane followed by ip injection of ketamine (60 mg/kg weight) and xylazine (10 mg/kg weight). Following a midline incision and thoracotomy, blood was collected via direct cardiac puncture into the left ventricle (5–10 mL into citrate), the right atrium was then cut, and the vasculature was perfused with sterile PBS. Plasma fractions were immediately separated and stored at -80 °C. The left kidney was frozen in liquid nitrogen for ensuing tissue studies, whereas the right kidney was stored in 10% v/v formalin for histological analysis. Thoracic aortae were harvested, rinsed with saline (0.9% w/v), stored in phosphate buffer (50 mM, pH 7.4) containing the phospho-diesterase inhibitor 3-isobutyl-1-methyl-xanthine (final concentration 100 μM), and then immediately frozen in liquid nitrogen for analysis of cyclic guanylyl monophosphate (cGMP).

Biochemistry

Biochemical analyses of plasma and urine were performed by the Diagnostic Pathology Unit (Concord Hospital, Sydney). Creatinine levels in plasma and urine were used to calculate the rate of creatinine clearance (CCr in units of mL/min) as an estimation of glomerular filtration rate as indicated below:

$$CCr = (U_{Cr} \times U_{24V})/(P_{Cr} \times 1440).$$

Here U_{Cr} = urinary creatinine concentration in milligrams per milliliter; U_{24V} = volume of urine passed in 24 h; P_{Cr} = plasma creatinine concentration in milligrams per milliliter; and 1440 = total min/24 h (time constant).

Tissue biochemistry

Frozen kidneys or aortae were thawed, diced with scissors, and snap-frozen in liquid nitrogen and pulverized to a fine powder with

a mortar and pestle. The powdered tissue was suspended in Buffer A (50 mM PBS, pH 7.4) containing 1 mM EDTA, 10 µM butylated hydroxytoluene and a Protease Inhibitor Cocktail tablet (Roche Diagnostics, Bern Switzerland), transferred to a glass tube, and homogenized with a rotating piston arrangement (Wheaton Specialty Glass, USA; 500 rpm) as described [13]. After 5 min, a sample (50 µL) was taken for protein analysis and the remaining fraction was split into two equal volumes. One sample was stored at -80 °C for mRNA extraction, and the other immediately extracted into a mixture of hexane and methanol (5:1 v/v): the lipid-soluble fraction was isolated, dried under reduced pressure, and resuspended in isopropanol for lipid analysis.

Assessment of lipid markers of oxidation

The tissue homogenate content of lipid-soluble vitamin E (as α-TOH, the most biological active form), free cholesterol (FC), cholesteryl esters (cholesteryl linoleate, C18:2, and cholesteryl arachidonate, C20:4, together referred to as CE), and CE-derived lipid hydroperoxides and hydroxides (referred to as CeO(O)H) were determined by HPLC analysis as described previously [29,30]. Where required, measurement of BP and its oxidized product, diphenoquinone (3,3′,5,5′-tetra-*tert*-butyl-4,4′-diphenoquinone) (DQ), was determined by gradient reversed-phase HPLC [31]. Lipids and antioxidants were quantified by area under the curve comparison with authentic standards.

Plasma and tissue levels of ascorbate and urate were determined by using an ion-paired, reversed-phase HPLC system in conjunction with oxidative electrochemical detection using a glassy carbon electrode (Bioanalytical Systems) with applied potentials of $+500$ mV versus the silver/silver chloride reference electrode as described previously [30]. Recovery of tissue ascorbate was corrected for adventitial oxidation by the addition of a known quantity of isoascorbate (final concentration 5 µM) during preparation of the individual homogenates, thereby acting as an internal standard in the processing of the sample. The average recovery of the internal standard for plasma and renal tissues was determined to be 86.3 ± 6.1 and $66.6 \pm 4.1\%$, respectively (not shown), and data were corrected for loss of the internal standard.

F_2-Isoprostanes (*8-iso*-prostaglandin $F_{2\alpha}$), nonenzymatic peroxidation products of arachidonic acid, were measured in plasma and renal tissues with a commercial immunoassay kit (Cayman, Ann Arbor, MI): detection limit of 5 pg/mL (plasma) and 12 pmol/mg protein (renal tissues). Plasma and tissue samples were initially hydrolyzed by saponification with 5 M NaOH, neutralized with 1 M HCl, and centrifuged ($3060\times g$), and the supernatant was collected for isoprostane determinations. The results were expressed as picograms per milliliter for plasma and normalized to total protein for renal tissues. Consistent with previous reports, the inter- and intraassay coefficients of variation were ~8 and 10%, respectively [32].

Determination of tissue protein content was performed using the BCA assay (Sigma, Sydney, Australia) with an Ultramark Microplate system (Bio-Rad, Sydney, Australia) and Microplate Manager software v5.1. All lipid- and water-soluble analytes in renal homogenates were normalized to total protein.

Urinary protein markers of kidney dysfunction

Urinary kidney injury molecule-1 (KIM-1) and clusterin were determined using a Rat Kidney Toxicity Multiplex Panel 1 (Millipore) and a Luminex system. Briefly, urine samples were diluted and incubated with antibody-immobilized beads overnight. After washing, detection antibodies were added and incubated for 1 h at 37 °C. Next, streptavidin-phycoerythrin was added and after a further 30 min incubation at 37 °C the samples were washed under vacuum and resuspended in PBS for analysis using a Luminex 200 xMAP platform (Abacus, Sydney Australia) and finally the median fluorescent intensity was converted to sample concentration using a standard curve.

Gene regulation

Isolation of total mRNA, conversion to cDNA, and assessment of gene regulation was determined by RT-PCR with an Eppendorf MasterCycler as described in detail elsewhere [13]. Primer pairs employed for the assessment of β-actin, SOD-1/2, and GPx-4 are collected in Table 1. Amplified cDNA was resolved on 1% w/v agarose gel containing ethidium bromide (2 µg/mL). Products were visualized and photographed under short-wavelength UV light and converted to TIFF using standard software. Densitometry was performed with ImageJ v1.42 (http://rsb.info.nih.gov/ij, NIH, USA). Gene expression in the control was arbitrarily assigned a unitary value and responses expressed as a relative fold-change.

Expression of monocyte chemoattractant protein 1

Determinations of the chemokine-2/monocyte chemoattractant protein-1 (CCL2/MCP-1) were performed using an AlphaLISA assay (PerkinElmer, Australia). Briefly, plasma samples were centrifuged, diluted, and incubated with Anti-m/r CCL2/MCP-1 acceptor beads and the corresponding biotinylated Anti-m/r CCL2/MCP-1 antibody. After 60 min, streptavidin donor beads were added and samples incubated further (30 min; 37 °C) and then measured using an Enspire plate reader (PerkinElmer, Australia).

Antioxidant enzyme activity

Glutathione peroxidase activity was determined by monitoring the time-dependent oxidation of NADPH ($\varepsilon_{340nm} = 6220$ M^{-1} cm^{-1}) at 5 min intervals over 15 min at 37 °C in the presence and absence of kidney homogenates as described previously [33]. For the assessment of total GPx activity, NADPH oxidation was initiated by addition of 350 µm H_2O_2. For GPx-4 activity, 100 µM phosphatidylcholine hydroperoxide was employed as the substrate (Cayman Chemicals, Ann Arbor, MI). In the absence of tissue, NADPH oxidation was negligible and independent of the presence or absence of phosphatidylcholine hydroperoxide (not shown). Enzyme activity was reported as a protein-normalized fold-change relative to the Sham.

SOD activity

Total SOD activity was assessed by measuring the inhibition of pyrogallol autooxidation monitored at 405 nm at 5 min intervals over 30 min at 37 °C as described previously [34]. Total SOD activity was expressed as a protein-normalized fold-change relative to the SOD activity determined in the Sham group.

Kidney histology

Kidneys were cut longitudinally and fixed in 10% v/v formalin solution. Tissues were embedded in paraffin wax, and 5 µm sections were stained with hematoxylin and eosin or periodic acid Schiff-base (PAS) stain. After staining, the images were viewed and captured using an Olympus Photo Microscope fitted with a digital camera and image system (Olympus DP Controller; v2.2.1.227). The images captured were converted to TIFF for manipulation with MS Power Point (2008, v7).

Table 1
Forward and reverse primer sequences used in gene analysis studies.

Gene	Sense	Antisense
β-Actin	5′-AGCGGTAGAGCTGCTTGAACT-3′	5′-CTCTCAGCTGTGGTGGTGAA-3′
SOD-1	5′- GAGATTGAGCGCAACAAGGA -3′	5′-AGCCATGTACGTAGCCATCC-3′
SOD-2	5′- GGAGATGAGACCCTTAGGTT -3′	5′-AGCAAGTGTAATCCAATAGC-3′
GPx-4	5′-TGAGAAGTGCGAGGTGAATG -3′	5′-AACACCGTCTGGACCTACCA -3′

Primers were obtained from Sigma (Australia) and diluted to 10 µM before use. Annealing temperatures were 60 °C for all primer sets employed.

Assessment of vascular function

Activation of the enzyme-soluble guanylyl cyclase by endothelial nitric oxide within VSMC promotes the conversion of intracellular guanosine diphosphate (GDP) to cGMP, which initiates vasorelaxation [35]. To determine the effect of extracellular Mb on the vascular function, aortic samples were first thawed then pulverized and homogenized in 1 mL buffer A containing 100 µM IBMX. Aortic cGMP was then determined with a commercial ELISA kit (Cayman Chemical) by monitoring absorbance (420 nm) with an Ultramark Microplate Reader (Bio-Rad, Australia) and Microplate manager v5.1. Finally, the levels of cGMP were normalized to homogenate protein.

Renal kinase activity

Assessment of the mitogen-activated protein kinase (MAPK) Erk activity in renal homogenates was determined using a luminescent ADP-Glo assay kit (Promega, Australia) to assess ADP production by the protein kinase reaction. The assay was performed at 30 °C for 15 min in a final volume of 25 µL containing kinase buffer, phospholipase-A_2 (substrate for Erk), and 2.5 mM ATP. The reaction was terminated by the addition of 25 µL of ADP-Glo stop reagent after 40 min. Next, 50 µL of kinase detection reagent was added, the reaction was incubated for a further 50 min, then luminescence was measured, and total ERK activity was calculated using a standard curve with correction for homogenate protein concentration.

Statistical analyses

Statistical analyses were performed with Prism (GraphPad, San Diego, CA). Data are presented as mean ± SD of replicate analyses from at least 3 independent experiments (or as indicated in the legends to the figures). Differences between data sets were assessed with one-way ANOVA with a Bonferroni correction for multiple comparisons. Significance was accepted at the 95% level; $P < 0.05$.

Results

Vitamin C synergizes with phenoxyl radicals generated from the polyphenol BP

To establish that BP was capable of interacting with Vit C, micellular dispersions of BP were subjected to irradiation and a radical product was detected with EPR spectroscopy (Fig. 1). Irradiated solutions of BP yielded a broad singlet (Fig. 1A) that was not detected in the absence of the light source (Fig. 1B). Based on these observations, the EPR signal was assigned as the phenoxyl radical derived from the one-electron oxidation of BP. Hyperfine coupling to H-atoms on the biphenyl rings were not resolved, even after decreasing modulation amplitude to 0.01 mT (data not shown). The potential for rapid electron transfer between the biphenyl ring structure and/or the molecular oxygen likely explains this line-broadening effect detected. In the presence of Vit C, the broad singlet feature was replaced by a doublet signal with hyperfine splitting ~0.2 mT (compare Figs. 1A and C), which has previously been assigned as the ascorbyl radical [36]. These data indicate that phenoxyl radicals derived from BP are chemically reduced by Vit C to yield ascorbyl radicals, overall regenerating BP in this process.

To assess whether this interaction between Vit C and BP inhibits oxidation in a biological context, we determined the impact of Vit C and BP cosupplementation on Mb-mediated lipid oxidation using low-density lipoprotein (LDL) as a target [37]. As anticipated, exposure of LDL to horse heart ferric Mb and H_2O_2 (final ratio Mb/H_2O_2 1:5 mol/mol) in the absence of antioxidant pretreatment resulted in the consumption of Vit E (α-tocopherol; α-TOH) and concomitant accumulation of CeO(O)H (hatched squares in Supplemental Figs. IA and B). Supplementation of LDL with BP alone prior to treatment
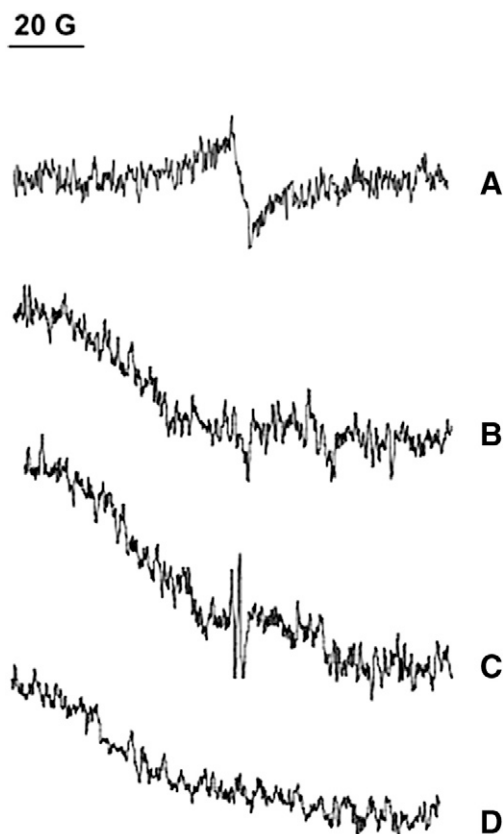

Fig. 1. Vitamin C chemically reduces the phenoxyl radical derived from the polyphenol BP to yield ascorbyl radicals. Micelles containing 100 µM BP were prepared as described in the methods section and then irradiated to generate a phenoxyl radical detected by EPR spectroscopy. Where required, vitamin C was added to the micellar dispersions. EPR spectra were obtained from (A) 100 µM BP irradiated with white light, (B) samples containing BP without irradiation, (C) 100 µM BP irradiated with white light and then treated with 250 µM vitamin C, and (D) samples containing BP and vitamin C without irradiation. Spectra were recorded at 9.41 GHz with modulation amplitude 0.8 G and modulation frequency 12.5 kHz and are the average of three cumulative scans.

with Mb/H_2O_2 inhibited the consumption of α-TOH and protected LDL lipids from oxidation and this coincided with depletion of BP prior to α-TOH (filled circles in Supplemental Figs. IA, B, and C). Introduction of Vit C at 25, 50, or 100 µM before supplementation with BP increased the time for onset of BP and α-TOH consumption and in turn inhibited CeO(O)H accumulation in a dose-dependent fashion (Supplemental Figs. IA, B, and C). Depletion of Vit C preceded BP followed by the consumption of α-TOH and accumulation of CeO(O)H (cf. Supplemental Figs. ID with A, B, and C): notably, the highest Vit C dose tested completely inhibited lipid oxidation and spared both BP and α-TOH. Thus, cosupplementation with low-molecular-weight antioxidants may lead to an enhanced antioxidant capacity through a synergistic mechanism that protects lipids from oxidation initiated by ferric Mb.

Antioxidant levels in supplemented animals

The antioxidant status of the animals was examined both before and after induction of RM. Consistent with the study design, animals treated with BP (0.12% w/w) in the diet contained both BP and the oxidation product DQ in both plasma (total drug 42.19 ± 8.3 µM; mean ± SD, $n = 8$) and renal tissue homogenate (total drug 6.6 ± 3.4 pmol/mg protein; $n = 8$), suggesting that a significant amount of the drug was present in the samples (Figs. 2A and B). Notably, the phenolic antioxidant was primarily present in its antioxidant active form (ratio of BP/DQ > 96.7%; $P < 0.05$) as opposed to its oxidized form *in*
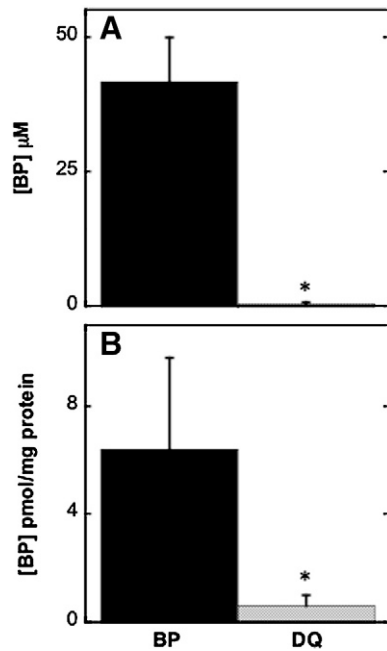
Fig. 2. Supplementation with dietary bisphenol increases the antioxidant content in plasma and renal tissues of rats. Animals were supplemented with BP (0.12% w/w in the diet) for 4 weeks. After treatment, they were euthanized and samples of kidney tissue and blood were obtained. Plasma was derived from whole blood and the kidney tissue was homogenized as detailed in the methods section. The concentration of BP and its oxidized product, DQ, in plasma (A) and kidney tissues (B) were determined by reversed-phase gradient liquid chromatography. Concentrations of renal antioxidants were normalized against total protein and expressed in units of ρmol/mg protein. Data represent mean ± SD; $n = 8$ for both groups. *Decreased relative to the BP concentration detected in the same samples, $P < 0.05$.
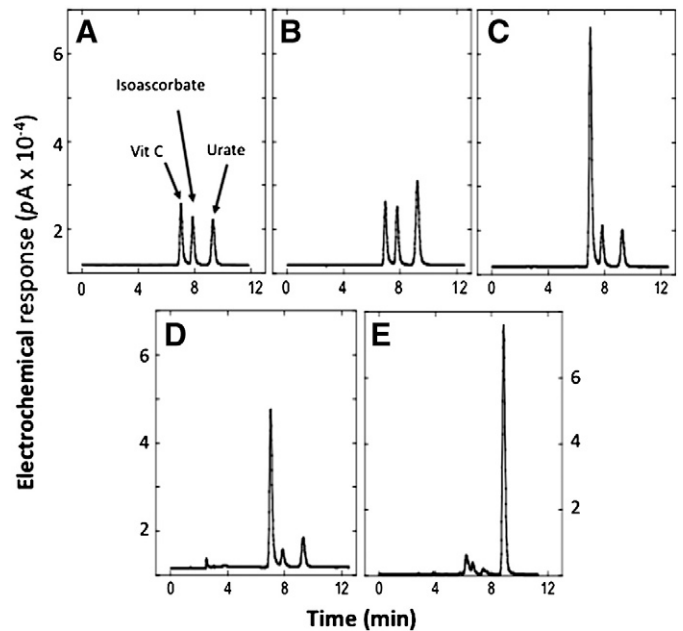

Fig. 3. Representative chromatograms showing changes in Vit C and urate in rats after induction of experimental RM. Animals were separated into different experimental groups and were supplemented with BP (0.12% w/w in the diet) for 4 weeks with and without vitamin C (500 mg/kg administered ip as a solution in PBS) as described in the methods section. After induction of experimental RM (or not Sham), animals were euthanized, blood and kidneys were harvested, plasma was isolated, and the renal tissues were homogenized. Next, the concentration of Vit C and urate was measured in the plasma (Panel B, Sham; Panel C, Vit C supplemented group) and renal tissue (Panel D, Vit C supplemented group; Panel E, Control) with liquid chromatography using electrochemical detection and concentrations determined by comparison to corresponding authentic standards (Panel A) 1 μM Vit C, 1 μM isoascorbate, and 1 μM urate. In all analyses, 5 μM isoascorbate was employed as the internal standard and values of Vit C were corrected against recovery of isoascorbate after sample workup as described previously [30].

vivo. In the absence of dietary supplementation no BP or DQ was detected in the Sham or Control groups.

The concentration of Vit C was also elevated significantly in the plasma and kidneys of ascorbate-treated animals compared with the Sham and Control animals (Figs. 3 and 4A and B): supplementation with BP had no affect on plasma or tissue levels of Vit C. Interestingly, after RM induction animals in the Control group showed a significant decrease in plasma Vit C, which was not apparent in samples from animals supplemented with BP, indicating that the synthetic bisphenol may ameliorate the depletion of endogenous Vit C after the induction of muscle myolysis. The impact of experimental RM on the plasma and tissue urate levels was also assessed by liquid chromatography (Fig. 3 and Figs. 4C and D). In the absence of antioxidant supplementation, urate increased markedly in plasma and renal tissues after RM. Supplementation with Vit C or BP either alone or in combination significantly prevented this increase in plasma urate, while in the kidney Vit C was more effective than BP in decreasing urate concentrations.

Lipid markers of oxidative damage

Analysis of lipid profiles afforded a comparison of plasma and renal tissue markers of lipid oxidation following experimental RM (Tables 2 and 3). Plasma concentrations of FC and CE remained unchanged in all groups except animals treated with both BP and Vit C whereas a significant increase in C20:4 was observed compared to the Sham group. Notably, plasma concentrations of CeO(O)H increased in the Control versus Sham groups, indicative of enhanced oxidative damage. In animals supplemented with BP, CeO(O)H levels were decreased to background levels detected in the Sham. While animals supplemented with Vit C alone showed a ~4-fold decrease in plasma CeO(O)H this level of lipid oxidation remained significantly higher than for the Sham group.

Animals treated with both BP and Vit C showed a 10-fold decrease relative to the Control group and this was not different from the effect of BP alone. Overall, α-TOH levels showed no significant changes

Fig. 4. Quantification of vitamin C and urate levels in plasma and renal tissues following experimental RM. The levels of the Vit C and urate in the plasma (A, C) and kidney homogenates (B, D) were measured as described in the legend to Fig. 3. Values were normalized using total protein and expressed in units of ρmol/mg protein. Data are expressed as mean ± SD for Sham ($n = 8$), Control ($n = 8$), BP ($n = 6$), Vit C ($n = 8$), and combined BP + Vit C ($n = 8$) groups. *Different to the Sham group, $P < 0.05$; #Different than animals supplemented with BP, $P < 0.05$.

Table 2
Plasma concentrations of native and oxidized lipids and vitamin E[a].

	Sham ($n=4$)[b]	Control ($n=4$)	BP ($n=4$)	Vitamin C ($n=8$)	BP + vitamin C ($n=8$)
[FC] mM	0.8 ± 0.3	0.8 ± 0.2	0.8 ± 0.2	0.7 ± 0.3	0.9 ± 0.1
[TOH] µM	7.3 ± 2.6	5.7 ± 1.8	7.4 ± 1.9	6.0 ± 4.3	5.6 ± 1.9
[CeO(O)H] nM	13 ± 2	37 ± 2[*]	10 ± 6[#]	16 ± 2[#]	10 ± 1[#]
[C18:2] mM	0.3 ± 0.02	0.3 ± 0.02	0.3 ± 0.3	0.4 ± 0.2	0.4 ± 0.2
[C20:4] mM	0.9 ± 0.4	1.1 ± 0.6	1.0 ± 0.5	2.1 ± 2.2	1.2 ± 0.4
[F$_2$-Isoprostanes] pg/mL	45.2 ± 2.7	138.5 ± 6.9[*]	80.1 ± 7.8[*,#]	68.8 ± 19.2[#]	39.8 ± 9.1[#]

[a] Animals supplemented with normal chow (Sham), vehicle-treated chow (Control), chow supplemented with bisphenol (BP; 0.12% w/w in the diet for 4 weeks) with or without Vit C coadministration (three consecutive ip injections as described in the methods section) were subjected to experimental RM (except Sham). After 24 h, animals were euthanized and samples of blood were obtained and the parameters listed were measured by liquid chromatography as described in the methods section. Data are expressed as mean ± (SD). FC, unesterified cholesterol; α-TOH, α-tocopherol (biologically active vitamin E); C18:2, cholesteryl linoleate; C20:4, cholesteryl arachidonate; CE, combined cholesteryl esters representing the sum of C18:2 and C20:4; CeO(O)H, CE-derived lipid hydroperoxides and hydroxides.
[b] Units of measurement and the numbers of samples tested (n) for all parameters are as indicated.
[*] Different to the Sham group; $P<0.05$.
[#] Different to the Control group; $P<0.05$.

irrespective of any treatment with regard to Sham and Control groups, indicating that inhibition of lipid peroxidation was unlikely directly dependent on this lipid-soluble antioxidant.

In renal homogenates the levels of FC and α-TOH remained unchanged in all groups indicating that antioxidant supplementation did not affect the tissue content of lipid-soluble vitamin E. In the animals treated with both BP and vitamin C renal tissues contained significantly higher levels of C20:4 than the Sham group, which was consistent with the increase in C20:4 detected in the plasma of the same animals. Levels of CeO(O)H increased in renal tissues after induction of experimental RM, whereas antioxidant supplementation significantly decreased oxidized lipid accumulation in renal tissues with all groups reaching baseline levels detected in the Sham group.

Relative to the Sham, total F$_2$-isoprostane concentration was elevated significantly in the Control group after RM. Thus similar to the marker of cell membrane of oxidation CeO(O)H, F$_2$-isoprostane levels increased ~3- and ~7-fold in plasma and renal tissues, respectively. Supplementation with either BP or Vit C prior to RM induction significantly inhibited the formation of F$_2$-isoprostanes in both plasma and renal tissues. Interestingly, cosupplementation with BP and Vit C was more efficient in inhibiting plasma F$_2$-isoprostanes than animals receiving Vit C or BP alone, suggesting that the synergy between Vit C and BP may have enhanced plasma antioxidant activity and protected plasma lipids from pro-oxidant Mb. By contrast, this enhanced antioxidant efficacy was not evident in renal tissues where the inhibition of F$_2$-isoprostanes was similar among all antioxidant-supplemented groups.

Expression of monocyte chemoattractant protein-1

The secreted protein MCP-1 displays chemotactic activity for monocytes and is produced in renal cells through activation of the NF-κB/TNF pathway [38]. The plasma concentration of MCP-1 increased 3-fold after induction of experimental RM compared to the Sham group, suggesting that enhanced inflammation may be linked to increased oxidative stress resulting from extracellular Mb accumulation in the kidney (Fig. 5A). All antioxidant treatments (alone or in combination) yielded a significant decrease in this inflammatory marker.

Aortic function

In the absence of antioxidant supplementation aortic cGMP decreased substantially in animals subjected to experimental RM (compare levels in Control and Sham groups, Fig. 5B). By contrast, aortic cGMP concentration was restored to near baseline levels in animals receiving BP or vitamin C compared with Control animals. The recovery of aortic cGMP levels in animals cosupplemented with BP and Vit C was greater than that determined in animals supplemented with BP or Vit C alone; however, this trend was not statistically significant.

Gene regulation in renal tissues

Next, the regulation of antioxidant response genes was examined in renal tissues (Table 4). In comparison with the Sham group, a ~6-fold increase in GPx-4 gene expression was determined in the Control group. Within the SOD family, only SOD-1 showed a marked elevation after RM induction. Supplementation with antioxidants inhibited Gpx-4 gene and SOD-1 gene regulation in renal tissues. Induction of RM also markedly increased expression of the transcription factor NF-κB coupled with a trend to increase TNF-α that did not reach statistical significance, at least when determined 24 h after RM induction (Table 4).

Table 3
Kidney tissue concentrations of native and oxidized lipids and vitamin E[a].

	Sham ($n=6$)[b]	Control ($n=6$)	BP ($n=6$)	Vit C ($n=8$)	BP + Vit C ($n=8$)
[FC] nmol/mg protein	0.2 ± 0.1	0.2 ± 0.1	0.3 ± 0.1	0.3 ± 0.1	0.4 ± 0.2
[TOH] pmol/mg protein	425 ± 207	388 ± 157	398 ± 190	385 ± 163	475 ± 185
[CeO(O)H] pmol/mg protein	2.4 ± 1.9	43.1 ± 8.8[*]	1.6 ± 1.2[#]	10.1 ± 2.1[*,#]	4.5 ± 1.7[#]
[C18:2] nmol/mg protein	0.03 ± 0.03	0.03 ± 0.01	0.02 ± 0.01	0.02 ± 0.01	0.03 ± 0.02
[C20:4] nmol/mg protein	0.06 ± 0.02	0.06 ± 0.01	0.07 ± 0.02	0.07 ± 0.04	0.13 ± 0.1
[F$_2$-Isoprostanes] pmol/mg protein	33.8 ± 6.9	227.2 ± 35.5[*]	61.9 ± 13.3[#]	51.2 ± 15.6[#]	44.3 ± 27.1[#]

[a] Animals supplemented with normal chow (Sham), vehicle-treated chow (Control), chow supplemented with bisphenol (BP; 0.12% w/w in the diet for 4 weeks) with or without vitamin C (Vit C) coadministration (three consecutive ip injections as described in the methods section) were subjected to experimental RM (except Sham). After 24 h, animals were euthanized, the kidneys were harvested and homogenized, lipids were extracted, and the parameters listed were measured by liquid chromatography as described in the methods section. Data are expressed as mean ± (SD). FC, unesterified cholesterol; α-TOH, α-tocopherol (biologically active vitamin E); C18:2, cholesteryl linoleate; C20:4, cholesteryl arachidonate; CE, combined cholesteryl esters representing the sum of C18:2 and C20:4; CeO(O)H, CE-derived lipid hydroperoxides and hydroxides.
[b] Units of measurement and the numbers of samples tested (n) for all parameters are as indicated.
[*] Different to the Sham group; $P<0.05$.
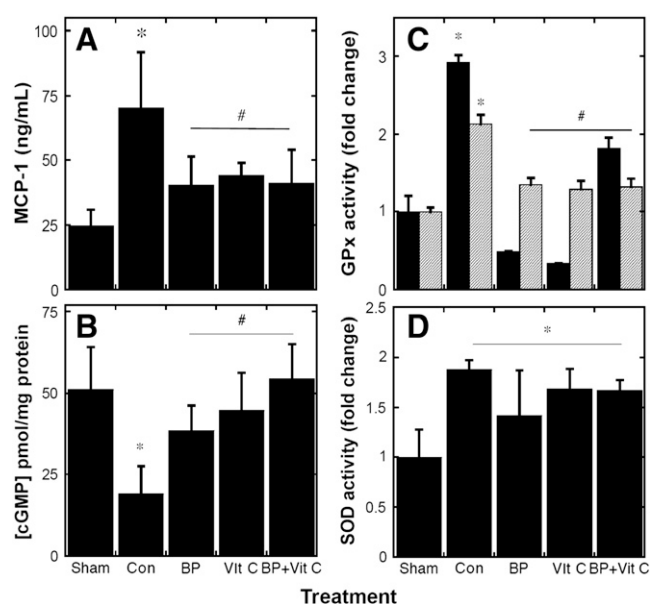[#] Different to the Control group; $P<0.05$.

Fig. 5. Plasma levels of monocyte chemoattractant protein 1, aortic content of cGMP, and renal antioxidant enzyme activity in rats exposed to experimental RM. Animals were separated into five experimental groups as described in the legend to Fig. 3 and exposed to experimental RM, and after 24 h the plasma, aorta and kidney were isolated as described in the methods section. Plasma was assessed for (A) MCP-1 concentration; (B) levels of cGMP were determined in aortic homogenates and kidney tissue homogenates were subjected to determinations of (C) total GPx (black bar) and specific GPx-4 activity (hatched bar) and (D) total SOD activity. Parameters were normalized to the corresponding total protein and where appropriate activity was expressed as a fold-change compared to the Sham (arbitrarily assigned unitary value). Data are expressed as mean ± SD for Sham ($n=8$), Control ($n=8$), BP ($n=6$), vitamin C ($n=8$), and BP + vitamin C ($n=8$). *Different to the Sham group, $P<0.05$. #Different to the Control group; $P<0.05$.

Enzyme activity

To further confirm the effects of RM and antioxidant treatment on the antioxidant response elements, activities for total GPx and SOD were determined in renal tissues as well as specific Gpx-4 activity (Figs. 5C and D). Overall, RM induced a ~3-fold increase in GPx activity, whereas antioxidant treatment (BP, Vit C, BP + Vit C) diminished this effect (Fig. 5C). Animals supplemented with BP or Vit C alone showed greater inhibition of GPx activity than the group treated with both BP and Vit C. Of the GPx isoforms GPx-4 is characterized by its ability to preferentially reduce phospholipid hydroperoxides

[39]. Consistent with this increase in total GPx activity, specific GPx-4 activity increased and this was also modulated by antioxidant supplementation (Fig. 5C). Similarly, renal SOD activity increased after RM (relative to the Sham group) (Fig. 5D). Unexpectedly, renal SOD activity remained elevated in animals supplemented with antioxidants despite the marked decrease in SOD-1 gene expression in the same animals.

Renal kinase activity

Measurement of Erk activity in renal homogenates was performed by using a commercial kit. Overall, RM induced a marked elevation in Erk activity as judged by comparing the Control and Sham groups, whereas animals supplemented with BP, Vit C, or the combination of both antioxidants showed lower activity levels, suggesting that diminished oxidative stress was linked to normalization of renal Erk activity (Fig. 6).

Kidney morphology

Histopathological assessment of renal sections from the Sham group (Fig. 7A) showed normal morphology in the glomerular tuft and tubular network. By contrast, the kidneys obtained from rats subjected to experimental RM (Fig. 7B) showed an abundance of tubule casts and disruption of the epithelial brush border of the renal tubule network. Supplementation with BP alone or in combination with Vit C had no marked effect on the renal histopathology (Figs. 7C and E), whereas animals supplemented with Vit C alone (Fig. 7D) showed decrease frequency of renal casts and near to normal appearance of epithelial brush borders.

Biochemical analysis of renal function

In the absence of antioxidant treatment, muscle myolysis stimulated significant increases in plasma urea and creatinine, while levels of most other mono- and divalent cations remained unchanged (Table 5). Elevation of urinary K^+ ion was determined, and this occurred concomitantly with a significant decrease in CCr (Table 5). Assessment of urinary markers of AKI indicated increased proteinuria accompanied by elevated levels of KIM-1 and clusterin, all consistent with significant renal dysfunction after RM (Fig. 8). Overall, supplementation with BP or Vit C had no or little effect on renal dysfunction induced by RM as judged by assessing CCr and blood nitrogen levels (Table 5) or urinary biomarkers of AKI (Figs. 8A–C). However,
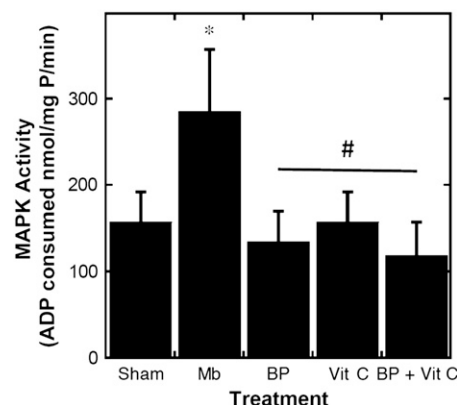
Table 4
Gene expression in renal tissues.

Treatment					
	Sham ($n=8$)	Control ($n=8$)	BP ($n=8$)	Vit C ($n=8$)	BP + Vit C ($n=7$)
SOD-1	1.0 (0.0)	3.1 (0.1)*	1.5 (0.1)#	1.2 (0.1)	1.3 (0.1)#
SOD-2	1.0 (0.3)	1.3 (0.2)	1.3 (0.1)	1.2 (0.1)	1.3 (0.0)
GPx-4	1.0 (0.1)	5.7 (0.1)*	2.7 (0.4)#	4.4 (0.2)	2.5 (0.0)#
NF-κB	1.0 (0.2)	2.7 (0.2)*	2.0 (0.4)*	1.4 (0.7)	2.0 (0.0)*
TNF-α	1.0 (0.4)	1.8 (0.8)	1.6 (0.1)	1.4 (1.1)	1.1 (0.1)*

Animals supplemented with normal chow (Sham), vehicle-treated chow (Control), and chow supplemented with BP (0.12% w/w in the diet for 4 weeks) with or without (Vit C) coadministration (three consecutive ip injections as described in the methods section) were subsequently subjected to experimental RM (except Sham). After 24 h, animals were euthanized, the kidneys harvested and homogenenized, and then total mRNA was isolated and the corresponding cDNA probed for gene regulation using RT-PCR as described in the methods section. Note, gene expression levels in the Sham were arbitrarily assigned a value = 1 and other data are expressed relative to this level. Data represent mean ± (SD) from $n=$ different animals as indicated.
*Significantly different to the Sham; $P<0.05$.
Significantly different to the corresponding Control group; $P<0.05$.

Fig. 6. Activation of the MAPK ERK in renal tissues after experimental RM. Animals were separated into five experimental groups as described in the legend to Fig. 3 and exposed to experimental RM, and after 24 h the kidneys were isolated and homogenized as described in the methods section. MAPK activity was determined using a commercial kit. Data are expressed as mean ± SD for Sham ($n=8$), Control ($n=8$), BP ($n=6$), vitamin C ($n=8$), and BP + vitamin C ($n=8$). *Significantly different to the Sham group, $P<0.05$. # Different to the Control group; $P<0.05$.
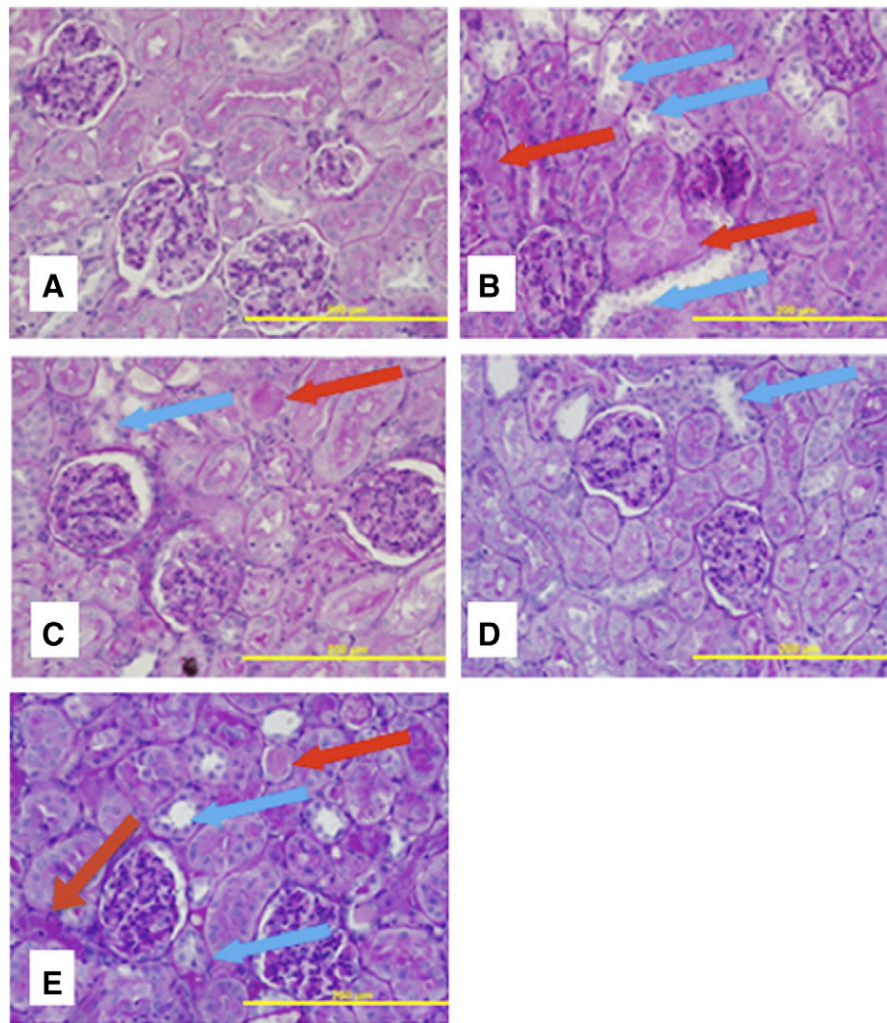
Fig. 7. Morphological changes in kidneys following experimental RM. Animals were separated into five experimental groups as described in the legend to Fig. 3 and exposed to experimental RM, and after 24 h the kidneys were isolated, stored in 4% v/v formalin, and prepared for histology. Representative sections shown are from (A) Sham, (B) Control, (C) BP-treated, (D) Vit C-treated, and (E) animals cosupplemented with both BP and Vit C. Figures are representative of at least four independent samples from each treatment group at two different fields of view ($40\times$magnification). Red arrows indicate cast formation; blue arrows indicate changes in brush border.

proteinuria decreased significantly in animals supplemented with Vit C alone (Fig. 8A), although CCr, blood nitrogen levels, and urinary concentrations of KIM-1 and clusterin remained elevated in this same group of animals (Table 5 and Figs. 8B and C).

Discussion

Despite advances in renal replacement therapies, AKI remains a prevalent clinical complication that is strongly associated with high

Table 5
Renal function assessed by plasma and urinary biochemistry [a].

Parameter	Sham ($n=8$)	Control ($n=16$)	BP ($n=12$)	Vit C ($n=8$)	Vit C + BP ($n=8$)
Urine					
Na$^+$ (mmol/L)	31.3 (16.0)	48.8 (12.9)	33.6 (13.3)	26.6 (13.8)	27.6 (13.0)
K$^+$ (mmol/L)	179.9 (32.3)	137.3 (27.3)[*]	121.4 (31.6)[*]	126.7 (49.4)[*]	99.5 (30.3)[*]
CCR (mL/min)	3.6 (1.2)	1.2 (0.8)[*]	1.3 (0.8)[*]	1.9 (0.9)[*]	1.4 (1.1)[*]
Plasma					
Na$^+$ (mmol/L)	178.3 (49.7)	190.3 (60.6)	167.1 (30.5)	211.1 (21.0)	207.4 (20.2)
K$^+$ (mmol/L)	4.6 (1.4)	4.4 (1.0)	5.1 (0.7)	4.0 (0.9)	4.1 (0.9)
Cl$^-$ (mmol/L)	119.9 (18.7)	108.1 (19.2)	113.0 (11.7)	106.3 (4.4)	104.5 (3.4)
Urea (mmol/L)	5.0 (0.8)	13.3 (6.2)[*]	17.5 (9.9)[*]	16.2 (8.9)[*]	19.5 (9.9)[*]
Creatinine (µmol/L)	16.8 (2.1)	56.3 (19.6)[*]	63.5 (21.0)[*]	48.8 (15.9)[*]	55.9 (27.6)[*]
Ca (mmol/L)	2.2 (0.4)	2.1 (0.6)	2.4 (0.3)	2.0 (0.3)	2.0 (0.2)

[a] Blood plasma and urine were collected 24 h after the induction of experimental RM and concentrations of different biochemical parameters were measured. Data are expressed as mean ± (SD). Units of measurement and the numbers of samples tested (n values for all parameters) are as indicated in the table. Creatinine clearance (CCR) was calculated as described in the methods section.
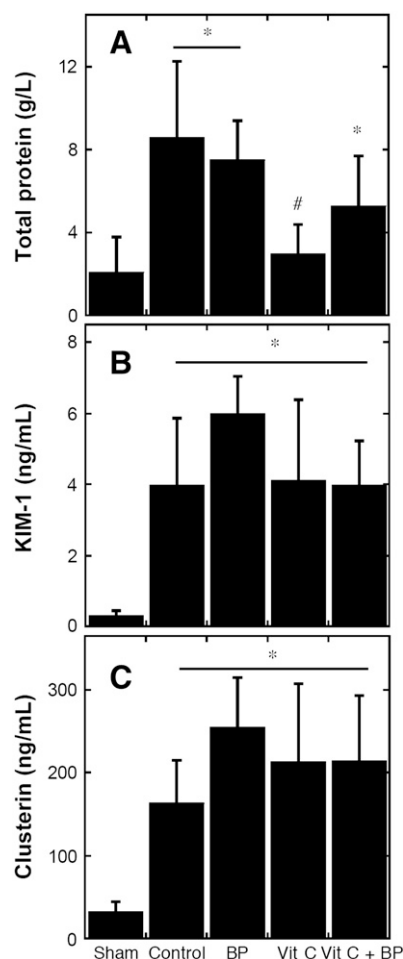 [*] Different to the Sham group; $P < 0.05$.

Fig. 8. Biochemical markers of renal function following experimental RM. Animals were separated into five experimental groups as described in the legend to Fig. 3 and exposed to experimental RM, and after 24 h of isolation urine was collected and analyzed for the content of (A) total protein, (B) KIM-1, and (C) clusterin. *Different to the Sham group, $P<0.05$. #Different to the Control group; $P<0.05$.

mortality rates in patients with RM subsequent to severe burns [8,40]. Studies assessing the peak levels of plasma Mb as a risk factor for renal failure suggest that Mb may be useful for predicting the extent of AKI in patients [41]. Although the use of urinary Mb as a marker requires further evaluation [42], it is known that redox cycling of the Mb from ferrous to ferric and to ferryl oxidation states can initiate lipid peroxidation and renal injury without invoking release of free iron [43,44]. Extracellular Mb is a pro-oxidant and causes the oxidation of a wide range of biological targets including low-molecular-weight phenols and amino acids in proteins [45,46]. Urinary malondialdehyde, used as an *in vivo* marker of *in vivo* oxidation, increases in thermal burn patients before the development of acute renal failure [47]. Therefore, antioxidants that inhibit Mb pro-oxidant activity and decrease oxidative damage have the potential to also regulate the extent of AKI during RM. Here we demonstrated that pharmacological concentrations of BP or Vit C (administered either separately or in combination) protected plasma constituents and renal tissues from oxidative damage (as assessed using two indices of lipid oxidation) and inflammation induced by experimental RM, yet only rats supplemented with Vit C alone were protected from renal failure as judged by monitoring some, though not all, markers of AKI in this animal model.

Renal tissues showed elevated SOD and Gpx activities, indicating an endogenous increase in antioxidant capacity in response to experimental RM. Despite this response, oxidative processes led to cumulative damage in renal tissues, decreased vascular function, and increases in

markers of AKI that reflect renal insufficiency after RM. Therefore, the idea to enhance antioxidant capacity prior to experimental RM has some merit. Overall, increasing plasma and tissue levels of BP, Vit C, or both BP and Vit C effectively inhibited CE oxidation and F_2-isoprostane accumulation in the plasma and renal tissues and this is likely due to the synergistic action of BP and Vit C that enhances their antioxidant efficacy (Supplemental Fig. I). Reduced oxidative damage in the kidney was associated with a decrease in renal inflammatory status, indicating that the low-molecular-weight antioxidants were highly effective in protecting the vasculature and renal tissues from Mb-mediated injury. With the exception of F_2-isoprostane accumulation in plasma, the effects of cosupplementation with BP and Vit C on markers of lipid oxidation and inflammation did not differ from supplementation with BP or Vit C administered separately, suggesting that optimal synergism between these antioxidants was already evident before increasing Vit C levels in these animals. These results taken together demonstrate that supplementation with either BP or Vit C efficiently bolsters antioxidant capacity *in vivo*; however, this does not consistently lead to improved renal function after challenge with experimental RM. Our data demonstrate that both Vit C and BP exhibit near identical antioxidant activity, yet only Vit C improves select markers of AKI, which suggests that other characteristics of this water-soluble antioxidant are important to renal protection.

Impaired renal perfusion by RM-induced vasoconstriction causes ischemic damage to kidney tissues including damage to the glomerular basement membrane and renal tubule epithelia that together promote AKI [29,48]. The importance of maintaining renal vascular perfusion is highlighted by studies demonstrating that administration of an NO donor and L-arginine, the substrate for endothelial nitric oxide synthase (eNOS), protects renal tissues from experimental RM [49]. Furthermore, renal perfusion is altered in eNOS-deficient mice [50,51], suggesting that maintenance of factors associated with normal vascular tone is crucial for sustained renal function. Notably, antioxidants are capable of protecting the renal vasculature through NO-dependent mechanisms [52] and through inhibiting the formation of F_2-isoprostanes [9,10] that also impact on vascular relaxation. Here we demonstrated that both BP and Vit C (either administered alone or together) restored aortic function to similar extents as judged by the yield of aortic cGMP from antioxidant-supplemented animals. If this result can be extrapolated to the renal (micro)vasculature then it suggests that, similar to the inhibition of oxidative stress in renal tissues, improved renal perfusion alone cannot be the only critical factor associated with protecting renal tissues from experimental RM.

The activation of Erk in renal epithelial cells [53] and other renal cell types [54] is considered a response to oxidant-induced stress and the current paradigm is that Erk activity is renal protective. However, not all studies support such a role for activated Erk. For example, Erk inhibition decreases damage in response to renal ischemia reperfusion injury [55]. Consistent with extracellular Mb stimulating ischemia in this animal model, we determined a Mb-mediated decrease in aortic cGMP with increases in renal Erk activity. Several mitogen-activated protein kinase (MAPK) pathways are activated in the kidney after experimental RM including Erk and the stress-activated kinase JNK and this response is associated with improved renal function following glycerol-mediated AKI [56], although not all studies support this conclusion [57]. Indeed, the MAPK inhibitor U0126 decreases TNF-α-mediated inflammation and apoptosis in renal injury induced by heavy metals [58]. Here we determined that BP and Vit C (supplemented separately or together) effectively inhibited Erk activation to similar extents, decreased both oxidative stress and the expression of the chemokine MCP-1 but did not consistently lead to renal protection. Therefore, the impact of Erk activation and its regulation by low-molecular-weight antioxidants warrants further study in this animal model.

Outcomes from this study indicate that Vit C ameliorates some markers of RM-induced AKI as judged by the restoration of urinary protein and plasma urate to near baseline levels and the presence of

fewer renal casts in the kidney tubule network: hyperuricemia is linked to the pathogenesis of RM-induced renal failure through promoting intratubular obstruction by precipitated urate [59]. However, other markers of renal damage/dysfunction remained unaffected in this interventional study. For example, irrespective of Vit C supplementation, both KIM-1, an early marker for epithelial cell dedifferentiation in response to renal tubular injury [60], and clusterin, a secreted protein that may play a role in apoptosis suppression and cell aggregation in the kidney [61], were elevated after induction of experimental RM and this result was similar to that obtained with rats supplemented with BP alone or in combination with Vit C. These data suggest that different biomarkers can indicate different outcomes within the same intervention and caution is required to assert renal protection unless a range of biomarkers of renal dysfunction is assessed in this animal model. Notably, KIM-1 and clusterin are currently being further evaluated in this regard. Diagnostic assessment of KIM-1 as a urinary biomarker for renal injury concluded that elevated levels in the urine correlated with injury in preclinical models of AKI and outperformed traditional biomarkers of evaluating renal damage [62]. In addition, age-adjusted levels of KIM-1 in the urine were higher in patients prior to death or where patients required renal replacement therapy when compared with survivors that did not require renal replacement therapy [63]. Although to date there has been no clinical study assessing the use of clusterin as a diagnostic marker of renal injury, preclinical testing has indicated that clusterin may be a useful biomarker when used in conjunction with traditional clinical biochemical markers and histopathological assessment of AKI in rodents [64,65].

The data obtained in this study indicate that antioxidants are effective in decreasing renal oxidative stress and inflammation following RM-mediated AKI; however, their therapeutic benefit is complicated by a lack of strong correlation between antioxidant activity and the array of biomarkers for assessing renal dysfunction. Data collected together in Supplemental Table I summarize outcomes from some antioxidant interventions using this model of experimental RM. These data are presented with the corresponding octanol/water partition coefficients for the agents tested and their antioxidant action. Overall, all antioxidants tested inhibited oxidative damage. In general, those agents with low partition coefficients (or enhanced water solubility) showed greater renal protective potential than the more lipid-soluble agents (i.e., hydrophobic agents with higher partition coefficients), at least when assessed using older generation biomarkers of renal damage. However, this trend is not always the case. For example, although the hydrophilic analgesic acetominophen shows reno-protection that is strongly associated with inhibiting plasma and urinary F_2-isoprostane accumulation, the hydrophilic antioxidant caffeic acid is unable to protect kidney tissues from experimental RM despite inhibiting malondialdehyde accumulation. Therefore, the question of whether antioxidants have a place in the prevention or therapy for AKI after RM and which markers of renal dysfunction best reflect reno-protective activity remains unclear and further studies evaluating RM-induced AKI using a combination of early and late markers of renal damage may be required to provide a definitive answer.

Acknowledgments

Appendix A. Supplementary data

Supplementary data to this article can be found online at doi:10.1016/j.freeradbiomed.2012.02.011.

References

[1] Lazarus, D.; Hudson, D. Fatal rhabdomyolysis in a flame burn patient. Burns 23:446–450; 1997.

[2] Holt, S.; Moore, K. Pathogenesis and treatment of renal dysfunction in rhabdomyolysis. Int. Care Med. 27:803–811; 2001.

[3] Holt, S.; Reeder, B.; Wilson, M.; Harvey, S.; Morrow, J.; Roberts, I. Increased lipid peroxidation in patients with rhabdomyolysis. Lancet 353:1241; 1999.

[4] Shulman, L.; Yuhus, Y.; Frolkis, I.; Gavendo, S.; Knecht, A.; Eliahon, H. E. Glycerol induced ARF in rats is mediated by tumor necrosis factor-alpha. Kidney Int. 43:1397–1401; 1993.

[5] Chrysopoulo, M. T.; Jeschke, M. G.; DzieswulskiD, P.; Barrow, R. E.; Herndon, D. N. Acute renal dysfunction in severely burned adults. J. Trauma 46:141–144; 1999.

[6] Holm, C.; Hörbrand, F.; von Donnersmarck, G.; Mühlbauer, W. Acute renal failure in severely burned patients. Burns 25:171–178; 1999.

[7] Zager, R. Heme protein-ischemic interactions at the vascular, intraluminal, and renal tubular cell levels: implications for therapy of myoglobin-induced renal injury. Ren. Fail. 14:341–344; 1992.

[8] Bosch, X.; Poch, E.; Grau, J. M. Rhabdomyolysis and acute kidney injury. N. Engl. J. Med. 361:62–72; 2009.

[9] Reeder, B. J.; Wilson, M. T. Hemoglobin and myoglobin associated oxidative stress: from molecular mechanisms to disease States. Curr. Med. Chem. 12:2741–2751; 2005.

[10] Badr, K. F.; Abi-Antoun, T. E. Isoprostanes and the kidney. Antioxid. Redox Signal. 7:236–243; 2005.

[11] Oken, D.; Arce, M.; Wilson, D. Glycerol-induced hemoglobinuric acute renal failure in the rat. I. Micropuncture study of the development of oliguria. J. Clin. Invest. 45:724–735; 1966.

[12] Li, C.; Hossieny, P.; Wu, B.; Qawasmeh, A.; Beck, K.; Stocker, R. Pharmacologic induction of heme oxygenase-1. Antioxid. Redox Signal. 9:2227–2240; 2007.

[13] Kim, H .-B.; Shanu, A.; Wood, S.; Parry, S. N.; Collett, M.; McMahon, A. C.; Witting, P. K. Phenolic antioxidants tert-butyl-bisphenol and vitamin E decrease oxidative stress and enhance vascular function in an animal model of rhabdomyolysis yet do not improve acute renal failure. Free Radic. Res. 45:1000–1012; 2011.

[14] Hill-Kapturczak, N.; Chang, S.; Agarwal, A. Heme oxygenase and the kidney. DNA Cell Biol. 21:307–321; 2002.

[15] Stocker, R. Antioxidant activities of bile pigments. Antioxid. Redox Signal. 6:841–849; 2004.

[16] Koyner, J. L.; Ali, R. S.; Murray, P. T. Antioxidants: do they have a place in the prevention or therapy of acute kidney injury? Exp. Nephrol. 109:e109–e117; 2008.

[17] Chander, V.; Singh, D.; Chopra, K. Catechin, a natural antioxidant protects against rhabdomyolysis-induced myoglobinuric acute renal failure. Pharmacol. Res. 48:503–509; 2003.

[18] Chander, V.; Singh, D.; Chopra, K. Reversal of experimental myoglobinuric acute renal failure in rats by quercetin, a bioflavonoid. Pharmacology 73:49–56; 2005.

[19] Stefanovic, V.; Savic, V.; Vlahovic, P.; Cvetkovic, T.; Najman, S.; Mitic-Zlatkovic, M. Reversal of experimental myoglobinuric acute renal failure with bioflavonoids from seeds of grape. Ren. Fail. 22:255–266; 2000.

[20] Rodrigo, R.; Bosco, C.; Herrera, P.; Rivera, G. Amelioration of myoglobinuric renal damage in rats by chronic exposure to flavonol-rich red wine. Nephrol. Dial. Transplant. 19:2237–2244; 2004.

[21] Vlahovic, P.; Cvetkovic, T.; Savic, V.; Stefanovic, V. Dietary curcumin does not protect kidney in glycerol-induced acute renal failure. Food Chem. Toxicol. 45:1777–1782; 2007.

[22] Aydogdu, N.; Atmaca, G.; Yalcin, O.; Batcioglu, K.; Kaymak, K. Effects of caffeic acid phenethyl ester on glycerol-induced acute renal failure in rats. Clin. Exp. Pharmacol. Physiol. 31:575–579; 2004.

[23] Azzi, A.; Gysin, R.; Kempná, P.; Munteanu, A.; Villacorta, L.; Visarius, T.; Zingg, J. M. Regulation of gene expression by alpha-tocopherol. Biol. Chem. 385:585–591; 2004.

[24] Sies, H. Oxidative stress: oxidants and antioxidants. Academic Press, New York; 1991.

[25] Witting, P. K.; Stocker, R. Ascorbic acid as an antioxidant in atherosclerosis. In: May, J.M., Hasard, A., Smirnoff, N. (Eds.), Vitamin C: it functions and biochemistry in animals and plants. Bios Scientific, Oxford, UK,pp. 261–290; 2004.

[26] Shanu, A.; Parry, S. N.; Wood, S.; Rodas, E.; Witting, P. K. The synthetic polyphenol tert-butyl-bisphenol inhibits myoglobin-induced dysfunction in cultured kidney epithelial cells. Free Radic. Res. 44:843–853; 2010.

[27] Witting, P. K.; Westerlund, C.; Stocker, R. A rapid and simple screening test for potential inhibitors of tocopherol-mediated peroxidation of LDL lipids. J. Lipid Res. 37:853–867; 1996.

[28] Ustundag, S.; Yalcin, O.; Sen, S.; Cukur, Z.; Ciftci, S.; Demirkan, B. Experimental myoglobinuric acute renal failure: the effect of vitamin C. Ren. Fail. 30:727–735; 2008.

[29] Sattler, W.; Mohr, D.; Stocker, R. Rapid isolation of lipoproteins and assessment of their peroxidation by high performance liquid chromatography postcolumn luminescence. Methods Enzymol. 233:469–489; 1994.

[30] Suarna, C.; Dean, R. T.; May, J.; Stocker, R. Human atherosclerotic plaque contains both oxidized lipids and relatively large amounts of alpha-tocopherol and ascorbate. Arterioscler. Thromb. Vasc. Biol. 15:1616–1624; 1995.

[31] Witting, P. K.; Pettersson, K.; Ostlund-Lindqvist, A. M.; Waberg, A. M.; Stocker, R. Dissociation of atherogenesis from aortic accumulation of lipid hydro(pero)xides in Watanabe heritable hyperlipidemic rabbits. J. Clin. Invest. 104:213–220; 1999.

[32] Pradelles, P.; Grassi, J.; Maclouf, J. Enzyme immunoassays of eicosanoids using AchE as label: an alternative to radioimmunoassay. Anal. Chem. 57:1170–1173; 1985.

[33] Wilson, S. R.; Zucker, P. A.; Huang, R. R. C.; Spector, A. Development of synthetic compounds with glutathione peroxidase activity. J. Am. Chem. Soc. 111:5936–5939; 1989.

[34] Parry, S. N.; Ellis, N.; Li, Z.; Maitz, P.; Witting, P. K. Myoglobin induces oxidative stress and decreases endocytosis and monolayer permissiveness in cultured kidney epithelial cells without affecting viability. *Kidney Blood Press. Res.* **31:**16–28; 2008.

[35] Thomas, S. R.; Witting, P. K.; Drummond, G. R. Redox control of endothelial function and dysfunction: molecular mechanisms and therapeutic opportunities. *Antioxid. Redox Signal.* **10:**1713–1765; 2008.

[36] Witting, P. K.; Upston, J. M.; Stocker, R. Role of alpha-tocopheroxyl radical in the initiation of lipid peroxidation in human low-density lipoprotein exposed to horse radish peroxidase. *Biochemistry* **36:**1251–1258; 1997.

[37] Witting, P. K.; Willhite, C. A.; Davies, M. J.; Stocker, R. Lipid oxidation in human low-density lipoprotein induced by metmyoglobin/H2O2: involvement of alpha-tocopheroxyl and phosphatidylcholine alkoxyl radicals. *Chem. Res. Toxicol.* **12:**1173–1181; 1999.

[38] Donadelli, R.; Abbate, M.; Zanchi, C.; Corna, D.; Tomasoni, S.; Benigni, A.; Remuzzi, G.; Zoja, C. Protein traffic activates NF-kB gene signaling and promotes MCP-1-dependent interstitial inflammation. *Am. J. Kidney Dis.* **36:**1226–1241; 2000.

[39] Schneider, M.; Forster, H.; Boersma, A.; Seiler, A.; Wehnes, H.; Sinowatz, F.; Neumuller, C.; Deutsch, M. J.; Walch, A.; Hrabe De Angelis, M.; Wurst, M.; Ursini, F.; Roveri, A.; Maleszewski, M.; Maiorinin, M.; Conrad, M. Mitochondrial glutathione peroxidase 4 disruption causes male infertility. *FASEB J.* **23:**3233–3242; 2009.

[40] Brusselaers, N.; Monstrey, S.; Colpaert, K.; Decruyenaere, J.; Blot, S. I.; Hoste, E. A. Outcome of acute kidney injury in severe burns: a systematic review and meta-analysis. *Intensive Care Med.* **36:**915–925; 2010.

[41] Kasaoka, S.; Todani, M.; Kaneko, T.; Kawamura, Y.; Oda, Y.; Tsuruta, R.; Maekawa, T. Peak value of blood myoglobin predicts acute renal failure induced by rhabdomyolysis. *J. Crit. Care* **25:**601–604; 2010.

[42] Rodríguez-Capote, K.; Balion, C. M.; Hill, S. A.; Cleve, R.; Yang, L.; El Sharif, A. Utility of urine myoglobin for the prediction of acute renal failure in patients with suspected rhabdomyolysis: a systematic review. *Clin. Chem.* **55:**2190–2197; 2009.

[43] Holt, S.; Moore, K. Pathogenesis of renal failure in rhabdomyolysis: the role of myoglobin. *Exp. Nephrol.* **8:**72–76; 2000.

[44] Moore, K. P.; Holt, S. G.; Patel, R. P.; Svistunenko, D. A.; Zackert, W.; Goodier, D.; Reeder, B. J.; Clozel, M.; Anand, R.; Cooper, C. E.; Morrow, J. D.; Wilson, M. T.; Darley-Usmar, V.; Roberts II, L. J. A causative role for redox cycling of myoglobin and its inhibition by alkalinization in the pathogenesis and treatment of rhabdomyolysis-induced renal failure. *J. Biol. Chem.* **273:**31731–31737; 1998.

[45] Ostdal, H.; Andersen, H. J.; Davies, M. J. Formation of long-lived radicals on proteins by radical transfer from heme enzymes—a common process? *Arch. Biochem. Biophys.* **362:**105–112; 1999.

[46] Reeder, B. J.; Svistunenko, D. A.; Cooper, C. E.; Wilson, M. T. The radical and redox chemistry of myoglobin and hemoglobin: from in vitro studies to human pathology. *Antioxid. Redox Signal.* **6:**954–966; 2004.

[47] Sabry, A.; El-Din, A. B.; El-Hadidy, A. M.; Hassan, M. Markers of tubular and glomerular injury in predicting acute renal injury outcome in thermal burn patients: a prospective study. *Ren. Fail.* **31:**457–463; 2009.

[48] Singh, D.; Chander, V.; Chopra, K. Rhabdomyolysis. *Methods Find. Exp. Clin. Pharmacol.* **27:**39–48; 2005.

[49] Chander, V.; Chopra, K. Molsidomine, a nitric oxide donor and L-arginine protects against rhabdomyolysis-induced myoglobinuric acute renal failure. *Biochim. Biophys. Acta* **1723:**208–214; 2005.

[50] Ortiz, P. A.; Garvin, J. L. Cardiovascular and renal control in NOS-deficient mouse models. *Am. J. Physiol. Regul. Integr. Comp. Physiol.* **284:**R628–R638; 2003.

[51] Mattson, D. L.; Meister, C. J. Renal cortical and medullary blood flow responses to L-NAME and ANG II in wild-type, nNOS null mutant, and eNOS null mutant mice. *Am. J. Physiol. Regul. Integr. Comp. Physiol.* **289:**R991–R997; 2005.

[52] Chander, V.; Tirkey, N.; Chopra, K. Resveratrol, a polyphenolic phytoalexin protects against cyclosporine-induced nephrotoxicity through nitric oxide dependent mechanism. *Toxicology* **210:**55–64; 2005.

[53] Gonzalez, J. E.; DiGeronimo, R. J.; Arthur, D. E.; King, J. M. Remodeling of the tight junction during recovery from exposure to hydrogen peroxide in kidney epithelial cells. *Free Radic. Biol. Med.* **47:**1561–1569; 2009.

[54] Kim, O. S.; Kim, Y. S.; Jang, D. S.; Yoo, N. H.; Kim, J. S. Cytoprotection against hydrogen peroxide-induced cell death in cultured mouse mesangial cells by erigeroflavanone, a novel compound from the flowers of *Erigeron annuus. Chem. Biol. Interact.* **180:**414–420; 2009.

[55] Alderliesten, M.; de Graauw, M.; Oldenampsen, J.; Qin, Y.; Pont, C.; van Buren, L.; van de Water, B. Extracellular signal-regulated kinase activation during renal ischemia/reperfusion mediates focal adhesion dissolution and renal injury. *Am. J. Pathol.* **171:**452–462; 2007.

[56] Ishizuka, S.; Yano, T.; Hagiwara, K.; Sone, M.; Nihei, H.; Ozasa, H.; Horikawa, S. Extracellular signal-regulated kinase mediates renal regeneration in rats with myoglobinuric acute renal injury. *Biochem. Biophys. Res. Commun.* **254:**88–92; 1999.

[57] Kim, J. H.; Lee, S. S.; Jung, M. H.; Yeo, H. D.; Kim, H. J.; Yang, J. I.; Roh, G. S.; Chang, S. H.; Park, D. J. N-Acetylcysteine attenuates glycerol-induced acute kidney injury by regulating MAPKs and Bcl-2 family proteins. *Nephrol. Dial. Transplant.* **25:**1435–1443; 2010.

[58] Jo, S. K.; Cho, W. Y.; Sung, S. A.; Kim, H. K.; Won, N. H. MEK inhibitor, U0126, attenuates cisplatin-induced renal injury by decreasing inflammation and apoptosis. *Kidney Int.* **67:**458–466; 2005.

[59] Steele, T. H. Hyperuricemic nephropathies. *Nephron* **81:**45–49; 1999.

[60] Koyner, J. L.; Vaidya, V. S.; Bennett, M. R.; Ma, Q.; Worcester, E.; Akhter, S. A.; Raman, J.; Jeevanandam, V.; O'Connor, M. F.; Devarajan, P.; Bonventre, J. V.; Murray, P. T. Urinary biomarkers in the clinical prognosis and early detection of acute kidney injury. *Clin. J. Am. Soc. Nephrol.* **5:**2154–2165; 2010.

[61] Rosenberg, M. E.; Silkensen, J. Clusterin: physiologic and pathophysiologic considerations. *Int. J. Biochem. Cell Biol.* **27:**633–645; 1995.

[62] Vaidya, V. S.; Ozer, J. S.; Dieterle, F.; Collings, F. B.; Ramirez, V.; Troth, S.; Muniappa, N.; Thudium, D.; Gerhold, D.; Holder, D. J.; Bobadilla, N. A.; Marrer, E.; Perentes, E.; Cordier, A.; Vonderscher, J.; Maurer, G.; Goering, P. L.; Sistare, F. D.; Bonventre, J. V. Kidney injury molecule-1 outperforms traditional biomarkers of kidney injury in preclinical biomarker qualification studies. *Nat. Biotechnol.* **28:**478–485; 2010.

[63] Vaidya, V. S.; Waikar, S. S.; Ferguson, M. A.; Collings, F. B.; Sunderland, K.; Gioules, C.; Bradwin, G.; Matsouaka, R.; Betensky, R. A.; Curhan, G. C.; Bonventre, J. V. Urinary biomarkers for sensitive and specific detection of acute kidney injury in humans. *Clin. Transl. Sci.* **1:**200–208; 2008.

[64] Nath, K. A.; Dvergsten, J.; Correa-Rotter, R.; Hostetter, T. H.; Manivel, J. C.; Rosenberg, M. E. Induction of clusterin in acute and chronic oxidative renal disease in the rat and its dissociation from cell injury. *Lab. Invest.* **71:**209–218; 1994.

[65] Harpur, E.; Ennulat, D.; Hoffman, D.; Betton, G.; Gautier, J. C.; Riefke, B.; Bounous, D.; Schuster, K.; Beushausen, S.; Guffroy, M.; Shaw, M.; Lock, E.; Pettit, S. On behalf of the HESI Technical Committee on Biomarkers of Toxicity, Nephrotoxicity Working Group. Biological qualification of biomarkers of chemical-induced renal toxicity in two strains of male rat. *Toxicol. Sci.* **122:**235–252; 2011.

Supplementary Experimental Section

Materials

Phosphate buffer (pH 7.4, 50 mM) was prepared from nanopure water and the corresponding conjugate acid and base. All reagents were of the highest purity available. Buffers were stored over Chelex-100 (Bio-Rad) at 4 °C for 24 h then treated with diethylentriamene pentaacetate (DTPA; final concentration 100 μM) to remove any contaminating transition metals. Ferric horse heart myoglobin (Mb), potassium bromide (KBr), diethylentriamene pentaacetate and hydrogen peroxide (H_2O_2; 30% w/v) were obtained from Sigma (Sydney Australia).

Isolation of low-density lipoprotein (LDL)

Blood was obtained from a non-fasted healthy donor (male 44 years of age), drawn into heparin-containing vacutainers, and LDL was isolated by ultracentrifugation using a KBr gradient as described previously [1]. The isolated LDL (0.25-0.5 mg apoB100/mL) was stored at 4 °C for 16 h before use. Immediately prior to use, KBr and remaining low-molecular mass, water-soluble antioxidants were removed by gel filtration (PD-10 column, Pharmacia, Uppsala, Sweden). LDL protein concentrations were determined with the using the BCA assay (Sigma, Sydney Australia) with an Ultramark Microplate system (Bio-Rad, Sydney, Australia) and Microplate Manager software v5.1.

Where required, isolated LDL was treated with an ethanolic solution of BP (diluted to a final concentration of 50 μM) or vehicle as control. LDL samples containing BP were then treated with ascorbate from a 5 mM stock solution to yield final concentrations of 25, 50 and 100 μM or vehicle to yield co-supplemented LDL samples and a sample containing BP in the absence of added Vit C. Next, the lipoprotein mixtures were chilled to 4 °C and combined with ferric Mb and H_2O_2 (Mb/H_2O_2 ratio 5:25 mol/mol/mol), and the reaction mixture was incubated at 37 °C and samples obtained after 0, 15, 30, 60 and 240 min.

Oxidation of isolated LDL

Analysis of lipid oxidation and consumption of lipid- and water-soluble antioxidants were performed by reversed-phase HPLC as described previously [1,2] except that accumulating lipid oxidation products were estimated using UV234nm rather than post-column chemiluminescence detection; cholesteryl linoleate hydroperoxides and hydroxides (together referred to as CeO(O)H)) exhibit similar retention times under the

HPLC conditions employed. Accumulating CeO(O)H were quantified by area comparison with an authentic standard of cholesteryl linoleate hydroperoxide.

Supplemental Table I. Intervention studies with lipid- and water-soluble antioxidants.

Antioxidant	Octanol-water partition coefficient	Renal function after RM	CCr	Proteinuria	Tubular casts/ epithelial damage	KIM-1	Clusterin	Oxidative damage	Source
Bisphenol	10.3	↓	↓	↑	↑	↑	↑	↓	[3, This study]
Vitamin E	12.2	↓	↓	↑	↑	n/a	n/a	↓	[3,4]
Resveratrol	1.87	↑	↑	↓	↓	n/a	n/a	↓	[5,6]
Caffeic acid	0.25	↓	↓	-	↑	n/a	n/a	↓	[5,7]
Quercetin	1.82	↑	↑	↓	↓	n/a	n/a	↓	[5,8]
Curcumin	3.29	↓	↓	-	-	n/a	n/a	↓	[9,10]
Vitamin C	-1.85	↑	↓	-	↓	n/a	n/a	↓	[5,11]
Acetaminophen	2.88	↑	↑	↓	↓	n/a	n/a	↓	[12,13]

Data are taken from the literature sources indicate. The upward arrow (↑) indicates improvement in the parameter indicated while the downward arrow (↓) indicates a poor outcome. The smaller arrows indicate a marginal effect. A relatively low value for the octanol-water partition coefficient is indicative of a water-soluble (hydrophilic) antioxidant, while higher values are indicative of a hydrophobic antioxidant. CCr = creatinine clearance; KIM-1 = kidney injury molecule-1; oxidative damage has been assessed using a variety of markers in plasma, urine and kidney tissues including malondialdehyde, F_2-isoprostane and cholesteryl ester hyroperoxides and hydroxides.

References

1. Sattler, W., Mohr, D., Stocker, R. Rapid isolation of lipoproteins and assessment of their peroxidation by HPLC postcolumn chemiluminescence. *Methods Enzymol.* 1994*;***233**:469-489.

2. Suarna, C., Dean, R. T., May, J. Stocker, R. Human atherosclerotic plaque contains both oxidized lipids and relatively large amounts of alpha-tocopherol and ascorbate. *Arterioscler. Thromb. Vasc. Biol.,* 1995;**15**, 1616-1624

3. Shanu, A., Parry, S.N., Wood, S., Rodas, E., Witting, P.K. The synthetic polyphenol tert-butyl-bisphenol inhibits myoglobin-induced dysfunction in cultured kidney epithelial cells. *Free Radic Res.* 2010;**44**:843-853

4. Kim, H-B., Shanu, A., Wood, S. Parry, S.N., Collett, M., McMahon, A.C., Witting, P.K. Phenolic antioxidants tert-butyl-bisphenol and vitamin E decrease oxidative stress and enhance vascular function in an animal model of rhabdomyolysis yet do not improve acute renal failure. *Free Rad. Res.* 2011;**45**:1000-1012

5. Moridani, M.Y., Galati, G., O'Brien, P.J. Comparative quantitative structure toxicity relationships for flavonoids evaluated in isolated rat hepatocytes and HeLa tumor cells. *Chem. Biol. Interact.* 2002;**139**:251-264.

6. Chander, V., Chopra, K. Protective effect of resveratrol, a polyphenolic phytoalexin on glycerol-induced acute renal failure in rat kidney. *Ren. Fail.* 2006;**28**:161-169

7. Aydogdu, N., Atmaca, G., Yalcin, O., Batcioglu, K., Kaymak, K. Effects of caffeic acid phenethyl ester on glycerol-induced acute renal failure in rats. *Clin. Exp. Pharmacol. Physiol.* 2004;**31**:575-579

8. Chander, V., Singh, D., Chopra, K. Reversal of experimental myoglobinuric acute renal failure in rats by quercetin, a bioflavonoid. *Pharmacology.* 2005;**73**:49-56

9. Patel, R., Singh, S.K., Singh, S, Sheth, N.R., Gendle, R. Development and Characterization of Curcumin Loaded Transfersome for Transdermal Delivery. *J. Pharm. Sci. & Res.* 2009;**1**:71-80.

10. Vlahovic, P., Cvetkovic, T., Savic, V., Stefanovic, V. 2007. Dietary curcumin does not protect kidney in glycerol-induced acute renal failure. *Food Chem. Toxicol.* 2007;**45**:1777-1782

11. Ustundag, S., Yalcin, O., Sen, S., Cukur, Z., Ciftci, S., Demirkan, B. Experimental myoglobinuric acute renal failure: the effect of vitamin C. *Ren. Fail.* 2008;**30**:727-735

12. Lorphensri O, Intravijit J, Sabatini DA, Kibbey TC, Osathaphan K, Saiwan C. Sorption of acetaminophen, 17alpha-ethynyl estradiol, nalidixic acid, and norfloxacin to silica, alumina. and a hydrophobic medium. *Water Res.* 2006;**40**:1481-91

13. Boutaud, O., Moore, K.P., Reeder, B.J., Harry, D., Howie, A.J., Wang, S., Carney, C.K., Masterson, T.S., Amin, T., Wright, D.W., Wilson, M.T., Oates, J.A., Roberts, L.J. 2nd. Acetaminophen inhibits hemoprotein-catalyzed lipid peroxidation and attenuates rhabdomyolysis-induced renal failure. *Proc. Natl. Acad. Sci.* U.S.A. 2010;**107**:2699-2704

6 Discussion

6.1 Oxidant Injury and Rhabdomyolysis-Induced Renal Failure

There is accumulating evidence for a causative role of Mb-mediated oxidative injury to the kidney in the development of RM-induced renal failure (Reeder, Hider et al. 2008). Herein, we tested two hypotheses to explain the mechanism by which Mb can cause injury to the kidney. First, we compared the ability of a novel chelator DFOB-AdA$_{OH}$ and its parent compound DFOB to protect cultured kidney epithelial cells in an established cell model of RM that mimics urinary Mb levels detected in severe electrical burn-induced muscle RM. Second, we compared the renal protection of a synthetic phenolic antioxidant BP in an experimental model of RM with or without Vit C co-supplementation. The outcomes from the studies undertaken here indicate that chelators and antioxidants may play a role in ameliorating damage to kidney cells and tissues but that this may not be sufficient to reverse the underlying acute kidney injury, leading to renal failure.

6.2 Desferrioxamine B

The release of free ferrous iron from Mb during degradative processes can lead to the generation of free radicals (*e.g.*, hydroxyl radicals via the Fenton reaction) and this may be causally linked to renal failure. Previous studies showed that desferrioxamine decreased RM-induced renal injury in the rat (Paller 1988) and protected kidney cells from direct exposure to Mb (Zager 1992; Zager and Burkhart 1997). However, there is a growing school of thought that it is the intact Mb protein itself rather than the iron that leads to myoglobinuric oxidative stress after induction of RM (Boutaud and Roberts 2011). The reactive oxygen species produced by Fenton reaction is the hydroxyl radical. Therefore, a wide range of compounds that scavenge •OH, such as dimethylthiourea, benzoate and mannitol were tested to protect the cells from the Mb-induced injury, but this approach has been largely unsatisfactory (Zager and Burkhart 1997).

The effects of DFOB observed both *in vivo* and in cell culture instead point to Mb acting via a pseudo-peroxidase manner, which mediates lipid peroxidation (Figure 5). Moreover, the urine of humans with RM contains increased levels of F$_2$-isoprostanes and hemoprotein cross-links, both outcomes indicative of Mb peroxidase activity

(Reeder, Sharpe et al. 2002). These data unambiguously demonstrate that Mb redox cycling occurs in the kidney of patients with RM, as the hemoprotein cross-link forms only by the reaction of the ferryl-heme and the globin radical (Reeder, Svistunenko et al. 2002).

In addition to the evidence presented above that supports a peroxidase action for Mb in the setting of RM, the ability of catalase, an endogenous scavenger of H_2O_2, to completely inhibit Mb induced damage *in vitro* confirms the importance of H_2O_2 in the Mb pro-oxidative mechanism (Zager and Burkhart 1997). Both ferric and ferrous Mb can react with H_2O_2 to produce water, and perferrylmyoglobin. Also known as Compound I, the ferryl Mb contains hypervalent iron that manifests as a radical porphyrin cation, a potent two-electron oxidant. This oxidant is able to react with a wide range of biological substrates, yielding oxidatively modified products. For example, Compound I reacts with phenols (including amino acids) to produce the corresponding quinones, and regenerates ferrous Mb in the process, thus continuing the cycle of damage (see Figure 5).

Oxidizing Mb reacts with low-molecular weight antioxidants such as ascorbate (Irwin, Østdal et al. 1999) and glutathione (GSH) (Galaris, Cadenas et al. 1989) and this can lead to a depletion of the cell antioxidant status and increased cellular oxidative stress. For example, depletion of GSH in the endothelium upon exposure to pro-oxidant Mb linked to the cytotoxicity of this hemoprotein (D'Agnillo, Wood et al. 2000).
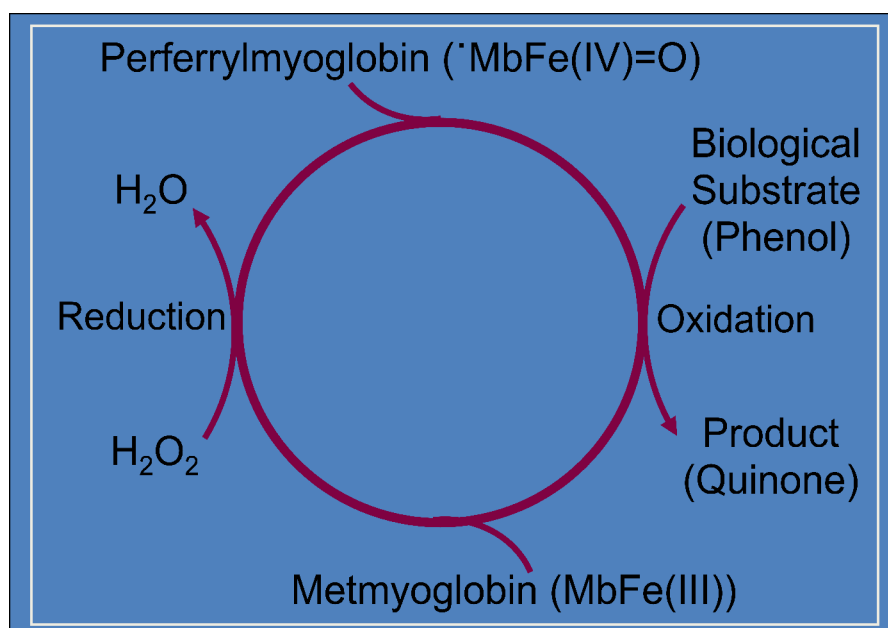
Figure 5   The pseudo-peroxidase activity of Myoglobin

Reduction of H_2O_2 to water results in oxidation of the Fe(III) heme to an Fe(IV) species that cycles back to Fe(III) heme in the presence of suitable substrates. Modified from Reeder et al. (2008). FRBM 44(3): 264-273.

This leads to a logical hypothesis that an appropriate antioxidant (for example, perhaps a synthetic polyphenol) may offer protection against this oxidative stress if it is preferentially oxidized by the various Mb-derived oxidants over other biological substrates.

The chelator DFOB is also known to be a reductant of ferryl-Mb (Rice-Evans, Okunade et al. 1989; Reeder, Hider et al. 2008), which would explain its beneficial effects apart from iron chelation. But even if it is a combination of these different mechanisms involving antioxidant and metal chelating activities, we have clearly shown that DFOB and its new derivative can intervene in both pathological pathways. First, we have shown that DFOB and DFOB-AdA$_{OH}$ bind Fe as a stable Fe(III)-chelator complex that does not redox cycle to the Fe(II)-complex (Liu, Obando et al. 2009). Second, we tested the ability of this new chelator to inhibit the peroxidase activity of Mb. We confirmed a similar antioxidant activity of DFOB-AdA$_{OH}$ compared to DFOB by the ability of the chelators to inhibit oxidizing Mb through formation of nitroxide radicals that lead to the depletion of DFOB-AdA$_{OH}$.

The advantage of DFOB lies in its broad spectrum of biological activity but is limited due to its relatively high toxicity. By conjugating DFOB to an adamantyl derivative we

have a new class of iron chelator with superior properties in regards of toxicity and lipophilicity. DFOB-AdA$_{OH}$ is not only a promising candidate in the prevention of ARF as a consequence of RM but also in the treatment of diverse iron overload diseases such as β-thalassemia (Liu, Obando et al. 2009).

6.3   Bisphenol and Vitamin C

The phenolic antioxidant BP exhibits biological activity that is in part based on its free radical scavenging (or antioxidant) activity. Synthetic BP was strategically designed through a structure-function study using the inhibition of lipoprotein oxidation and synergism with Vit C was used in this study for developing an improved antioxidant (Witting, Westerlund et al. 1996). Notably, studies performed with BP supplementation in animal models of atherosclerosis showed both inhibition of aortic accumulation of oxidized lipids and a concomitant reduction of markers of aortic oxidative damage. However, the studies produced conflicting results in terms of pathological outcome with BP-supplementation inhibiting atherosclerosis in genetically modified low-density lipoprotein deficient mice (Witting, Pettersson et al. 1999), but being unable to inhibit lesion development in Watanabe heritable hyperlipidaemic rabbit (Witting, Pettersson et al. 1999). Nevertheless, these data demonstrated that supplemented BP was active *in vivo* and readily inhibited aortic lipid oxidation consistent with its molecular design.

Vit C is capable of scavenging/neutralizing an array of reactive oxygen species and can regenerate/recycle other phenolic antioxidants. Similar to the polyphenol BP, Vit C reacts with lipid-derived free radicals to protect cell membranes from oxidation (Retsky, Chen et al. 1999) and this has been shown to be beneficial in some animal models where oxidative damage is reported to play a central role in disease progression (Bendich and Langseth 1995).

A range of outcomes investigated in this study confirmed increasing oxidative stress in the modified-glycerol model of RM. Most notably, there is evidence of increased lipid (per)oxidation in both the circulating blood and renal tissues that occurs concomitantly with the release of extracellular Mb. In line with other studies our experiments support the role of Mb redox cycling in the development of RM-induced renal failure. The high levels of Mb accumulating in the kidney have been shown to cause lipid peroxidation in that target organ as reflected by markedly increased F_2-isoprostane and CE oxidation in the plasma and accumulation of F_2-isoprostanes in the kidney in the rat model of RM

(Moore, Holt et al. 1998). Supplementation with BP, Vit C or both BP and Vit C inhibited lipid peroxidation and inflammation but only Vit C, when administered alone, improved renal function in this animal model of RM.

This enhanced oxidative damage was paralleled by a decrease in the aortic content of cGMP suggesting that nitric oxide (•NO) production is decreased during RM-induced acute renal failure and that changes in vascular function may be centrally related to impaired renal function in this animal model. The balance between vaso-constriction and vaso-relaxation acts to maintain vascular tone and regulate circulating blood pressure (Andriambeloson and Witting 2002). Indeed, it has been suggested that vascular dysfunction induced by myoglobinuria plays a role in limiting blood supply to the kidney and exacerbating damage to the renal tissues (Wakabayashi and Kikawada 1996).

Experimental administration of an •NO donor or the •NO precursor L-arginine have the potential to protect the kidneys from injury after RM (Chander and Chopra 2005). Endothelium-derived •NO is the primary vaso-dilating agent produced in the vasculature, which is produced by the action of endothelial nitric oxide synthase on L-arginine. This process generates L-citrulline and •NO as products, and •NO plays a vital role in vessel dilation by regulating peripheral vascular resistance and ultimately blood pressure (Andriambeloson and Witting 2002). To initiate vessel dilation, •NO binds to and activates its molecular target protein, the enzyme soluble guanylyl cyclase (sGC) within the underlying vascular smooth muscle cells (VSMC). The binding of •NO to sGC activates the enzyme by up to 200-fold and this catalyses the conversion of GTP to the effector molecule cGMP. Subsequently, synthesised cGMP activates a cascade of effector proteins that initiate vessel dilation by stimulating VSMC relaxation.

However, •NO is highly reactive with free radicals such as superoxide radical anion, and both peroxyl and hydroxyl radicals. Importantly, extracellular Mb is potentially toxic to the vascular endothelium (D'Agnillo, Wood et al. 2000) and has the potential to bind or chemically modify •NO on the physiological timescale, promoting vascular dysfunction (Zager 1996; Andriambeloson and Witting 2002). In vitro studies have also shown that oxygenated ferrous Mb rapidly reacts with dissolved •NO gas ($k \sim 107$ M-1s-1) to yield higher order N-oxides such as nitrate (Doyle and Hoekstra 1981). Together, these chemical reactions have the potential to effectively scavenge •NO within its expected lifetime in biological systems. As mentioned before, RM produces a large

amount of F_2-isoprostanes, which have been shown to be potent vasoconstrictors. Vasoconstriction is mediated by activation of thromboxane receptors and specific antagonists have been shown to prevent vasoconstriction in a rat model of RM (Chander and Chopra 2005).

Consistent with this idea, our study demonstrated that extracellular Mb causes vascular dysfunction, and this is associated with oxidative stress. The decrease in cGMP level in aorta from myoglobinuric rats may be taken as an evidence of diminished bioavailability of •NO, which was improved by BP and Vit C supplementation through a mechanism that likely involved diminution of oxidative stress.

The kidney tissue also exhibited a selective increase in the (early) antioxidant gene response. Although not exhaustive, our studies demonstrate that the cellular antioxidant response to Mb insult is confined to an induction of SOD-1 gene and GPx-4 activities. No significant inflammatory response was evident in the absence of antioxidant supplementation at least for the time period (24 h post glycerol injection) monitored. These latter observations effectively rule out RM-inducing an early inflammatory response in the renal tissues and dissociate inflammation as a causal factor in ARF (at least up to 24 h after initiation of RM). Whether inflammatory responses become increasing relevant to the renal pathology at later times (>24 h) is not clear and this issue was not addressed in this study.

Overall, the data obtained in this study demonstrates that administration of either BP or Vit C to rats prior to induction of RM prevents the accumulation of oxidative damage, in both the vasculature and kidneys, which is normally evident in myoglobinuria-induced ARF. Supplementation also reverses the decrease in aortic cGMP content as well as the increase of GPx activity. Notably, BP and Vit C alone showed a greater inhibition of oxidative damage than the group treated with both BP and Vit C in kidneys of myoglobinuric animals. Unexpectedly, supplementation with antioxidants did not reduce SOD-1 activity despite the marked decrease in SOD-1 gene expression in the same animals.

Assessment of renal function showed increases in plasma urea and creatinine concomitantly with a significant decrease in C_{Cr}. Though other studies showed improvement in kidney function assessed by the classical marker creatinine and filtration rate (Ustundag, Yalcin et al. 2008), these results might need to be reconsidered. Creatinine concentration is based on the constant release from the body

into the blood and secretion through the kidneys (Perrone, Madias et al. 1992). As RM means an instant release of creatinine from the damaged muscle fibers, the high plasma concentration of creatinine is rather due to the exhausted excretion capacity of the kidneys and may not reflect glomerular filtration. Therefore, kidney markers in animal models of ARF after RM should be reassessed with a focus on early markers of renal damage. In this study, various other biomarkers were employed to investigate renal function. For example, Kidney Injury Molecule-1 (KIM-1) which has been found to serve as a novel biomarker for renal proximal tubule injury (Han, Bailly et al. 2002) and clusterin (Vaidya, Ferguson et al. 2008) increased in all groups with RM regardless of the intervention therapy. Even in the Vit C group, which had a significant decrease in proteinuria, urinary biomarkers remained elevated. Taken together, a re-evaluation of markers of renal damage in animals supplemented with antioxidants is vital to obtain a definite assessment of the relationship between inhibiting oxidative damage and reinstating renal function.

Treatment with BP showed an inhibition of oxidative stress however this did not seem to have an effect on renal damage. In comparison, Vit C treatment was seen to remove oxidative stress in this investigation and also, showed a restoration of renal morphology and decreased proteinuria. However, co-supplementation of BP with Vit C was seen to lower the oxidative stress but did not seem to ameliorate renal dysfunction as evident when assessing renal histology. One possible analogy could be that BP due to its lipophilic nature is directed to the capillaries in the glomerular tuft and hence, is not able to exercise its antioxidant effects on the kidneys. However, Vit C due to its water-soluble nature does not stick to the glomerular tuft and is present in the blood and the extracellular fluid and can exercise its antioxidant effects since it has access to the site of damage within the kidney. Due to this compartmentalization where BP is stuck in the glomerular tuft and Vit C being available in the blood and the extracellular fluid could indicate the reversal of renal dysfunction in samples treated with Vit C. Hence, BP did not have a significant effect on renal morphology. This could mean that water solubility and lipophilicity may play an important role in the antioxidant affecting renal damage.

Previous studies have employed various other antioxidants to inhibit oxidative stress and thus, reverse renal damage. One such group of water-soluble polyphenolic antioxidants that have been reported to exhibit potent antioxidant and free radical scavenging activities are the flavonoids. They may function to scavenge reactive

oxygen species and chelate metal ions. Also, they may act as chain-breaking antioxidants by scavenging lipid peroxyl radicals or portion in to the lipid bi-layer to prevent lipid damage. Some flavonoids used in previous studies to protect renal function against damage from RM induced myoglobinuria include catechins (found in green tea and black tea) (Chander, Singh et al. 2003), Naringin (found in grapefruit) (Singh, Chander et al. 2004) and resveratrol (found in red wine) (Jang and Surh 2003). The aforementioned polyphenolic compounds have been successful in the restitution of renal function by inhibiting oxidative damage albeit limited to traditional markers of renal damage. Therefore, in future studies the use of water-soluble phenolic antioxidants could be considered and may assist in defining the necessary physical properties of suitable antioxidant therapies to combat RM-induced ARF.

Overall, the data obtained in this investigation suggest that oxidative stress may not be causally associated with renal damage. Although, co-supplementation with antioxidants (BP with Vit C) was to some extent seen to be successful in removing oxidative stress, it was not successful in improving renal insufficiency. In addition, this study demonstrated that co-supplementation of BP with Vit C improved vascular function *in vivo*, but still renal dysfunction was not affected. Hence, it could be concluded that supplementation with an antioxidant to inhibit vascular oxidation in union with tissue oxidation does not lead to protection of renal tissues from RM-induced ARF. Results obtained indicate that oxidative stress could be an outcome of myoglobinuria, which affects vessel function and this may have a significant role in RM and ARF. Further investigation in this direction could be conducted using water-soluble phenolic antioxidants and the inclusion of other markers to detect renal changes such as NGAL or cystatin-C (Parikh and Devarajan 2008). In addition, the animal model employed in this study was limited by its timescale. Assessment of injury was only conducted on the first 24 h following RM, whereas early-onset ARF may occur up to 5 days post-burn. Therefore, other complications or delayed effects may have been missed and not taken into consideration. Hence, a suitable timescale incorporating other factors could be employed in future research. Prospective studies could also involve examination of intratubular cast material and other inflammatory responses in regards to myoglobinuria induced ARF. It could be that administration of these other factors together with oxidative stress may have a protective effect on RM induced renal damage.

Another possibility is that, although oxidative stress has an evidential role in ARF, it is a combination of several factors that include, but are not limited to, cytokines released during RM, shock, dehydration and acidosis (Bosch, Poch et al. 2009). Whether limiting Mb pro-oxidant activity also impacts on these other factors is not clear and warrants further study.

6.4   Clinical Implication of this Study

The development of ARF with delay of intensive management of burn lesions impacts significantly on survival (Chrysopoulo, Jeschke et al. 1999). A significant population of patients with severe AKI require hemodialysis or hemo-filtration, and their in-hospital mortality rate ranges from 45 to 70% (Wald, Quinn et al. 2009). Among those who survive, 15% require dialysis at the time of discharge (Silvester, Bellomo et al. 2001; Uchino, Kellum et al. 2005). Dialysis has improved prognosis and survival rates in burns patients with ARF, however the mortality rate among these patients remains unacceptably high. Moreover, little is known about burns patients who survive ARF especially once they leave the hospital and recover enough kidney function to be free of dialysis in the short term. Hence, it is not yet known if the improved survival is a lasting effect or if further severe clinical pathologies in addition to renal complications arise in any portion of this population.

An improved therapy to prevent RM-induced renal failure should aim to reverse the main critical events: decrease of the glomerular filtration rate, reduced blood flow to the glomerulus, tubular obstruction by myoglobin casts, damage through direct cyotoxicity of myoglobin and oxidative stress by both free iron and Mb pro-oxidant activity. The gold standard in shock patients and renal diseases is infusion with large volumes to restore normovolemia and perfusion of the kidneys.

Several intervention therapies have been suggested such as supplementation with mannitol or bicarbonate. Mannitol was thought to increase the removal of Mb in the renal tubule through its diuretic effect. Bicarbonate increases the urine pH and therefore prevents from the accumulation of Tamm-Horsfall-proteins. Another side effect of this is that the pro-oxidant activity of Mb is decreased at a higher pH. However, clinical studies did not confirm the potential benefits of mannitol and bicarbonate (Homsi, Barreiro et al. 1997).

Though oxidative stress may only be one aspect that leads to ARF in RM patients, it still plays a central role in the pathology. Based on our results, another approach for an intervention therapy could be to further investigate the antioxidative capacity of DFOB-AdA$_{OH}$ and the other DFOB derivatives. As we have shown, DFOB and its derivative DFOB-AdA$_{OH}$ are able to effectively bind Fe and therefore inhibit any iron-mediated (oxidative) processes. Further research should test if experiments *in vivo* confirm the ability of these compounds to reduce Mb *in vitro* as seen in EPR spectoscropy. If this is the case, generation of radicals and F$_2$-isoprostanes should be inhibited and •NO levels restored resulting in an improved microcirculation in the kidneys and an increased glomerular filtration. If necessary, a suitable antioxidant should be added to restore the antioxidant capacity of the chelator similar to the Vit C/BP concept. If this needs to be a lipophilic or hydrophilic antioxidant requires further evaluation.

DFOB-AdA$_{OH}$ and the other derivatives were primarily developed to become orally available and to reach intracellular compartements. Therefore, penetration to a precise site in the membrane or intracellular space may be an important feature of the protection against ROS and minimize oxidative stress in the lipid phase. However, the animal studies revealed certain benefits of the water-soluable antioxidant Vit C raising the question if the initiating process for ARF starts in the aqueous phase.

7 Summary

Therapeutic approaches to minimise acute renal failure in an animal model of myoglobinuria

Ludwig K. Groebler

Burns are one of the main causes leading to lethal acute renal failure (ARF). Coagulative necrosis of the skin and the underlying subcutaneous tissue including muscle cells, a process termed RM (rhabdomyolysis), leads to the release of toxic factors including extracellular skeletal myoglobin (Mb). If its amount in the circulation exceeds the binding capacity of the protein haptoglobin, Mb is filtered by the glomeruli and is secreted in the urine, a condition termed myoglobinuria. Accumulating Mb can damage the kidneys by intrarenal vasoconstriction, direct and ischemic tubule injury and tubular obstruction. However, the exact mechanisms are yet unclear. It has been proposed that the release of free iron from the heme group can generate hydroxyl radicals and cause cellular injury. In addition, extracellular myoglobin can undergo redox cycling to yield ferric Mb and from then to the pro-oxidative ferryl state. The ferryl form can initiate lipid peroxidation and renal injury without invoking release of free iron. Furthermore, Mb is a pro-oxidant and initiates the oxidation of biological targets including cell membranes, proteins and DNA. This study tested whether chelators or antioxidants are able to ameliorate ARF through inhibiting oxidative stress. In a cell model using cultured kidney epithelial cells the chelators inhibited Mb-induced oxidative stress and inflammation and improved epithelial cell function. The new iron chelator DFOB-AdAOH showed similar activity to DFOB and due to its low toxicity may be a promising candidate in the treatment of iron overload disease as well as a potential therapeutic strategy to combat ARF after RM.

In an animal model of RM, co-supplementation with tetra-tert-butyl bisphenol (BP) and vitamin C (Vit C) or both BP and Vit C inhibited lipid peroxidation and inflammation but only Vit C, when administered alone, improved renal function as monitored by selected markers of AKF. These data indicate that lipid- and water-soluble antioxidants may differ in terms of their therapeutic impact on RM-induced renal dysfunction. However, the lack of correlation between antioxidant activity and biomarkers of renal

dysfunction makes it difficult to evaluate renal damage. Although oxidative stress has an evidential role in ARF, it seems to be a combination of several factors that include, but are not limited to, cytokines released during RM, shock, dehydration and acidosis. Therefore, a therapeutic intervention should aim to restore glomerular filtration rate, increase blood flow to the glomerulus, and inhibit tubular obstruction by Mb casts. Finally, our studies indicate that further work with the chelator DFOB-AdaOH is warranted. Thus, whether DFOB-AdaOH diminishes oxidative stress caused by both free iron and Mb pro-oxidant activity and whether this can protect the kidneys from experimental ARF should be evaluated further using in vivo models in the future.

8 Zusammenfassung

Therapeutische Ansätze zur Verminderung von akutem Nierenversagen in einem Tiermodell der Myoglobinurie

Ludwig K. Gröbler

Verbrennungen sind eine der Hauptursachen für akutes Nierenversagen (ARF). Nekrosen der Haut und des darunterliegenden Gewebes einschließlich der Muskulatur, RM (Rhambdomyolyse) genannt, führen zur Freisetzung von toxischen Substanzen wie extrazellulärem Myoglobin. Wenn dessen Menge im Blutsystem die Bindungskapazität des Proteins Haptoglobin übersteigt wird Mb von den Glomeruli ausgeschieden und über den Urin entfernt (Myoglobinurie). Die Akkumulation von Myoglobin kann durch intrarenale Vasokonstriktion, direkte und ischämische Schäden des Tubulus oder durch Blockade des Tubulus zu Nierenschäden führen. Trotzdem sind die genauen Ursachen noch unbekannt. Eine Theorie ist, dass die Freisetzung von freiem Eisen aus dem Häm Hydroxylradikale produziert und diese Zellschäden verursachen. Des weiteren kann extrazelluläres Mb durch „redox cycling" den $Fe(III)$- und daraufhin den pro-oxidativen $Fe(IV)$-Zustand annehmen. Die $Fe(IV)$-Form kann auch ohne die Beteiligung von freiem Eisen zu Lipidoxidation und Nierenschäden führen. Zusätzlich ist Mb ein Pro-Oxidant und fördert die Oxidation von Zellmembranen, Proteinen und DNA. In dieser Studie wurde getestet, ob Chelatoren oder Antioxidantien durch die Verminderung von oxidativem Stress die Entstehung von ARF verhindern können. In einem *in vitro*-Modell mit Nierenepithelzellen reduzierten die Chelatoren oxidativen Stress, unterdrückten Entzündungsprozesse und verbesserten die Funktion der Zellen. Der neuentwickelte Eisenchelator DFOB-AdA$_{OH}$ zeigte ähnliche Eigenschaften wie DFOB und könnte aufgrund seiner geringeren Toxizität sowohl für die Behandlung von Eisenüberschuss als auch für die Prävention von ARF nach RM ein aussichtsreicher Wirkstoff sein.

In einem Tiermodell der RM verminderte die Verabreichung von tetra-*tert*-butyl bisphenol (BP) und Vitamin C (Vit C) oder in Kombination Lipidoxidation und Entzündungsprozesse, aber nur Vit C allein verbesserte ausgewählte Marker des akuten Nierenversagens. Die gewonnenen Daten deuten darauf hin, dass lipid- und wasserlösliche Antioxidantien unterschiedlichen Einfluss auf durch RM verursachtes Nierenversa-

gen haben können. Allerdings bestehen aufgrund der mangelnden Korrelation von antioxidativer Wirkung und Nierenschaden Schwierigkeiten diesen korrekt zu erfassen. Obwohl oxidativer Stress zweifelsfrei eine wichtige Rolle bei ARF spielt, scheint es eine Kombination aus verschiedenen Faktoren wie Freisetzung von Zytokinen, Schock, Dehydration und Azidose zu sein. Daher sollte eine mögliche Therapie darauf zielen, die glomeruläre Filtrationsrate zu erhalten, den Blutfluss zum Glomerulus zu erhöhen und die Blockade durch Mb-Zylinder zu lösen. Aufgrund dieser Ergebnisse scheinen weitere Studien mit dem Chelator DFOB-AdA$_{OH}$ notwendig. Daher sollte in einem *in vivo* Experiment untersucht werden, ob DFOB-AdA$_{OH}$ sowohl den durch freies Eisen als auch den durch die pro-oxidative Wirkung des Myoglobins enstandenen oxidativen Stress vermindert und ob dies ARF verhindern kann.

9   List of Figures

10   List of Tables

11   References

Ames BN, Shigenaga MK, Hagen TM (1993) Oxidants, antioxidants, and the degenerative diseases of aging. Proceedings of the National Academy of Sciences 90(17):7915

Andriambeloson E, Witting P (2002) Chemical regulation of nitric oxide: a role for intracellular myoglobin? Redox Report 7(3):131-136

Aydogdu N, Atmaca G, Yalcin O, Taskiran R, Tastekin E, Kaymak K (2006) Protective effects of L-Carnitine on myoglobinuric acute renal failure in rats. Clinical and Experimental Pharmacology and Physiology 33(1-2):119-124

Azzi A (2007) Molecular mechanism of [alpha]-tocopherol action. Free Radical Biology and Medicine 43(1):16-21

Bendich A, Langseth L (1995) The health effects of vitamin C supplementation: a review. Journal of the American College of Nutrition 14(2):124-136

Bosch X, Poch E, Grau JM (2009) Rhabdomyolysis and acute kidney injury. New England Journal of Medicine 361(1):62-72

Boutaud O, Roberts LJ (2011) Mechanism-based therapeutic approaches to rhabdomyolysis-induced renal failure. Free Radical Biology and Medicine 51(5):1062-1067

Bywaters E, Beall D (1941) Crush injuries with impairment of renal function. British Medical Journal 1(4185):427-437

Bywaters EGL, Delory GE, Rimington C, Smiles J (1941) Myohaemoglobin in the urine of air raid casualties with crushing injury. Biochemical Journal 35(10-11):1164-1168

Chander V, Chopra K (2005) Molsidomine, a nitric oxide donor and L-arginine protects against rhabdomyolysis-induced myoglobinuric acute renal failure. Biochimica et Biophysica Acta (BBA)-General Subjects 1723(1-3):208-214

Chander V, Singh D, Chopra K (2003) Catechin, a natural antioxidant protects against rhabdomyolysis-induced myoglobinuric acute renal failure. Pharmacological Research 48(5):503-509

Chrysopoulo M, Jeschke M, Dziewulski P, Barrow R, Herndon D (1999) Acute renal dysfunction in severely burned adults. The Journal of Trauma 46(1):141

Criddle LM (2003) Rhabdomyolysis: Pathophysiology, recognition, and management. Critical Care Nurse 23(6):14-30

D'Agnillo F, Wood F, Porras C, Macdonald VW, Alayash AI (2000) Effects of hypoxia and glutathione depletion on hemoglobin-and myoglobin-mediated oxidative

stress toward endothelium. Biochimica et Biophysica Acta (BBA)-Molecular Cell Research 1495(2):150-159

Davies KJA (1995) Oxidative stress: the paradox of aerobic life. Biochemical Society Symposium, 61:1-31

Doyle MP, Hoekstra JW (1981) Oxidation of nitrogen oxides by bound dioxygen in hemoproteins. Journal of Inorganic Biochemistry 14(4):351-358

Dylewski DF, Froman DM (1992) Vitamin C supplementation in the patient with burns and renal failure. Journal of Burn Care & Research 13(3):378-380

Fenton H (1894) LXXIII.-Oxidation of tartaric acid in presence of iron. Journal of the Chemical Society, Transactions 65: 899-910

Gabutti V, Piga A (1996) Results of long-term iron-chelating therapy. Acta Haematologica 95(1):26-36

Genova ML, Pich MM, Biondi A, Bernacchia A, Falasca A, Bovina C, Formiggini G, Castelli GP, Lenaz G (2003) Mitochondrial production of oxygen radical species and the role of coenzyme Q as an antioxidant. Experimental Biology and Medicine 228(5):506-513

Gordon JL (1986) Extracellular ATP: effects, sources and fate. Biochemical Journal 233(2):309-319

Haber F, Weiss J (1932) Über die Katalyse des Hydroperoxydes. Naturwissenschaften 20(51):948-950

Halliwell B (2007) Biochemistry of oxidative stress. Biochemical Society, Transactions 35(5):1147-1150

Han WK, Bailly V, Abichandani R, Thadhani R, Bonventre JV (2002) Kidney injury molecule-1 (KIM-1): a novel biomarker for human renal proximal tubule injury. Kidney International 62(1):237-244

Hendryk S, Czuba Z, Jędrzejewska-Szypułka H, Bażowski P, Doleżych H, Król W (2010) Increase in activity of neutrophils and proinflammatory mediators in rats following acute and prolonged focal cerebral ischemia and reperfusion. Brain Edema XIV 106:29-35

Holm C, Hörbrand F, Henckel von Donnersmarck G, Mühlbauer W (1999) Acute renal failure in severely burned patients. Burns 25(2):171-178

Homsi E, Barreiro MFFL, Orlando JMC, Higa EM (1997) Prophylaxis of acute renal failure in patients with rhabdomyolysis. Renal Failure 19(2):283-288

Huerta-Alardin AL, Varon J, Marik PE (2005) Bench-to-bedside review: Rhabdomyolysis-an overview for clinicians. Critical Care 9(2):158-169

Ide T, Tsutsui H, Kinugawa S, Utsumi H, Dongchon K, Hattori N, Uchida K, Arimura KI, Egashira K, Takeshita A (1999) Mitochondrial electron transport complex I is a potential source of oxygen free radicals in the failing myocardium. Circulation Research 85(4):357-363

Irwin JA, Østdal H, Davies MJ (1999) Myoglobin-induced oxidative damage: evidence for radical transfer from oxidized myoglobin to other proteins and antioxidants. Archives of Biochemistry and Biophysics 362(1):94-104

Ison MG, Hayden FG (2001) Therapeutic options for the management of influenza. Current Opinion in Pharmacology 1(5):482-490

Jang JH, Surh YJ (2003) Protective effect of resveratrol on [beta]-amyloid-induced oxidative PC12 cell death. Free Radical Biology and Medicine 34(8):1100-1110

Jovanovic SV, Steenken S, Hara Y, Simic MG (1996) Reduction potentials of flavonoid and model phenoxyl radicals. Which ring in flavonoids is responsible for antioxidant activity? Journal of the Chemical Society, Perkin Transactions 2(11):2497-2504

Kavdia M, Tsoukias NM, Popel AS (2002) Model of nitric oxide diffusion in an arteriole: impact of hemoglobin-based blood substitutes. American Journal of Physiology-Heart and Circulatory Physiology 282(6):H2245-H2253

Khan F (2009) Rhabdomyolysis: a review of the literature. The Netherlands Journal of Medicine 67(9):272-283

Kim HB, Shanu A, Wood S, Parry SN, Collet M, McMahon A, Witting PK (2011) Phenolic antioxidants tert-butyl-bisphenol and vitamin E decrease oxidative stress and enhance vascular function in an animal model of rhabdomyolysis yet do not improve acute renal dysfunction. Free Radical Research 45(9):1000-1012

Knochel JP (1993) Mechanisms of rhabdomyolysis. Current Opinion in Rheumatology 5(6):725-731

Lewin P, Moscarello M (1966) Cardiac myoglobin in myoglobinuria. Canadian Medical Association Journal 94(3):129-131

Liu J, Obando D, Schipanski LG, Groebler LK, Witting PK, Kalinowski DS, Richardson DR, Codd R (2010) Conjugates of desferrioxamine B (DFOB) with derivatives of adamantane or with orally available chelators as potential agents for treating iron overload. Journal of Medicinal Chemistry 53(3):1370-1382

Miwa S, Brand M (2003) Mitochondrial matrix reactive oxygen species production is very sensitive to mild uncoupling. Biochemical Society, Transactions 31(6):1300-1301

Moore KP, Holt SG, Patel RP, Svistunenko DA, Zackert W, Goodier D, Reeder BJ, Clozel M, Anand R, Cooper CE (1998) A causative role for redox cycling of

myoglobin and its inhibition by alkalinization in the pathogenesis and treatment of rhabdomyolysis-induced renal failure. Journal of Biological Chemistry 273(48):31731-31737

Moses Old Testament 11:31-35

Mosmann T (1983) Rapid colorimetric assay for cellular growth and survival: application to proliferation and cytotoxicity assays. Journal of Immunological Methods 65(1-2):55-63

Mustonen KM, Vuola J (2008) Acute renal failure in intensive care burn patients (ARF in burn patients). Journal of Burn Care & Research 29(1):227-237

Nick H (2007) Iron chelation, quo vadis? Current Opinion in Chemical Biology 11(4):419-423

Padayatty SJ, Katz A, Wang Y, Eck P, Kwon O, Lee JH, Chen S, Corpe C, Dutta A, Dutta SK (2003) Vitamin C as an antioxidant: evaluation of its role in disease prevention. Journal of the American College of Nutrition 22(1):18-35

Paller M (1988) Hemoglobin- and myoglobin-induced acute renal failure in rats: role of iron in nephrotoxicity. American Journal of Physiology - Renal Physiology 255(3):539-544

Parikh CR, Devarajan P (2008) New biomarkers of acute kidney injury. Critical Care Medicine 36(4):S159-165

Parry SN, Ellis N, Li Z, Maitz P, Witting PK (2008) Myoglobin induces oxidative stress and decreases endocytosis and monolayer permissiveness in cultured kidney epithelial cells without affecting viability. Kidney and Blood Pressure Research 31(1):16-28

Pentón-Rol G, Cervantes-Llanos M, Martínez-Sánchez G, Cabrera-Gómez JA, Valenzuela-Silva CM, Ramírez-Nuñez O, Casanova-Orta M, Robinson-Agramonte MA, Lopategui-Cabezas I, López-Saura PA (2009) TNF-alpha and IL-10 downregulation and marked oxidative stress in neuromyelitis optica. Journal of Inflammation 618-627

Perkoff GT, Hill RL, Brown DM, Tyler FH (1962) The characterization of adult human myoglobin. Journal of Biological Chemistry 237(9):2820-2827

Perrone RD, Madias NE, Levey AS (1992) Serum creatinine as an index of renal function: new insights into old concepts. Clinical Chemistry 38(10):1933-1953

Porter J, Rafique R, Srichairatanakool S, Davis B, Shah F, Hair T, Evans P (2005) Recent insights into interactions of deferoxamine with cellular and plasma iron pools: Implications for clinical use. Annals of the New York Academy of Sciences 1054(1):155-168

Reeder B, Sharpe M, Kay A, Kerr M, Moore K, Wilson M (2002) Toxicity of myoglobin and haemoglobin: oxidative stress in patients with rhabdomyolysis and subarachnoid haemorrhage. Biochemical Society, Transactions 30(4):745-748

Reeder BJ, Hider RC, Wilson MT (2008) Iron chelators can protect against oxidative stress through ferryl heme reduction. Free Radical Biology and Medicine 44(3):264-273

Reeder BJ, Svistunenko DA, Sharpe MA, Wilson MT (2002) Characteristics and mechanism of formation of peroxide-induced heme to protein cross-linking in myoglobin. Biochemistry 41(1):367-375

Retsky KL, Chen K, Zeind J, Frei B (1999) Inhibition of copper-induced LDL oxidation by vitamin C is associated with decreased copper-binding to LDL and 2-oxo-histidine formation. Free Radical Biology and Medicine 26(1-2):90-98

Rice-Evans C, Okunade G, Khan R (1989) The suppression of iron release from activated myoglobin by physiological electron donors and by desferrioxamine. Free Radical Research 7(1):45-54

Rodrigo R, Bosco C, Herrera P, Rivera G (2004) Amelioration of myoglobinuric renal damage in rats by chronic exposure to flavonol-rich red wine. Nephrology Dialysis Transplantation 19(9):2237-2244

Sabry A, Wafa I, AB E, El-Hadidy A, Hassan M (2009) Early markers of renal injury in predicting outcome in thermal burn patients. Saudi Journal of Kidney Diseases and Transplantation 20(4):632-638

Sharp LS, Rozycki GS, Feliciano DV (2004) Rhabdomyolysis and secondary renal failure in critically ill surgical patients. The American Journal of Surgery 188(6):801-806

Sies H (1997) Oxidative stress: oxidants and antioxidants. Experimental Physiology 82(2):291-295

Silvester W, Bellomo R, Cole L (2001) Epidemiology, management, and outcome of severe acute renal failure of critical illness in Australia. Critical Care Medicine 29(10):1910-1915

Singh D, Chander V, Chopra K (2004) Protective effect of naringin, a bioflavonoid on glycerol-induced acute renal failure in rat kidney. Toxicology 201(1-3):143-151

Smirnoff N, Running JA, Gatzek S (2004) Ascorbate biosynthesis: a diversity of pathways. Vitamin C: its Functions and Biochemistry in Animals and Plants: 7-29

Spasov A, Khamidova T, Bugaeva L, Morozov I (2000) Adamantane derivatives: Pharmacological and toxicological properties (review). Pharmaceutical Chemistry Journal 34(1):1-7

Stefanovic V, Savic V, Vlahovic P, Cvetkovic T, Najman S, Mitic-Zlatkovic M (2000) Reversal of experimental myoglobinuric acute renal failure with bioflavonoids from seeds of grape. Renal Failure 22(3):255-266

Stintzi A, Barnes C, Xu J, Raymond KN (2000) Microbial iron transport via a siderophore shuttle: a membrane ion transport paradigm. Proceedings of the National Academy of Sciences 97(20):10691-10696

Toufektsian MC, Boucher F, Tanguy S, Morel S, De Leiris J (2001) Cardiac toxicity of singlet oxygen: implication in reperfusion injury. Antioxidants and Redox Signaling 3(1):63-69

Uchino S, Kellum JA, Bellomo R, Doig GS, Morimatsu H, Morgera S, Schetz M, Tan I, Bouman C, Macedo E (2005) Acute renal failure in critically ill patients. JAMA: The Journal of the American Medical Association 294(7):813-818

Ueda N, Baliga R, Shah SV (1996) Role of 'catalytic' iron in an animal model of minimal change nephrotic syndrome. Kidney International 49:370-373

Ustundag S, Yalcin O, Sen S, Cukur Z, Ciftci S, Demirkan B (2008) Experimental myoglobinuric acute renal failure: the effect of vitamin C. Renal Failure 30(7):727-735

Vaidya VS, Ferguson MA, Bonventre JV (2008) Biomarkers of acute kidney injury. Annual Review of Pharmacology and Toxicology 48:463-493

Valko M, Rhodes C, Moncol J, Izakovic M, Mazur M (2006) Free radicals, metals and antioxidants in oxidative stress-induced cancer. Chemico-Biological Interactions 160(1):1-40

Vanholder R, Sever MS, Erek E, Lameire N (2000) Rhabdomyolysis. Journal of the American Society of Nephrology 11(8):1553-1561

Vlahovic P, Cvetkovic T, Savic V, Stefanovic V (2007) Dietary curcumin does not protect kidney in glycerol-induced acute renal failure. Food and Chemical Toxicology 45(9):1777-1782

Wakabayashi Y, Kikawada R (1996) Effect of L-arginine on myoglobin-induced acute renal failure in the rabbit. American Journal of Physiology - Renal Physiology 270(5):F784-F789

Wald R, Quinn RR, Luo J, Li P, Scales DC, Mamdani MM, Ray JG (2009) Chronic dialysis and death among survivors of acute kidney injury requiring dialysis. JAMA: The Journal of the American Medical Association 302(11):1179-1185

Walsh MB, Miller SL, Kagen LJ (1982) Myoglobinemia in severely burned patients: correlations with severity and survival. The Journal of Trauma 22(1):6-10

Winterbourn CC (1995) Toxicity of iron and hydrogen peroxide: the Fenton reaction. Toxicology Letters 82:969-974

Witting P, Pettersson K, Östlund-Lindqvist A, Westerlund C, Wågberg M, Stocker R (1999) Dissociation of atherogenesis from aortic accumulation of lipid hydro (pero) xides in Watanabe heritable hyperlipidemic rabbits. Journal of Clinical Investigation 104(2):213-220

Witting P, Westerlund C, Stocker R (1996) A rapid and simple screening test for potential inhibitors of tocopherol-mediated peroxidation of LDL lipids. Journal of Lipid Research 37(4):853-867

Witting PK, Pettersson K, Östlund-Lindqvist AM, Westerlund C, Eriksson AW, Stocker R (1999) Inhibition by a coantioxidant of aortic lipoprotein lipid peroxidation and atherosclerosis in apolipoprotein E and low density lipoprotein receptor gene double knockout mice. The FASEB Journal 13(6):667-675

Zager R (1992) Combined mannitol and deferoxamine therapy for myohemoglobinuric renal injury and oxidant tubular stress. Mechanistic and therapeutic implications. Journal of Clinical Investigation 90(3):711-719

Zager RA (1996) Rhabdomyolysis and myohemoglobinuric acute renal failure. Kidney International 49(2):314-326

Zager RA, Burkhart K (1997) Myoglobin toxicity in proximal human kidney cells: Roles of Fe, Ca2+, H2O2, and terminal mitochondrial electron transport. Kidney International 51(3):728-738

12   Presentations and Publications

Publications arising directly from this work:

1. Joe Liu, Daniel Obando, Liam G. Schipanski, <u>Ludwig K. Groebler</u>, Paul K. Witting, Danuta S. Kalinowski, Des R. Richardson, Rachel Codd.

Conjugates of desferrioxamine B (DFOB) with derivatives of adamantane or with orally available chelators as potential agents for treating iron overload. Journal of Medicinal Chemistry 2009; 53: 1370-1382

Konjugate von Desferrioxamine B (DFOB) mit Derivaten von Adamantan oder oral verfügbaren Chelatoren als potentielle Wirkstoffe zur Behandlung von Eisenüberschuss.

DOI: 10.1021/jm9016703

2. <u>Ludwig K. Groebler</u>, Joe Liu, Rachel Codd and Paul K. Witting.

Comparing the potential renal protective activity of desferrioxamine B and the novel chelator desferrioxamine B-N-(3-hydroxyadamant-1-yl)carboxamide in a cell model of myoglobinuria. Biochemical Journal 2011; 435: 669-677

Der Vergleich der Wirkung von Desferrioxamin B und dem neuen Eisenchelator Desferrioxamin B-N-(3-hydroxyadamant-1-yl)carboxamid zum Schutz der Niere in einem in vitro-Modell von Myoglobinurie.

DOI: 10.1042/BJ20101728

3. <u>Ludwig K. Groebler</u>, Hyun Bo Kim, Anu Shanu, Farjaneh Hossain, Aisling C. McMahon, Paul K. Witting.

Co-supplementation with a synthetic polyphenol and vitamin C inhibits oxidative damage and improves vascular function yet does not inhibit acute renal injury in an animal model of rhabdomyolysis. Free Radical Biology and Medicine 2012; 52(9): 1918-28

Die parallele Verabreichung von einem synthetischem Polyphenol und Vitamin C verhindert oxidative Gewebeschäden und verbessert die Gefäßfunktion in einem Tiermodell der Rhabdomyolyse ohne dabei akutes Nierenversagen zu verhindern.

DOI: 10.1016/j.freeradbiomed.2012.02.011

Publications arising from methodology and assays developed in this work, but not part of this particular thesis:

Daniel E. Morrison, Fatiah Issa, Mohan Bhadbhade, Paul K. Witting, <u>Ludwig K. Groebler</u>, Peter J. Rutledge and Louis M. Rendina. Boronated phosphonium salts containing arylboronic acid, closo-carborane or nido-carborane: X-ray diffraction, in vitro cytotoxicity, and cellular uptake. J Biol Inorg Chem. 2010 Nov; 15(8): 1305-18.

Presentations (presenter underlined):

<u>**Ludwig K. Groebler**</u>,* Joe Liu, Rachel Codd, and Paul K. Witting. 2. December 2010 "Novel Chelators as Inhibitors of Renal Cell Dysfunction". Society for Free Radical Research (Australasia) Annual Meeting, Akaroa, New Zealand.

* First author awarded with an internationally competitive travel grant (Young Investigator Award) to attend this meeting.

13   Author Contribution

Publication 1 (J. Med. Chem. 2010)

Specifically, LG (Ludwig Groebler) developed and performed MTT cell viability assays for the MDCK II cell lines employed throughout this study. LG was involved in reviewing and updating the text associated with the revised manuscript and for collegial intellectual input into design of experiments.

Publication 2 (Biochem. J. 2011)

LG was responsible for carrying out the majority of the work in the present study with guidance from the senior researcher. Together with Paul Witting, LG was involved in formulating research direction and in drafting the manuscript and subsequent redrafting of the text. In particular, LG prepared, cultured and harvested the cell lines used in this study. He planned and performed the experiments necessary for flow cytometry, RT-qPCR, fluorescence microscopy and inulin transport across cell monolayers. He was also responsible for performing and assessing an AlphaLISA assay for the measurement of MCP-1 which was supplied by the company PerkinElmer$^{®}$ as a beta test.

Publication 3 (FRBM 2012)

LG was responsible for carrying out the majority of the work in the present study with guidance from the senior researcher. Together with Paul Witting, LG was involved in formulating a draft manuscript and subsequent redrafting of the text. In particular, LG planned and organized the animal studies, monitored the animals, performed the experimental procedure and was responsible for post experimental ethical care of the animals. At the required time LG was responsible for the harvest of tissues from the experimental animal. He planned and performed the experiments necessary for HPLC, RT-qPCR, histology and enzyme activity assays. LG was beta user for the AlphaLISA assay for the measurement of MCP-1. LG was involved in the establishment of the Luminex$^{®}$ system in the Bosch Molecular Biology Facility, received special training and was contact person for other users.

14   Acknowlegements

15   Selbständigkeitserklärung

Hiermit bestätige ich, dass ich die vorliegende Arbeit selbständig angefertigt habe. Ich versichere, dass ich ausschließlich die angegebenen Quellen und Hilfen in Anspruch genommen habe.

Hamburg, den 07. Juni 2012

Ludwig K. Gröbler